

INVESTIGATION OF PLANT DERIVED SUBSTANCES THAT PROMOTE THE  
BIOSYNTHESIS OF COLLAGEN; DEVELOPMENT OF COSMETIC AND  
DERMATOLOGICAL SKIN CARE PRODUCTS

A THESIS SUBMITTED TO  
THE GRADUATE SCHOOL OF NATURAL AND APPLIED SCIENCES  
OF  
MIDDLE EAST TECHNICAL UNIVERSITY

BY

ASLIGÜL KURT

IN PARTIAL FULFILLMENT OF THE REQUIREMENTS  
FOR  
THE DEGREE OF DOCTOR OF PHILOSOPHY  
IN  
THE DEPARTMENT OF BIOCHEMISTRY

SEPTEMBER 2015



Approval of the Thesis:

**INVESTIGATION OF PLANT DERIVED SUBSTANCES THAT PROMOTE  
THE BIOSYNTHESIS OF COLLAGEN; DEVELOPMENT OF COSMETIC  
AND DERMATOLOGICAL SKIN CARE PRODUCTS**

submitted by **ASLIGUL KURT** in partial fulfillment of the requirements for the  
degree of **Doctor of Philosophy in Biochemistry Department, Middle East  
Technical University** by,

Prof. Dr. Gülbin Dural Ünver \_\_\_\_\_  
Dean, Graduate School of **Natural and Applied Sciences**

Prof. Dr. Orhan Adalı \_\_\_\_\_  
Head of Department, **Biochemistry**

Assoc. Prof. Dr. Nursen Çoruh \_\_\_\_\_  
Supervisor, **Chemistry Dept., METU**

Prof. Dr. Orhan Adalı \_\_\_\_\_  
Co-Supervisor, **Biology Dept., METU**

**Examining Committee Members:**

Prof. Dr. Musa Doğan \_\_\_\_\_  
Biology Dept., METU

Assoc. Prof. Dr. Nursen Çoruh \_\_\_\_\_  
Chemistry Dept., METU

Prof. Dr. İsmet Deliloğlu Gürhan \_\_\_\_\_  
Bioengineering Dept., Ege University

Assoc. Prof. Dr. Mesut Muyan \_\_\_\_\_  
Biology Dept., METU

Assoc. Prof. Dr. Nilgün Yücel \_\_\_\_\_  
Chemistry Dept., Dokuz Eylül University

Date: 30.09.2015

**I hereby declare that all information in this document has been obtained and presented in accordance with academic rules and ethical conduct. I also declare that, as required by these rules and conduct, I have fully cited and referenced all material and results that are not original to this work.**

Name, Last name : Aslıgül Kurt

Signature :

## ABSTRACT

### INVESTIGATION OF PLANT DERIVED SUBSTANCES THAT PROMOTE THE BIOSYNTHESIS OF COLLAGEN; DEVELOPMENT OF COSMETIC AND DERMATOLOGICAL SKIN CARE PRODUCTS

Kurt, Aslıgöl

Ph.D., Department of Biochemistry

Supervisor: Assoc. Prof. Dr. Nursen Çoruh

Co-Supervisor: Prof. Dr. Orhan Adalı

September 2015, 102 pages

Extracellular matrix provides a healthy functional condition for skin; it is composed largely of collagen and secreted by fibroblasts. As the aging develops, cellular proteins change shapes which prevents the proteins from proper communications resulting in the loss of extracellular matrix and collagen. Finally, the wrinkles and aging effects start building up. Meanwhile, the use of collagen stimulating products can reverse this process. Many herbal products have been produced for the repair of aging effects. Besides the benefits, some of those manufactured herbal products have the adverse effects as a result of unscientific production.

In this study, in-vitro experimental steps were planned for the search of herbal ingredients to help the induction of collagen biosynthesis. Plant samples that are used were selected from the effective facial mask recipes, as seed cotyledon of *Aesculus hippocastanum* and aerial parts of *Hypericum perforatum*, *Primula vulgaris*, *Achillea millefolium*.

The plant samples were extracted in methanol and experimental steps were started with the anti-oxidant tests. *Hypericum perforatum* extract revealed the highest anti-oxidant effect. Then, human fibroblasts were exposed to each extract and the effects of crude extracts were investigated on the expression level of type 1 collagen by qPCR and western blot analysis. In qPCR analysis *Achillea millefolium* extract and in western blot analysis *Primula vulgaris* extract had the highest induction rate. Those two extracts were fractionated with appropriate solvents (hexane, chloroform, ethyl acetate, water respectively). The effects of the ethyl acetate and water fractions as well as the crude extracts were again investigated on the expression level of type 1 collagen. The highest induction rate of collagen was found with the crude extract treatments.

In conclusion, the crude extract of *Primula vulgaris* was found to reveal the highest induction on collagen biosynthesis, which can be used in dermatological skin care products.

**Keywords:** Fibroblast, Collagen, *Aesculus hippocastanum*, *Hypericum perforatum*, *Primula vulgaris*, *Achillea millefolium*.

## ÖZ

### KOLAJEN BİYOSENTEZİNİ TEŞVİK EDEN BİTKİ KAYNAKLI MADDELERİN ARAŞTIRILMASI; KOZMETİK VE DERMATOLOJİK CİLT BAKIM ÜRÜNLERİ GELİŞTİRİLMESİ

Kurt, Aslıgül

Doktora, Biyokimya Bölümü

Tez Yöneticisi: Assoc. Prof. Dr. Nursen Çoruh

Ortak Tez Yöneticisi: Prof. Dr. Orhan Adalı

Eylül 2015, 102 sayfa

Ekstraselüler matriks deri için sağlıklı fonksiyonel ortamı sağlar; çoğunlukla kolajenden oluşmuştur ve fibroblast hücreleri tarafından salgılanır. Yaşın ilerlemesiyle birlikte, hücresel proteinler şekil değiştirerek uygun iletişim yapamaz hale gelirler ki bu da ekstraselüler matriks ve kolajen kaybı ile sonuçlanır. Son olarak, kırışıklıklar ve yaşlanma belirtileri ortaya çıkmaya başlar. Bu arada, kolajen uyarıcı ürünlerin kullanılması bu süreci tersine çevirebilir. Yaşlanmanın etkilerini onarabilmek için birçok bitkisel ürün geliştirilmiştir. Bu bitkisel ürünler bilimsel olmayan üretim sonucu faydalarının yanı sıra yan etkilere de sahiptir.

Bu çalışmada, kolajen biyosentezini başlatmaya yardımcı bitkisel içeriklerin araştırılması için in vitro deney adımları planlanmıştır. *Aesculus hippocastanum*'un tohum kotiledonu ve *Hypericum perforatum*, *Primula vulgaris*, *Achillea*

*millefolium*'un toprak üstü kısımları kullanılmıştır ve bu bitki örnekleri etkin yüz maskesi tariflerinden seçilmiştir.

Bitki örnekleri metanolde özütü elde edilmiş ve deney adımları anti-oksidan testlerle başlamıştır. *Hypericum perforatum* özütü en yüksek anti-oksidan etkiyi göstermiştir. Sonrasında insan fibroblast hücreleri her bir özüte maruz bırakılmış ve total özütlerin etkisi kolajen tip-1 seviyesinde qPCR ve Western blot analizleriyle araştırılmıştır. qPCR analizinde *Achillea millefolium* özütü ve Western blot analizinde *Primula vulgaris* özütü en yüksek tetikleyici etkiye sahip olmuştur. Bu iki özüt uygun çözücülerle (sırasıyla hekzan, kloroform, etil asetat, su) fraksiyonlarına ayrılmıştır. Etil asetat ve su fraksiyonlarının yanı sıra total özütün kolajen tip-1 ifade seviyesi de yeniden araştırılmıştır. En yüksek kolajen tetikleme oranı total özüt uygulamasında tespit edilmiştir.

Sonuç olarak, dermatolojik cilt bakım ürünlerinde kullanılacak *Primula vulgaris* total özütünün kolajen biyosentezinde en yüksek tetikleyici etkiye sahip olduğu gözlenmiştir.

**Anahtar Kelimeler:** Fibroblast, Kolajen, *Aesculus hippocastanum*, *Hypericum perforatum*, *Primula vulgaris*, *Achillea millefolium*.

To My Family,

## ACKNOWLEDGEMENTS

I am deeply grateful to my supervisor Assoc. Prof. Dr. Nursen oruh for her valuable guidance, patient, continued advice and critical discussion, her kindness and generosity throughout this study.

I am deeply grateful to my first co-supervisor Prof. Dr. Mesude İřcan for her support and help.

I am also deeply grateful to my co-supervisor Prof. Dr. Orhan Adalı for his guidance and advices throughout this study.

I thank to my thesis monitoring committee members Prof. Dr. İsmet Delilođlu Gűrhan and Assoc. Prof. Dr. Mesut Muyan for their suggestions and criticism.

I want to thank to Prof. Dr. Musa Dođan for his guidance.

I especially thank to Merve Akkulak and Serdar Karakurt for their beautiful friendship, support and encouragements to complete this thesis.

I am grateful to my lab mates řule řahin, Yeřim Kűmbet and Nizamettin Őzdođan for their beautiful friendship, support and help.

I am also thankful to my husband Oytun Kurt for his endless support and love.

I want to thank to my born to be baby for his patience to write this thesis.

I wish to thank The Ministry of Science, Industry and Technology and Ars Arthro Biotechnology for financial support as San-Tez Project (1507.STZ.2012-2).

This study is dedicated to my family, whose help, advice, patience, support, and love are undeniable and unforgettable. Without them I couldn't have done this.

## TABLE OF CONTENTS

<b>ABSTRACT</b> .....	<b>v</b>
<b>ÖZ</b> .....	<b>vii</b>
<b>ACKNOWLEDGEMENTS</b> .....	<b>x</b>
<b>TABLE OF CONTENTS</b> .....	<b>xi</b>
<b>LIST OF TABLES</b> .....	<b>xiv</b>
<b>LIST OF FIGURES</b> .....	<b>xv</b>
<b>LIST OF SYMBOLS AND ABBREVIATIONS</b> .....	<b>xxi</b>
<b>CHAPTERS</b> .....	<b>1</b>
<b>1. INTRODUCTION</b> .....	<b>1</b>
1.1 Animal Extracellular Matrix.....	1
1.1.1 Collagen .....	2
1.1.1.1 Type 1 Collagen .....	4
1.2 COL1A1 Gene.....	5
1.3 Insulin-like Growth Factor-I.....	5
1.3.1.Mitogen Activated Protein (MAP) Kinase Patway and PI3K/akt Patway... 6	
1.3.1.1 Insulin Receptor Substrate-1 .....	7
1.3.1.2 ERK ½ .....	7
1.4 Plants in Cosmetic Industry .....	7
1.4.1 <i>Achillea millefolium</i> .....	7
1.4.2 <i>Aesculus hippocastanum</i> .....	8
1.4.3 <i>Hyperricum perforatum</i> .....	8
1.4.4 <i>Primula vulgaris</i> .....	8
1.5 Aim of the Study .....	9
<b>2. MATERIALS AND METHODS</b> .....	<b>11</b>
2. 1. Materials .....	11
2.1.1 Cell Line .....	11
2.1.2 Plant Samples.....	11
2.2 Methods .....	12
2.2.1 Preparation of Plants .....	12
2.2.2 Extraction of Plants.....	12
2.2.3 Evaluation of Antioxidant Activity.....	13
2.2.3.1 Free Radical Scavenging Activity by DPPH Method .....	13

2.2.3.2. Free Radical Scavenging Activity by ABTS Method .....	13
2.2.3.3 Cuprac Assay.....	14
2.2.3.4 Determination of Total Phenolic Content .....	14
2.2.3.5 Determination of Total Flavonoids Content.....	155
2.2.4 Cell Culture .....	155
2.2.4.1 Cell Culture Conditions.....	155
2.2.4.2 Cell Thawing .....	16
2.2.4.3 Subculturing the Cell Lines.....	16
2.2.4.4 Cell Freezing .....	16
2.2.5 AlamarBlue Cell Viability Assay .....	17
2.2.5.1 Growth Curve of Cells .....	18
2.2.6 Determination of mRNA Expression.....	19
2.2.6.1 Isolation of Total RNA from Fibroblast Line .....	19
2.2.6.2 Determination of RNA Concentration .....	19
2.2.6.3 cDNA Synthesis .....	20
2.2.6.4 Quantitative Real-Time PCR .....	20
2.2.6.5 Qualification of qRT-PCR Products by Agarose Gel Electrophoresis	22
2.2.7 Protein Extraction .....	22
2.2.8 Determination of Protein Concentration .....	22
2.2.9 Determination of Protein Expression.....	23
2.2.9.1 Western Blotting .....	23
2.2.10 Fractionation of Crude Extract.....	26
<b>3. RESULTS.....</b>	<b>27</b>
3.1 EXTRACTION OF PLANT SAMPLES.....	27
3.2 Antioxidant Activity Determination.....	28
3.2.1 DPPH (2,2-diphenyl-1-picrylhydrazyl) Method.....	28
3.2.1.1 Determination of Antioxidant Capacities of <i>A. millefolium</i> , <i>H. perforatum</i> , <i>P. vulgaris</i> aerial parts and <i>A. hippocastanum</i> seed cotyledon Extracts by DPPH Method. ....	29
3.2.2. ABTS [2,2'-azinobis-(3-ethylbenzothiazoline-6-sulfonic acid)] Method	30
3.2.2.1 Determination of Free Radical Scavenging Capacities of <i>A. millefolium</i> , <i>H. perforatum</i> , <i>P. vulgaris</i> Aerial Parts and <i>A. hippocastanum</i> Seed Cotyledon Extracts by ABTS Method.....	31
3.2.3 CUPRAC ASSAY .....	32
3.2.3.1 Determination of Free Radical Scavenging Capacities of <i>A. millefolium</i> , <i>H. perforatum</i> , <i>P. vulgaris</i> Aerial Parts and <i>A. hippocastanum</i> Seed Cotyledon Extracts by CUPRAC Assay.....	33
3.2.4 Total Phenolic Content Determination. ....	34
3.2.4.1 Total Phenolic Content of <i>A. millefolium</i> , <i>H. perforatum</i> , <i>P. vulgaris</i> Aerial Parts and <i>A. hippocastanum</i> Seed Cotyledon Extracts.....	35
3.2.5 Total Flavonoids Content.....	36

3.3 Determination of Cell Viability (AlamarBlue <sup>®</sup> Assay).....	39
3.4 COL1A1 mRNA Expression in the Fibroblast Line .....	46
3.4.1 COL1A1 mRNA Expression in Fibroblast Line.....	46
3.5 Protein Concentrations of Lysates of the Treated and Non-Treated Cells.....	50
3.6 Protein Expression Analyze of COL1A1 in the Treated and Non-Treated Fibroblasts .....	51
3. 7 Fractionation of Crude Extract .....	54
3.8 Determination of Cell Viability (AlamarBlue <sup>®</sup> Assay of Chloroform, Etyhl Acetate and Water-Soluble Extracts) .....	57
3.9 COL1A1 mRNA Expression in the Fibroblast Line .....	61
3.10 Protein Expression Analysis of COL1A1 in the Treated and Non-Treated Fibroblasts .....	64
3.10.1 COL1A1 Protein Expression in Fibroblast Line.....	64
3.11 MAPK, IGF-I and IGF-IR mRNA Expressions in the Fibroblast Line .....	66
3.11.1 MAPK mRNA Expression in the Fibroblast Line .....	66
3.11.2 IGF-I mRNA Expression in the Fibroblast Line .....	69
3.11.3 IGF-IR mRNA Expression in the Fibroblast Line.....	72
3.12 Protein Concentrations of Lysates of the Treated and Non-Treated Cells.....	74
3.13 Protein Expression Analysis of ERK ½, p-ERK ½ IGF-I, IRS-1, p-IRS-1 in the Treated and Non-Treated Fibroblasts .....	75
3.13.1 ERK 1/2 Protein Expression in Fibroblast Line. ....	75
3.13.2 p-ERK 1/2 Protein Expression in Fibroblast Line.....	77
3.13.3 IGF-I Protein Expression in Fibroblast Line. ....	78
3.13.4 IRS-1 Protein Expression in Fibroblast Line.....	80
3.13.5 p-IRS-1 Protein Expression in Fibroblast Line.....	81
<b>4. DISCUSSION .....</b>	<b>83</b>
<b>5. CONCLUSION.....</b>	<b>91</b>
<b>REFERENCES .....</b>	<b>93</b>
<b>CURRICULUM VITAE.....</b>	<b>93</b>

## LIST OF TABLES

### TABLES

- Table 2.1** Collection localities and collection times of the studied plants
- Table 2.2** Molar extinction coefficients for alamarBlue at different wavelengths
- Table 2.3** Primer sequences, annealing temperatures and product sizes of the genes
- Table 3.1** Yield of crude extracts
- Table 3.2** DPPH scavenging activity of *A. millefolium*, *H. perforatum*, *P. vulgaris* aerial parts and *A. hippocastanum* seed cotyledon extracts. Activities were measured at 15<sup>th</sup> incubation period, at 517 nm, in percent versus concentrations (mg/mL)
- Table 3.3** Trolox equivalent anti-oxidant capacities (TEAC) of *A. millefolium*, *H. perforatum*, *P. vulgaris* aerial parts and *A. hippocastanum* seed cotyledon extracts
- Table 3.4** Trolox equivalent anti-oxidant capacities (TEAC) of *A. millefolium*, *H. perforatum*, *P. vulgaris* aerial parts and *A. hippocastanum* seed cotyledon extracts
- Table 3.5** Total phenolic content results of *A. millefolium*, *H. perforatum*, *P. vulgaris* aerial parts and *A. hippocastanum* seed cotyledon extracts
- Table 3.6** Comparison of selected anti-oxidant methods for *A. millefolium* aerial parts, *H. perforatum* aerial parts, *P. vulgaris* aerial parts and *A. hippocastanum* seed cotyledon
- Table 3.7** The method of Livak (A method to calculate relative mRNA expression)
- Table 3.8** Average protein concentrations of whole cell lysates of the cells
- Table 3.9** Summary of the mRNA and protein expression analysis of Col1A1 from plant extract treated cells relative to non-treated cells
- Table 3.10** Results of the mRNA and protein expression analysis of Col1A1 from plant fractionated extract treated cells relative to non-treated cells

## LIST OF FIGURES

### FIGURES

- Figure 1.1** Animal extracellular matrix (Mescher, 2013)
- Figure 1.2** Triple helix structure of collagen in detail (Berisio, 2002, Bella1994)  
(a) Structure of collagen (ProHypGly)<sub>4</sub>–(ProHypAla)–(ProHypGly)<sub>5</sub>  
(b) Triple helix with the three strands (space-filling, ball-and-stick, and ribbon representation). (c) Ball-and-stick image of a segment of collagen triple helix, showing hydrogen bonds. (d) Stagger of the three strands in the segment.
- Figure 1.3** Production steps of collagen fibrils in the endoplasmic reticulum (ER) of fibroblasts (Canty & Kadler, 2005).
- Figure 1.4** The structure of collagen, from the tropocollagen helix to the fiber (Alberts, 2008)
- Figure 1.5** Scheme of the IGF1R activation by its ligand (IGFs) and downstream signaling (Hematulin, 2010).
- Figure 2.1** Western blot sandwich.
- Figure 2.2** Solvent-solvent fractionation scheme of *Achillea millefolium* aerial parts crude methanol extract using different solvents of increasing polarity sequentially
- Figure 3.1** DPPH radical scavenging activity of *A. millefolium*, *H. perforatum*, *P. vulgaris* aerial parts and *A. hippocastanum* seed cotyledon extracts. Radical scavenging activities were measured at 15th incubation period, at 517 nm, in percent versus extract concentrations (mg/mL)
- Figure 3.2** Trolox standard curve to calculate Trolox equivalent anti-oxidant capacities of the extracts (at 734 nm). Each data were calculated by means of three independent experiments in triplicates.
- Figure 3.3** Trolox standard curve to calculate Trolox equivalent anti-oxidant capacities of the extracts (at 734 nm). Each data were calculated by means of three independent experiments in triplicates.

- Figure 3.4** Gallic acid standard curve. Each data was collected by means of three independent experiments in triplicates.
- Figure 3.5** Catechin standard curve.
- Figure 3.6** Fibroblast number and alamarBlue<sup>®</sup> fluorescence correlation (cell volume was adjusted to  $4 \times 10^4$  cells/wells)
- Figure 3.7** Growth curve of primary human dermal fibroblasts (ATCC: Catalog no. PCS-201-012)
- Figure 3.8** Fibroblasts were treated with increasing concentration of *A. hippocastanum* seed cotyledon extract. Fibroblasts were dosed for 48 h with extract then 3 hours with alamarBlue
- Figure 3.9** Fibroblasts were treated with increasing concentration of *Achillea millefolium* aerial parts extract. Fibroblasts were dosed for 48 h with extract then 3 hours with alamarBlue.
- Figure 3.10** Fibroblasts were treated with increasing concentration of *Primula vulgaris* aerial parts extract. Fibroblasts were dosed for 48 h with extract then 3 hours with alamarBlue
- Figure 3.11** Fibroblasts were treated with increasing concentration of *H. Perforatum* aerial parts extract. Fibroblasts were dosed for 48 h with extract then 3 hours with alamarBlue<sup>®</sup>.
- Figure 3.12** Fibroblasts treated with increasing concentration of *Aesculus hippocastanum* seed cotyledon extract. Fibroblasts were dosed for 48 h with extract then 3 hours with alamarBlue<sup>®</sup>.
- Figure 3.13** Fibroblasts treated with increasing concentration of *Achillea millefolium* aerial parts extract. Fibroblasts were dosed for 48 h with extract then 3 hours with alamarBlue<sup>®</sup>.
- Figure 3.14** Fibroblasts treated with increasing concentration of *P. Vulgaris* aerial parts extract. Fibroblasts were dosed for 48 h with extract then with alamarBlue<sup>®</sup>.
- Figure 3.15** Fibroblasts treated with increasing concentration of *H. Perforatum* aerial parts extract. Fibroblasts were dosed for 48 h with extract then 3 hours with alamarBlue<sup>®</sup>.

- Figure 3.16** Standard curves generated from serial dilutions of control cDNA to calculate quantities of COL1A1 mRNAs in the treated and non treated fibroblast line
- Figure 3.17** Amplification curve showing the accumulation of fluorescence emission at each reaction cycle
- Figure 3.18** Melting curve showing the fluorescence emission change versus temperature. Detection of single peak means single PCR product (Annealing Temp. is 60°C)
- Figure 3.19** Comparison of COL1A1 mRNA expression of treated and non-treated fibroblast line (Data was evaluated with student t-test \*\*\* $p < 0.0001$ )
- Figure 3.20** Immunoreactive protein bands of cell lines representing COL1A1 and  $\alpha$ -tubulin used as internal standard.
- Figure 3.21** Comparison of COL1A1 protein expressions of treated and non-treated fibroblast lines. The band quantifications are expressed as mean  $\pm$  SD of the relative intensity of three independent experiments (Data was evaluated with student t-test. \*\*\* $p < 0.0001$ , \*\* $p = 0.0081$ )
- Figure 3.22** Solvent – solvent fractionation scheme of *A. millefolium* aerial parts crude methanol extract using different solvents of increasing polarity sequentially.
- Figure 3.23** Solvent – solvent fractionation scheme of *P. vulgaris* aerial parts crude methanol extract using different solvents of increasing polarity sequentially.
- Figure 3.24** Fibroblasts were treated with increasing concentration of *Primula vulgaris* aerial parts chloroform extract. Fibroblasts were dosed for 48 h with extract then 3 hours with alamarBlue.
- Figure 3.25** Fibroblasts were treated with increasing concentration of *Primula vulgaris* aerial parts ethyl acetate extract. Fibroblasts were dosed for 48 h with extract then 3 hours with alamarBlue<sup>®</sup>.
- Figure 3.26** Fibroblasts were treated with increasing concentration of *Primula vulgaris* aerial parts water-soluble extract. Fibroblasts were dosed for 48 h with extract then 3 hours with alamarBlue<sup>®</sup>.

- Figure 3.27** Fibroblasts were treated with increasing concentration of *Achillea millefolium* aerial parts chloroform extract. Fibroblasts were dosed for 48 h with extract then 3 hours with alamarBlue<sup>®</sup>.
- Figure 3.28** Fibroblasts were treated with increasing concentration of *Achillea millefolium* aerial parts ethyl acetate extract. Fibroblasts were dosed for 48 h with extract then 3 hours with alamarBlue<sup>®</sup>.
- Figure 3.29** Fibroblasts were treated with increasing concentration of *Achillea millefolium* aerial parts water-soluble extract. Fibroblasts were dosed for 48 h with extract then 3 hours with alamarBlue<sup>®</sup>.
- Figure 3.30** Standard curve generated from serial dilutions of control cDNA to calculate quantities of COL1A1 mRNAs in the treated and non-treated fibroblast line
- Figure 3.31** Amplification curve showing the accumulation of fluorescence emission at each reaction cycle
- Figure 3.32** Melting curve showing the fluorescence emission change versus temperature. Detection of single peak means single PCR product (Annealing Temp. is 60°C).
- Figure 3.33** Comparison of COL1A1 mRNA expression of treated and non-treated fibroblast line (Data was evaluated with student t-test \*\*\*p<0,0001, \*\*p=0,0044).
- Figure 3.34** Immunoreactive protein bands of cell lines representing COL1A1 and β-actin used as internal standard.
- Figure 3.35** Comparison of COL1A1 protein expressions of treated and non-treated fibroblast lines. The band quantifications are expressed as mean ± SD of the relative intensity of three independent experiments (Data was evaluated with student t-test \*\*\*p=0,0009).
- Figure 3.36** Standard curves generated from serial dilutions of control cDNA to calculate quantities of MAPK mRNAs in the treated and non treated fibroblast line.
- Figure 3.37** Amplification curve showing the accumulation of fluorescence emission at each reaction cycle.

- Figure 3.38** Melting curve showing the fluorescence emission change versus temperature. Detection of single peak means single PCR product (Annealing Temp. is 60°C).
- Figure 3.39** Comparison of MAPK mRNA expression of treated and non-treated fibroblast line (Data was evaluated with student t-test \*\*\*p<0,0001, \*\*p=0,0026).
- Figure 3.40** Standard curves generated from serial dilutions of control cDNA to calculate quantities of IGF1 mRNAs in the treated and non treated fibroblast line.
- Figure 3.41** Amplification curve showing the accumulation of fluorescence at each reaction cycle.
- Figure 3.42** Melting curve showing the fluorescence emission change versus temperature. Detection of single peak means single PCR product (Annealing Temp. is 62°C).
- Figure 3.43** Comparison of IGF-I mRNA expression of treated and non-treated fibroblast line (Data was evaluated with student t-test \*\*\*p<0,0001)
- Figure 3.44** Standard curve generated from serial dilutions of control cDNA to calculate quantities of IGF-IR mRNAs in the treated and non treated fibroblast line.
- Figure 3.45** Amplification curve showing the accumulation of fluorescence at each reaction cycle.
- Figure 3.46** Melting curve showing the fluorescence emission change versus temperature. Detection of single peak means single PCR product (Annealing Temp. is 62°C)
- Figure 3.47** Comparison of IGF-IR mRNA expression of treated and non-treated fibroblast line (Data was evaluated with student t-test \*\*\*p<0,0001)
- Figure 3.48** Immunoreactive protein bands of cell lines representing ERK ½ and alpha tubulin used as internal standard
- Figure 3.49** Comparison of ERK ½ protein expressions of treated and non-treated fibroblast lines. The band quantifications are expressed as mean ± SD of the relative intensity of three independent experiments (Data

was evaluated with student t-test \*\*\*p<0,0001, \*\*p=0,0015, \*p>0,0189)

**Figure 3.50** Immunoreactive protein bands of cell lines representing p-ERK ½ and alpha tubulin used as internal standard.

**Figure 3.51** Comparison of p-ERK ½ protein expressions of treated and non-treated fibroblast lines. The band quantifications are expressed as mean ± SD of the relative intensity of three independent experiments (Data was evaluated with student t-test \*\*p=0,0015, \*p=0,01)

**Figure 3.52** Immunoreactive protein bands of cell lines representing IGF1 and alpha tubulin used as internal standard.

**Figure 3.53** Comparison of IGF-1 protein expressions of treated and non-treated fibroblast lines. The band quantifications are expressed as mean ± SD of the relative intensity of three independent experiments (Data was evaluated with student t-test \*\*p=0,0015, \*p<0,05).

**Figure 3.54** Immunoreactive protein bands of cell lines representing IRS-I and alpha tubulin used as internal standard.

**Figure 3.55** Comparison of IRS-1 protein expressions of treated and non-treated fibroblast lines. The band quantifications are expressed as mean ± SD of the relative intensity of three independent experiments (Data was evaluated with student t-test \*\*\*p<0,0001, \*\*p=0,0015, \*p>0,0189).

**Figure 3.56** Immunoreactive protein bands of cell lines representing p-IRS-I and alpha tubulin used as internal standard

**Figure 3.57** Comparison of p-IRS-1 protein expressions of treated and non-treated fibroblast lines. The band quantifications are expressed as mean ± SD of the relative intensity of three independent experiments (Data was evaluated with student t-test \*\*\*p<0,0001)

## LIST OF SYMBOLS AND ABBREVIATIONS

<b>ABTS</b>	2,2'-azinobis-(3-ethylbenzothiazoline-6-sulfonic acid)
<b>ATCC</b>	American Type Culture Collection
<b>BCIP</b>	5-bromo 4-chloro 3-indoyl phosphate
<b>BSA</b>	Bovine serum albumin
<b>BCA</b>	Bicinchoninic acid
<b>cDNA</b>	Complementary DNA
<b>CE</b>	Crude extracts
<b>Ct</b>	Threshold cycle
<b>CTFA</b>	Cosmetic, Toiletry and Fragrance Association
<b>DEPC</b>	Diethylpyrocarbonate
<b>DMSO</b>	Dimethyl sulfoxide
<b>DMEM</b>	Dulbecco's modified Eagle's medium
<b>DNA</b>	Deoxyribonucleic acid
<b>DPPH</b>	2,2-diphenyl-1-picrylhydrazyl
<b>EC50</b>	50% effective concentration
<b>ECM</b>	Extracellular matrix
<b>EDTA</b>	Ethylenediaminetetraacetic acid
<b>ERB</b>	Electronic running buffer
<b>FBS</b>	Fetal bovine serum

<b>FDA</b>	Food and Drug Administration
<b>GAE</b>	Equivalents of gallic acid
<b>GAPDH</b>	Glyceraldehydes 3-phosphate dehydrogenase
<b>IGF</b>	Insulin-like growth factor
<b>IL</b>	Interleukin
<b>IRS</b>	Insulin receptor substrate-1
<b>kDa</b>	kilo Dalton
<b>LA</b>	Lipoic acid
<b>MAP</b>	Mitogenactivated protein
<b>mRNA</b>	Messenger RNA
<b>MMPs</b>	Matrix metalloproteinases
<b>NBT</b>	Nitrotetrazolium blue chloride
<b>Nfr2</b>	Nuclear factor erythroid 2-related factor 2
<b>NTC</b>	No template control
<b>OD</b>	Optical density
<b>PBS</b>	Phosphate buffered saline
<b>PCR</b>	Polymerase chain reaction
<b>Pen-Strep</b>	Penicillin-Streptomycin
<b>PH</b>	Pleckstrin homology
<b>PMSF</b>	Phenylmethylsulfonyl fluoride
<b>PVDF</b>	Polyvinylidene difluoride
<b>qPCR</b>	Quantitative polymerase chain reaction

<b>qRT-PCR</b>	Quantitative real time polymerase chain reaction
<b>RIPA</b>	Radioimmunoprecipitation assay
<b>rpm</b>	Revolutions per minute
<b>RNA</b>	Ribonucleic acid
<b>SDS</b>	Sodium dodecyl sulfate
<b>SDS-PAGE</b>	Sodium dodecyl sulfate-polyacrylamide gel electrophoresis
<b>TBE</b>	Tris – Borate - EDTA
<b>TBST</b>	Tris-buffered saline and tween 20
<b>TEAC</b>	Trolox equivalent antioxidant capacity
<b>TEMED</b>	Tetramethylethylenediamine
<b>TF</b>	Total flavonoid
<b>TGF</b>	Transforming growth factor
<b>TP</b>	Total phenol



# CHAPTER 1

## INTRODUCTION

### 1.1 Animal Extracellular Matrix

Animal extracellular matrix (ECM) is a collection of extracellular molecules secreted by fibroblasts helps maintain healthy skin. It is composed largely of proteoglycans and glycoproteins which are able to bind on other glycoproteins making the matrix a highly crosslinked gel.

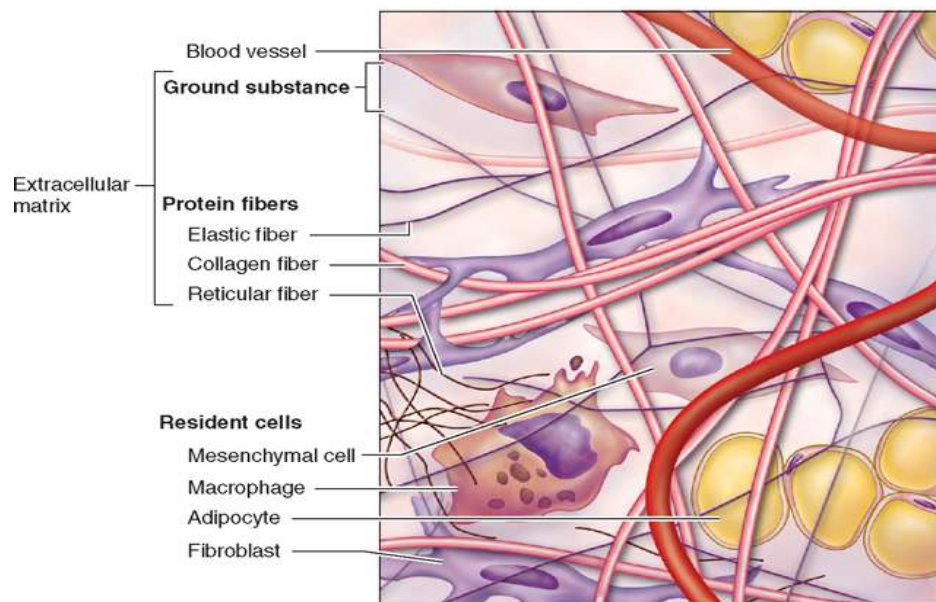


**Figure 1.1** Animal extracellular matrix (Mescher, 2013)

Although ECM is accounted for by a few dominant types of molecule, there are approximately a hundred known ECM components. These dominant molecule types are, collagens, elastin, fibrillins, fibronectins, hydroxyapatite, laminins, matrix metalloproteinases (MMPs) and nidogen. ECM provides a healthy functional condition for skin; it is composed mainly of collagen (Teli,1992).

### 1.1.1 Collagen

Collagens have a large family with nineteen related glycoproteins. They possess triple helix structure and a tight right-handed helix of three collagen chains. Also, these chains have left-handed helix structure. In order to triple helix formation occur, every third amino acid must face to the helix center with little space. This condition can only be obtained with glycine amino acid, which is the smallest one.

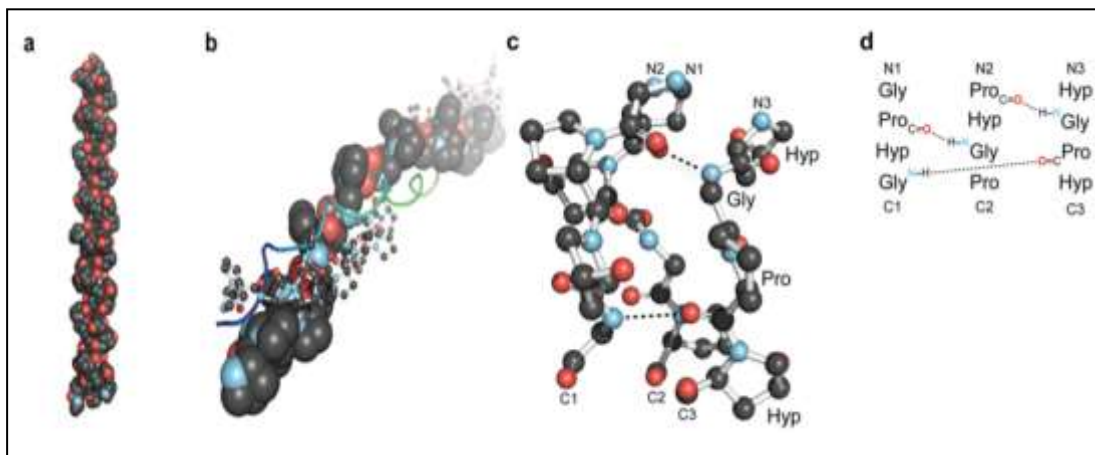


**Figure 1.2** Triple helix structure of collagen in detail (Berisio, 2002, Bella1994) (a) Structure of collagen (ProHypGly)<sub>4</sub>–(ProHypAla)–(ProHypGly)<sub>5</sub> (b) Triple helix with the three strands (space-filling, ball-and-stick, and ribbon representation). (c) Ball-and-stick image of a segment of collagen triple helix, showing hydrogen bonds. (d) Stagger of the three strands in the segment.

There are many types of collagens which are from collagen I to collagen XIX. In normal skin contain collagen type I mostly with approximately 90% of its dry weight (Nigel, 2005). Collagen precursors are synthesized in the endoplasmic reticulum (ER) of the cell and transported to the Golgi apparatus in order to secrete into the extracellular spaces and mature form of collagen can be occurred (Orgel, 2011).

According to Mays (1998) and Mehta (2007), decreases in the amount of the extracellular matrix triggers skin aging. With the aid of this information, providing to increase in collagen synthesis can be effective against skin aging. Insulin-like growth factor-I (IGF-I) has role in many biologic pathway and its structure is %49 homologous to pro-insulin (Baserga, 1997 & Schmid, 1995).

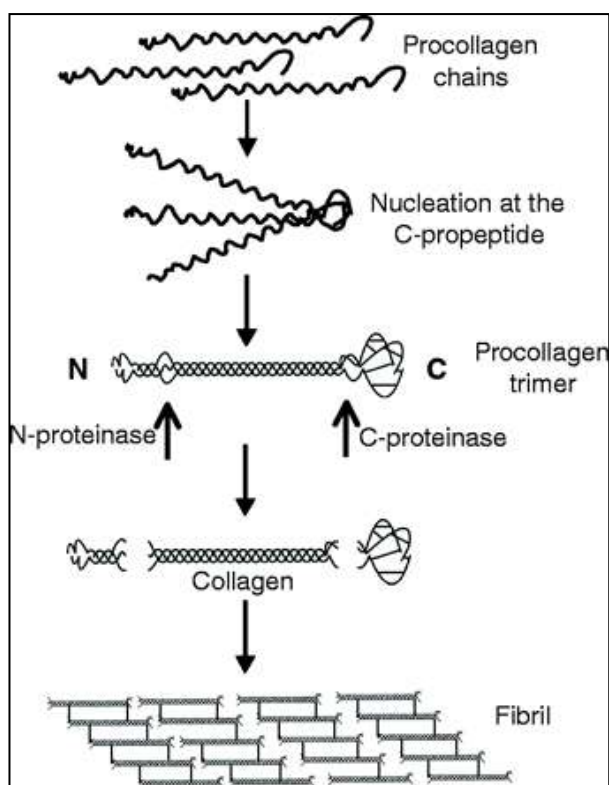


**Figure 1.3** Production steps of collagen fibrils in the endoplasmic reticulum (ER) of fibroblasts (Canty & Kadler, 2005).

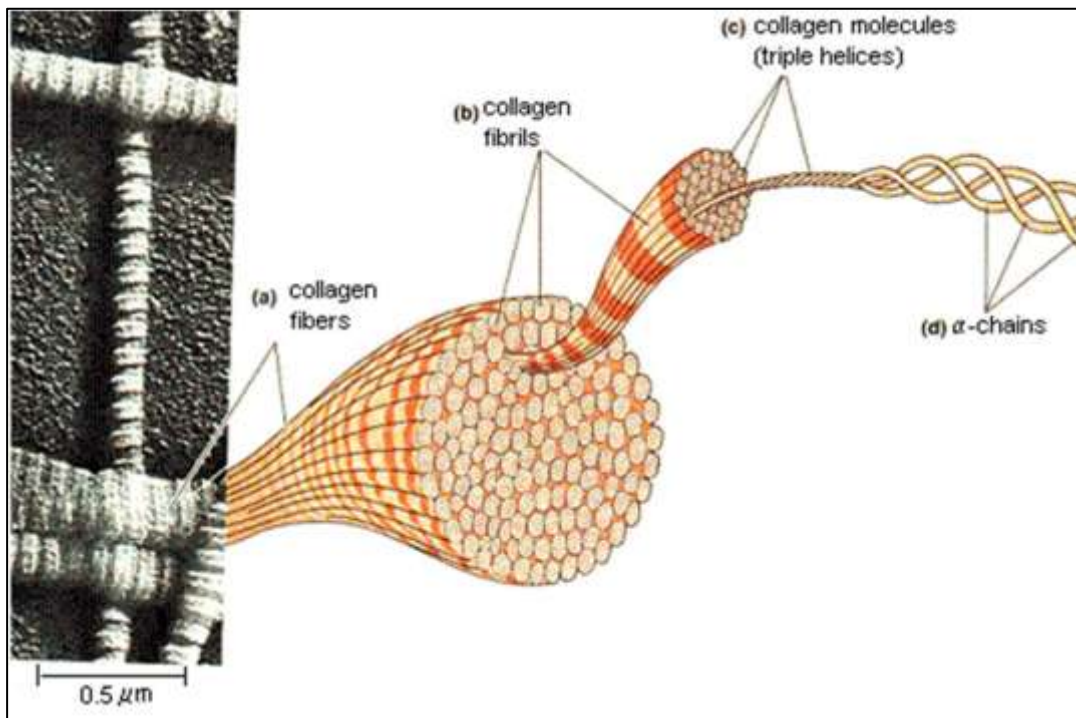


**Figure 1.4** The structure of collagen, from the tropocollagen helix to the fiber (Alberts, 1995).

### 1.1.1.1 Type 1 Collagen

Type I collagen is the main structural component of extracellular matrix. It consists of one  $\alpha 2$  chain and two  $\alpha 1$  chains, which are encoded on chromosome 7 and 17 in humans (Prockop, 1979). Pro-collagen chains are assembled into fibrils and then into fibres. These fibres can be degraded only by a few specific metalloproteases (Prockop, 1984). Although, type I collagen is the main structural protein, its abnormal accumulation causes fibrotic diseases.

Osteoblasts, fibroblasts and odontoblasts are the cell types which are responsible for type I collagen synthesis (Rossert, 1995, Bou-Gharios, 1996). In vitro studies using those discrete cell types have shown that biosynthesis of collagen can be triggered by different molecules. Type I collagen biosynthesis can be modulated by cytokines,

growth factors, vasoactive peptides or other molecules such as lipid peroxidation products in fibroblasts (Rossert, 1996).

## **1.2 COL1A1 Gene**

Type I collagen is composed of triple helix, has three chains (one  $\alpha 2$  and two  $\alpha 1$ ) (Malone, 2004). This is an extracellular matrices protein expressed in fibrils of tendon, ligaments and bones. COL1A1 consists of 1464 amino acids with an approximate molecular weight of 136514 Da and contains 1 VWFC domain .The gene of this protein contains 51 exons that spans 1754 kb and maps to 17q21.33. Promoter activity of COL1A1 is sensitive to DNA methylation and the COL1A1 gene is methylated in cancer cells with decreased collagen expression levels (Sengupta, 2005). Mutations in this gene are associated with some diseases such as idiopathic osteoporosis, osteogenesis imperfect and Ehlers-Danlos syndrome (Kuivaniemi, 1991). TGF-beta (transforming growth factor beta) stimulates protein complex formation on a TAE (TGF-beta response element) found in the distal portion (-1624) of the COL1A1 promoter (Sun, 2001). COL1A1 and Platelet-derived growth factor (PDGF) fusion is characteristic of a disease named dermatofibrosarcoma protuberans (Shimizu, 1999).

Thrombin has a crucial role in the coagulation of blood and it acts as a serine protease. It stimulates COL1A1 mRNA production and works during normal wound healing by triggering procollagen production in fibroblasts (Chambers, 1998). Biosynthesis of type 1 collagen increases by the effect of Insulin-like growth factor-I (IGF-I) in dermal fibroblasts (Gillery, 1992, Svegliati-Baroni, 1999).

## **1.3 Insulin-like Growth Factor-I**

In many cell systems, IGF-I signaling pathways have been well documented (Butler, 1998) these pathways activated include the phosphoinositide 3-kinase (PI3K) and mitogenactivated protein kinase (MAPK) pathways (Werner, 2000) and the major growth factor increases biosynthesis of type 1 collagen in dermal fibroblasts is IGF-1 (Gillery, 1992)

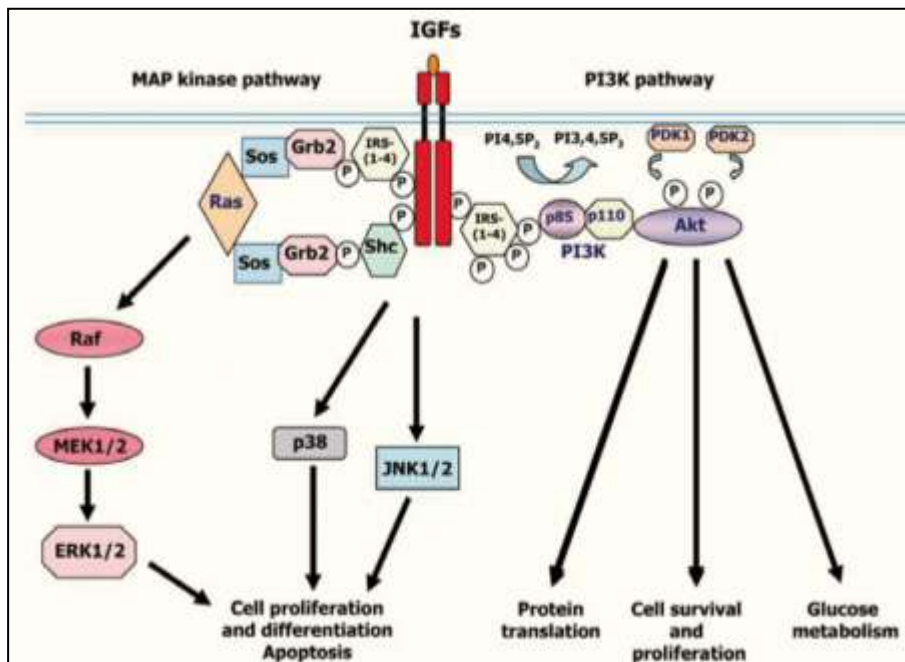


**Figure 1.5** Scheme of the IGF1R activation by its ligand (IGFs) and downstream signaling (Hematulin, 2010).

### 1.3.1. Mitogen Activated Protein (MAP) Kinase Pathway and PI3K/Akt Pathway

Several studies (Scheid et al., 1999) have shown that MAPK and PI-3K/Akt pathways are play critical role in cell survival (Bonni et al., 1999; Fang et al., 1999). In addition to cell survival, the MAP kinase pathway is involved in differentiation, proliferation, apoptosis and the PI3K/Akt pathway is involved in glucose metabolism, protein translation and proliferation (Lavan, 1997; Laron 2001).

### **1.3.1.1 Insulin Receptor Substrate-1**

Insulin receptor substrate-1 (IRS-1) has a critical role in transmitting signals from the insulin receptor and insulin-like growth factor-1 receptor to the PI3K/Akt and MAP kinase pathways (Sun, 1991). Extracellular ligand binding phosphorylates the tyrosine residue of insulin receptor or IGF-1 receptor, phosphorylation induces the binding of IRS-1 to these receptors in the cytoplasm. IRS-1 plays important biological function for many pathways (Xux, 2008).

### **1.3.1.2 ERK ½**

One of the important signaling pathways in IGF1 receptor activation is the MAPK pathway (Hematulin, 2010). In this pathway's downstream signaling the serine/threonine kinase ERK is the main component (Chambard, 2007). It controls cell cycle and fate decisions by regulating transcription and translation (Chambard, 2007; Meloche, 2007). The inactivation of ERK1/2 prevents proliferation in mammals (Li, 2006).

## **1.4 Plants in Cosmetic Industry**

Use of collagen stimulating cosmetic products can reverse aging process. There have been many herbal products developed to repair the aging defects. These herbal products were build up based on the information from past to present and still continues to expand rapidly across the world. In addition to the benefits, some of those manufactured herbal products have the adverse effects as a result of unscientific production (Dweck, 1996; Marks, 1997). *Hypericum perforatum*, *Primula vulgaris*, *Achillea millefolium*, *Aesculus hippocastanum* were selected from effective and simple herbal face masks recipes.

### **1.4.1 *Achillea millefolium***

*Achillea millefolium* is a member of the Asteraceae family. It is commonly known as yarrow (Simonetti, 1990). *A. millefolium* extract is known as a biological cosmetic

additive. 65 cosmetic products were submitted to the FDA as using extract of *A. millefolium* as a cosmetic ingredient (FDA 1998).

#### **1.4.2 *Aesculus hippocastanum***

*A. hippocastanum*, commonly known as horse-chestnut, is a large deciduous tree (BSBI List, 2007). Horse chestnut extract contains a saponin called escin and it is a good remedy to treat different parts of the body (Proserpio, 1980). It has been used as a cosmetic ingredient in many commercial products, including toothpastes and lotions (Leung, 2014). It has been shown that *A. hippocastanum* extract is very effective in reducing the effects of active oxygen species. Since there is a link between dermal aging and active oxygen species, *A. hippocastanum* can be used as a cosmetic ingredient (Masaki, 1995).

#### **1.4.3 *Hypericum perforatum***

*Hypericum perforatum*, commonly known as Perforate St John's-wort (Wölflle, 2014; Klemow, 2011) is a medicinal plant described for the treating wounds, psychological disorders and diseases of the alimentary tract (Butterweck, 2003; Maisenbacher and Kovar, 1992). Extract of this plant (*Hypericum perforatum* L.) is also used in cosmetic products but little research has been done about cosmetic formulations.

#### **1.4.4 *Primula vulgaris***

*Primula vulgaris*, known as primrose is an aerial partsing plant. It is native to Western and southern parts of Europe, southwest part of Asia and northwest part of Africa (Mabey, 1996). People have become more interested in primrose in recent years as it has different areas to be applied especially within the food and cosmetic world (Demir, 2014).

## 1.5 Aim of the Study

It is previously reported that the use of products that stimulate cells to produce collagen can reverse aging process of the skin. There are many herbal products developed to repair the emergence of aging defects. These herbal products are based on information from past to present and continues to expand rapidly across the world. In addition to the benefits, manufactured products from these plants have adverse effects as a result of incorrect uses. Consequently, the aim of this study is to search for plants which trigger type I collagen biosynthesis using human dermal fibroblasts.

*In-vitro* experiment steps were planned for the plants which were selected from effective and simple herbal face masks recipes. It has been known that free radicals have important roles in living organisms. They can cause many diseases and also can lead to skin aging therefore anti-oxidants play critical roles in skin aging to make comparison antioxidant capacities were evaluated. Then, cell culture experiments were started. Human fibroblasts were exposed to the extracts and the effects of each extract were investigated. For this purpose, the levels of pro-type 1 collagen was calculated by qPCR and westernblot analysis. Among these extracts, the extracts, which have the highest induction rates were focused and fractionated. This time fractions and crude extracts were investigated on type 1 collagen expression level.

It is reported in a previous study, thioctic acid mimics transforming growth factor- $\beta$  and triggers collagen biosynthesis in dermal fibroblasts (Tsuji, 2010). But little work has been done to understand mimicking effects of other natural plant extracts on collagen biosynthesis. Furthermore, fractions of active plants were searched, and revealed if they could trigger the IGF-I signaling pathway.



## CHAPTER 2

### MATERIALS AND METHODS

#### 2. 1. Materials

##### 2.1.1 Cell Line

In this study, *in-vitro* experiment steps were planned to search for anti-aging effects of various plants using human dermal fibroblasts. Human dermal fibroblast line PCS-201-012 was purchased from ATCC (Manassas, VA) and cells were used at passage 2-5 in the laboratory.

##### 2.1.2 Plant Samples

Plants were (*Hypericum perforatum*, *Primula vulgaris*, *Achillea millefolium*, *Aesculus hippocastanum*) selected from effective and simple herbal face masks recipes which have anti-aging benefits. Seed samples from *A. hippocastanum* and aerial part samples from *H. perforatum*, *P. vulgaris*, *A. millefolium* were identified by Prof. Dr. Musa Doğan from Biology Dept., METU. Collected from Turkey with the approval number (42353) taken from ministry of forestry and water affairs in their appropriate seasons and the specimens were deposited in the Department of Chemistry, METU. The plant specimens with their localities and the necessary field records were written and enumerated.

**Table 2.1** Collection localities and collection times of the studied plants

TAXON	COLLECTION LOCALITY	COLLECTION TIME
<i>A. millefolium</i>	Ankara: Mountain steppe, entrance of Kızılcahamam, Turkey.	24.06.2013 – 01.07.2013
<i>A. hippocastanum</i>	Ankara: Middle East Technical University, Turkey.	01.09.2013-15.10.2013
<i>H. perforatum</i>	Muğla: Surrounding of Milas, Kazıklı Village, Turkey.	20.07.2013-30.07.2013
<i>P. vulgaris</i>	Ankara: Kızılcahamam, Işık Mountain, Turkey.	01.04.2013-15.05.2013

## 2.2 Methods

### 2.2.1 Preparation of Plants

Plants were pressed, dried according to herbarium techniques and identified in accordance with the Flora of Turkey (Davis, 1965-1988).

### 2.2.2 Extraction of Plants

Seeds of *A. hippocastanum* and aerial parts of *H. perforatum*, *P. vulgaris*, *A. millefolium* were collected and extracted in 1:6 ratio of methanol for 24 hours rotational incubator at 25°C temperature. Mixtures filtered through a rough filter paper and solvents of filtrate were evaporated with help of evaporator (Heidolph Laborota 4000) at 25 °C until drying. Dried extracts were weighted out the percent yield of extraction was calculated. The resulting extracts were dissolved in suitable solvents for further studies. All samples were kept at 4°C until use.

## 2.2.3 Evaluation of Antioxidant Activity

### 2.2.3.1 Free Radical Scavenging Activity by DPPH Method

The stable 2, 2-diphenyl-1-picrylhydrazyl (DPPH) radical scavenging activity was determined by the method of Blois (Blois, 1958). This assay is often used to evaluate the antioxidant ability of plant extracts. DPPH, a stable radical with purple color, changes into a stable yellow compound (diphenyl-picrylhydrazine) on reacting with an antioxidant. DPPH scavenging activities of seeds of *A. hippocastanum* and aerial parts of *H. perforatum*, *P. vulgaris*, *A. millefolium* were assessed by using IC<sub>50</sub> values. A low IC<sub>50</sub> value indicates strong antioxidant activity. A suitable antioxidant such as gallic acid was employed as the reference.

For this purpose 0.1ml dry extracts were dissolved in ethanol and were mixed with 1.4 ml DPPH solution ( $1.5 \times 10^{-4}$  M). With this process a series of extract solutions with varying concentrations were prepared. Then the absorbances of the solutions (at 517 nm) were recorded after 30 min of incubation at room temperature.

Inhibition of DPPH in percent (I%) was calculated as given below:

$$\text{DPPH radical scavenging (\%)} = [(A_0 - A_1)] / A_0 \times 100$$

Where A<sub>0</sub> is the absorbance of the control reaction (containing all reagents except the test sample), and A<sub>1</sub> is the absorbance of the extracts/reference. Analyses were run in triplicates and 50 % effective concentration (EC<sub>50</sub>) values were calculated after constructing the percent radical scavenging versus extract concentration plots.

### 2.2.3.2. Free Radical Scavenging Activity by ABTS Method

The ability of the dry extracts to scavenge ABTS•+ radical cation were compared to Trolox standard. The ABTS•+ radical cation was pregenerated by mixing 7 mM ABTS stock solution with 2.45 mM potassium persulfate (final concentration) and incubated for 12–16 h in the dark at room temperature until the reaction completed and the absorbance is stable. The absorbance of the ABTS•+ solution was equilibrated to 0.70 (± 0.02) by diluting with water at room temperature, then 1 ml

was mixed with 100  $\mu\text{l}$  of the test sample ( $0.05^{-10}$  mg/ml) and the absorbance was measured at 734 nm after 6 min. All experiments were repeated six times. The decrease in absorbance caused by the addition of sample was compared with that of a standard curve by use of Trolox (20-200  $\mu\text{mol/L}$ ) (Hazra, 2008).

### **2.2.3.3 Cuprac Assay**

$\text{CuCl}_2$  solution,  $1.0 \times 10^{-2}$  M, was prepared by dissolving 0.17 g  $\text{CuCl}_2 \cdot 2\text{H}_2\text{O}$  in water, and diluting to 100 mL. Ammonium acetate buffer at pH 7.0, 1.0 M, was prepared by dissolving 19.27 g  $\text{NH}_4\text{Ac}$  in water and diluting to 250 mL. Neocuproine (Nc) solution,  $7.5 \times 10^{-3}$  M, was prepared daily by dissolving 0.039 g Nc in 96% ethanol. 50  $\mu\text{l}$   $\text{CuCl}_2$  solution ( $10^{-2}$  M), 50  $\mu\text{l}$  neocuproine alcoholic solution ( $7.5 \times 10^{-3}$  M) and 50  $\mu\text{l}$   $\text{NH}_4\text{Ac}$  buffer solution, 27,5  $\mu\text{l}$  sample and 27,5  $\mu\text{l}$  water were added to wells. The mixture mixed well and incubated the microwell strips at room temperature ( $18^\circ$  to  $25^\circ\text{C}$ ) for about 30 min. in dark. Absorbance was measured against a reagent blank at 450 nm. Since the molar absorptivity of Trolox in the CUPRAC method is  $\epsilon = 1.66 \times 10^4$  l/mol/cm, and the calibration curve for Trolox is a line passing through the origin, the Trolox equivalent molar concentration of the herbal extract sample in the final solution may be found by dividing the observed absorbance by the  $\epsilon$  for Trolox.

The Trolox equivalent antioxidant capacity may be traced back to the original extract considering all dilutions, and proportionated to the initial mass of herbal material taken to find a capacity in the units of  $\mu\text{mol TR/g}$  dry matter (Apak, 2004).

### **2.2.3.4 Determination of Total Phenolic Content**

Total concentrations of phenolic compounds in extracts were determined as the method of Singleton and Rossi (Singleton and Rossi 1965) with some modifications. A number of dilutions of gallic acid were obtained to prepare a calibration curve. 100 $\mu\text{l}$  extracts and gallic acid dilutions were mixed with 100 $\mu\text{l}$  of 50 % Folin–Ciocalteu’s reagent and incubated for 5 minutes, then 2% sodium carbonate ( $\text{Na}_2\text{CO}_3$ ) solution was added. The tubes were then vortexed and incubated at room

temperature for 30 min. At the end of the 30 minutes of incubation period, absorbances of each mixture were monitored at 750 nm and blanks were subtracted using ethanol at the same wavelength. All tests were performed six times. The phenolic content was evaluated from a gallic acid standard curve. Results were recorded as milligrams of total phenolics contained in milligrams of extract as the gallic acid equivalents (GAE).

#### **2.2.3.5 Determination of Total Flavonoids Content**

Determination of total flavonoid content was done as slightly modified version which described by Zhishen et al. (1999). 0.2 mL various concentrations of rutin as standard was diluted with water and 0.075 mL 5% NaNO<sub>2</sub> was added. Then after 5 minutes 0.15 mL of 10% AlCl<sub>3</sub> was added. 6 minutes later 0.5 mL 1 M NaOH was added and solution made up to 3 mL with water. The solution mixed well and the absorbance measured against blank solution at 510 nm immediately.

Same procedure applied for extract solutions. Calibration curves of the standard and extracts were plotted as absorbance at 510 nm against concentration. Then total flavonoid content was calculated as catechin equivalent from catechin standard curve equation  $y=mx+n$ .

#### **2.2.4 Cell Culture**

##### **2.2.4.1 Cell Culture Conditions**

Primary human dermal fibroblasts (ATCC: catalog no. PCS-201-012) were cultured in Dulbecco's modified Eagle's medium (DMEM) containing final concentrations of 10% fetal bovine serum (FBS) and 1% penicillin-streptomycin (Pen-Strep) solution according to the vendor's instruction. Cultures were incubated at 37 °C with 5% carbon dioxide (CO<sub>2</sub>) and 95% humidity in EC 160 NÜVE incubator. The cell culture studies were carried out in NÜVE MN 090 Class II Safety Cabinet. The growth media of culture were renewed in 2-3 days for appropriate growth conditions.

#### **2.2.4.2 Cell Thawing**

Before thawing the cells, 13 mL of pre-warmed growth medium was transferred into T75 cell culture flasks. After that, cryotubes were taken from the liquid nitrogen and the cells were defrosted at 37°C water bath and immediately transferred to T75 cell culture flask containing growth medium. Cells were incubated in CO<sub>2</sub> incubator at 37°C. After 24 hours, medium was renewed to eliminate dimethylsulfoxide (DMSO) and placed in CO<sub>2</sub> incubator.

#### **2.2.4.3 Subculturing the Cell Lines**

After cells were 80% confluent in the T75 flask, the medium was removed and cells were washed with 10 mL of 10 mM Ca<sup>+2</sup>, Mg<sup>+2</sup> free phosphate buffered saline (PBS). 1:4 split of cell line was performed by adding 2 ml of prewarmed trypsin to flask and placing the T75 flask in 37°C until cells were detached and 6 mL of growth medium was added to the flask to inactivate the trypsin and the 2 ml of this mixture was transferred into new T75 flask. Then 10 mL of growth medium was added to new T75 flask and the culture was placed in 37°C, CO<sub>2</sub> incubator. This procedure was repeated in every 3-4 days.

#### **2.2.4.4 Cell Freezing**

After cells were 80% confluent in the T75 flask, the medium was removed and cells were washed with 10 mL of PBS. 2 mL of pre-warmed trypsin was added to flask and placed in 37°C, CO<sub>2</sub> incubator for 5 minutes. After all the cells were detached, 2 mL of growth medium was added into the flask to inactivate the trypsin. The cells in the flask with trypsin and growth medium were transferred into an 15 mL centrifuge tube and centrifuged at 400 x g for 5 minutes at room temperature. After centrifugation, supernatant was discarded and pellet was resuspended in 1 ml growth medium by pipetting. Then the cell suspension was transferred to cryotube and 100 µl DMSO was added as cryoprotectant. Cryotube was immediately placed in the -80°C freezer and after two hour it was transferred to liquid nitrogen tank for longer term storage.

### 2.2.5 AlamarBlue<sup>®</sup> Cell Viability Assay

The alamarBlue<sup>®</sup> assay, a fluorometric indicator of cellular metabolic activity, was obtained from Invitrogen (Lot: 156603SA). The alamarBlue<sup>®</sup> assay is a proprietary assay designed to quantify cell proliferation, cytotoxicity and viability. For experimental use, the alamarBlue<sup>®</sup> was diluted into the culture medium without serum (1x alamar +10x ml medium). The assay solution was prepared immediately before each use to avoid possible precipitation. For fluorescence measurements, the cells were transferred into a sterile flat bottom multi-well cell culture plate. Optimization of cell number and alamarBlue<sup>®</sup> intensity was done and cell volume was adjusted to  $4 \times 10^4$  cells/well for 24-well plates and 660 $\mu$ l of medium were added to each well. The cells were then allowed to grow for one day in an incubator to form a confluent cell monolayer (not confluent). Plant extracts were melted in the medium respectively with an increasing order (0.1mg/ml, 0.5mg/ml, 1mg/ml, 5mg/ml, 10mg/ml), cells were treated with these media. The culture medium was carefully aspirated from each well, and the cells were washed with PBS buffer. Then 660 $\mu$ l (600 $\mu$ l medium + 60 $\mu$ l alamar) was put for each well of 24 well-plate.

The cells were further incubated in an incubator for three hours to allow the dye to be taken up by the cells. After the incubation, 100 $\mu$ l was taken from each well and fluorescence measurements were performed with UV visible spectrophotometer at 570 and 600 nm.

Calculations were performed by the following formula;

$$\text{Percentage reduction of alamarBlue}^{\text{®}} = \frac{(\text{O2} \times \text{A1}) - (\text{O1} \times \text{A2})}{(\text{R1} \times \text{N2}) - (\text{R2} \times \text{N1})} \times 100$$

Where:

O1= Molar extinction coefficient (E) of oxidized alamarBlue® (Blue) at 570 nm

O2= E of oxidized alamarBlue® at 600 nm

R1= E of reduced alamarBlue® (Red) at 570 nm

R2= E of reduced alamarBlue® at 600 nm

A1= Absorbance of test wells at 570 nm

A2= Absorbance of test wells at 600 nm

N1= Absorbance of negative control well (media plus alamarBlue® but no cells) at 570 nm

N2= Absorbance of negative control well (media plus alamarBlue® but no cells) at 570 nm

**Table 2.2** Molar extinction coefficients for alamarBlue® at different wavelengths

Wavelength	Reduced (R)	Oxidized (O)
540 nm	104395	47619
570 nm	155677	80586
600 nm	14652	117216
630 nm	5494	34798

### 2.2.5.1 Growth Curve of Cells

$4 \times 10^4$  cells/well were seeded into 24 well plates for 6 days to determine growth curve of fibroblasts. alamarBlue® cell viability assay as described section 2.2.5 was applied to determine cell growth for each day at the same time

## **2.2.6 Determination of mRNA Expression**

### **2.2.6.1 Isolation of Total RNA from Fibroblast Line**

All plastic and glass equipments used for total RNA isolation were treated with distilled water containing 0.1% (v/v) diethylpyrocarbonate (DEPC) in order to inhibit RNase activity. After the evaporation of excess DEPC, the equipments were autoclaved.

Fibroblast line was seeded into 6 well plates for RNA isolation. Next day, treatment of cells was done with plant extracts. Two days later, growth medium in the wells was removed and cells were washed three times by using PBS buffer. After that, 1 mL of QIAzol® was added into the wells and incubated for 5 minutes at room temperature.

After incubation, the cells were detached by pipetting and QIAzol® solution containing the cell lysate in the well was transferred into a 2 mL eppendorf tube. 200 µl of chloroform was added to tube and the tube was shaken vigorously. The tube was centrifuged at 12000 x g for 15 minutes at 4°C which produce three layers. The upper aqueous phase containing RNA was taken and same amount of cold isopropanol was added into the tube and the tube was shaken gently. The mixture was incubated at room temperature for 10 minutes. Then it was centrifuged at 12000 x g for 20 minutes at 4°C. the supernatant was removed and the pellet was mixed with 1 mL of 75% ethanol. The tube was centrifuged again at 7500 x g for 5 minutes at 4°C; the pellet was taken and excess amount of ethanol was evaporated in hood. Finally, RNA was dissolved in 25 µl of nuclease-free distilled water and stored at -80°C.

### **2.2.6.2 Determination of RNA Concentration**

Concentration of the isolated RNA was quantified by measuring the absorbance at 260 nm. Purity was assessed by the 260/280 nm ratio. The ratio of OD<sub>260</sub>/OD<sub>280</sub> must be between 1.8 and 2.2. Below 1.8 refers the DNA contamination while above 2.2 referring the protein contamination. The optical density of 1.0 corresponded to the 40

µg/mL for RNA. The concentration and purity of the RNA were measured at NanoDrop™ 2000 (Thermo Scientific).

### **2.2.6.3 cDNA Synthesis**

#### Reagents:

5X Reaction Buffer: 250 mM Tris-HCl pH 8.3, 250 mM KCl, 20mM MgCl<sub>2</sub> and 50 mM DDT.

M-MuLV-RT: Moloney-Murine Leukemia Virus Reverse Transcriptase

Ribolock: RNase inhibitor

dNTP: Deoxyribonucleotide triphosphate (10mM)

Reverse transcription of RNA to cDNA was performed by mixing 1 µg of total RNA isolated from cell lines and 1 µL of oligo dT primer (Fermentas, Hanover, MD, USA) in an eppendorf tube. The final volume of the mixture was completed to 12 µL with nuclease-free distilled water. The solution was mixed gently and spun down by microfuge.

Mixture was incubated at 70 °C for 5 minutes and it was chilled on ice. After that 4 µL of 5X reaction buffer, 1 µL Ribolock and 2 µL of 10 mM dNTP were added. The tube was mixed gently and spun down by microfuge. It was incubated at 37 °C for 1 hour. Finally, the reaction was stopped by keeping at 70 °C for 10 minutes and chilled on ice. cDNA was stored at -20 °C for further use.

### **2.2.6.4 Quantitative Real-Time PCR**

The expressions of MAPK1, IGF-I, IGF-IR and COL1A1 genes in fibroblast line were analyzed by quantitative real time PCR (qRT-PCR) using a real time PCR machine, Corbett Rotor Gene 6000 (Corbett Life Science, PO Box 435, Concorde, NSW 2137). The 25 µL of final reaction mixture containing 100 ng cDNA, 0.5 mM reverse and forward primers, 1 X Maxima® SYBR Green qPCR Master Mix (Fermentas, Glen, Burni, MD) and RNase free distilled water.

In order to detect any contamination, no template control (NTC) was used. As an internal standard, GAPDH (glyceraldehydes 3-phosphate dehydrogenase) gene was used. The DNA amplification was carried out in a reaction mixture containing specific nucleotide sequence for related gene is given in Table 2.3. The qRT-PCR program consisted of the following cycling profile; initial melting at 95°C for 10 minutes, amplification and quantification program repeated 45 times containing melting at 95°C for 20 seconds, annealing at 58-62°C (depending on the gene) for 30 seconds and extension at 72°C 20 seconds with a single fluorescent measurement. After cycling, melting curve program 50-99°C with a heating rate of 0.1°C/s and continuous fluorescence measurement was added.

Melting curve analysis of the amplification product was done at the end of each amplification reaction to confirm the detection of a PCR product. Quantities of specific mRNAs in the sample were measured according to corresponding gene and relative standard curve method.

Each standard curve was derived from dilution series (1:10, 1:100, 1:500, 1:1000, 1:5000) of control non-treated cDNA for each gene. Light cycler quantification software was used to draw the standard curve.

**Table 2.3** Primer sequences, annealing temperatures and product sizes of the genes.

GENE	Forward Primer (5'→3')	Reverse Primer (5'→3')	Annealing Temp. (C)	Product Size (bp)
GAPDH	GAGCGAGATCCCTCCAAAAT	GGCTGTTGTCATACTTCTCATGG	58	197
MAPK1	GCGCTACACCAACCTCTCGT	GGTTCTCTGGCAGTAGGTCT	60	136
COL1A1	GCCAAGACGAAGACATCCCA	CACAGATCACGTCATCGCAC	60	138
IGF1	CAGTTCGTGTGTGGAGACAG	CTGACTTGGCAGGCTTGAGG	60	166
IGF1R	GTACAACCTACCGCTGCTGGA	AGGATGTTGGCGCAGAAGTC	60	258

### **2.2.6.5 Qualification of qRT-PCR Products by Agarose Gel Electrophoresis**

Qualification of qRT-PCR products was checked on 2% (w/v) agarose gel by using horizontal agarose gel electrophoresis unit. 2% (w/v) agarose was prepared by mixing 2 g of agarose with 100 ml 0.5 X tris – borate-EDTA (TBE) buffer, pH 8.3. Agarose was dissolved in a microwave oven. The solution was cooled approximately 60 °C. 7 µL of ethidium bromide solution (10 mg/mL) was added and the solution was mixed thoroughly. Agarose gel solution was poured into electrophoresis tray and the comb was placed for well formation. After the gel polymerization, gel tank was filled with 0.5 X TBE buffer. The comb was removed. 5 µL of qRT-PCR products was mixed with 1 µL of 6 X loading dye and the mixture was loaded into wells. Electrophoresis was performed at 90 mV for 1 hour. The gel was observed and photographed under UV light.

### **2.2.7 Protein Extraction**

Cells were seeded to 100 x 20 mm tissue culture petri dish for protein extraction. Next day treatment of cells was done with plant extracts. Two days later, growth medium in the dish was removed and the cells were washed three times by using cold (4°C) PBS buffer. 1X RIPA buffer was prepared by dilution of commercially available 10X RIPA buffer (Cell Signaling Technology) with distilled water and 1mM phenylmethanesulfonyl fluoride (PMSF) was added just prior to use to prevent protease activity. 400 µl of the diluted RIPA buffer was added into the dish for lysis of the cells. Dish was incubated on ice for 5 minutes and the cells were scraped. The lysate was sonicated for 5 minutes and centrifuged at 14000 x g in a cold microfuge for 10 minutes. Supernatant was collected and stored at -80°C freezer.

### **2.2.8 Determination of Protein Concentration**

Protein concentrations of cell culture lysates were determined by the BCA (Bicinchoninic Acid) method using crystalline bovine serum albumin as a standard (Smith et al. 1985). This method depends on reduction of Cu<sup>2+</sup> ions with peptide bonds under alkaline conditions and chelation of two molecules of bicinchoninic acid

with each  $\text{Cu}^{2+}$  ion, forming a purple color that absorbs light at a wavelength of 562 nm and the absorbance at this wavelength proportional to the protein concentration.

### **Reagents:**

Reagent A: 0.4 g of  $\text{CuSO}_4 \cdot 5\text{H}_2\text{O}$  was dissolved in 10 ml  $\text{dH}_2\text{O}$

Reagent B: 8 g of  $\text{Na}_2\text{CO}_3 \cdot \text{H}_2\text{O}$  and 1.6 g of  $\text{NaKC}_4\text{H}_4\text{O}_6$  was dissolved with  $\text{dH}_2\text{O}$  and titrated with  $\text{NaHCO}_3$  to pH 11.25 and the volume was completed to 100 mL with  $\text{dH}_2\text{O}$ . The pH of the solution was checked at the end.

Reagent C: 4 g of BCA was dissolved in 100 mL of  $\text{dH}_2\text{O}$

BCA Solution: Reagent A, Reagent B and Reagent C were mixed in the same order with the ratio of 1:25:25.

## **2.2.9 Determination of Protein Expression**

### **2.2.9.1 Western Blotting**

#### **Reagents**

Transfer Buffer: (25 mM Tris, 192 mM Glycine)

3.03 g trisma-base and 14.4 g glycine was dissolved in 200 mL methanol, and the volume was made up to 1 L with distilled water.

TBST: (20 mM Tris-HCL pH 7.4, 500 mM NaCl, 0.05% Tween 20)

9.5 g of NaCl was dissolved in water and 6.5 mL of 1M tris-HCl buffer was added. Then pH of the solution was adjusted to 7.4. Finally, 165  $\mu\text{L}$  tween 20 was added and volume was made up to 350 mL distilled water.

Blocking Solution: (5% Non-Fat Dry Milk)

5g non-fat dry milk was dissolved in 100 mL TBS

Primary Antibody: 1/500 dilution

Secondary Antibody: 1/2000 dilution

ECL Substrate Solution: (Pierce ECL Western Blotting Substrate) 1 mL of peroxide solution and 1 mL of luminol enhancer solution were mixed and 2 mL of this mixture was used for each membrane.

Alkaline Phosphatase Substrate Solution:

Solution A: 2.67 mL of 1.5 M Tris-HCl Buffer (pH 8.8), 4 mL of 1 M NaCl, 96  $\mu$ L of Diethanolamine, 820  $\mu$ L of 100 mM MgCl<sub>2</sub>, 40  $\mu$ L of 100 mM ZnCl<sub>2</sub> and 12.2 mg of nitrotetrazolium blue chloride (NBT) were mixed and the pH of the mixture was adjusted to 9.55 with saturated Tris. Then the volume was made up to 40 mL with distilled water.

Solution B: 2 mg of Phenazine Methosulfate was dissolved in 1 mL of distilled water.

Solution C: 5.44 mg of BCIP (5-bromo 4-chloro 3-indoyl phosphate) was dissolved in 136  $\mu$ L of N-N-dimethylformamide.

To prepare the substrate solution, 20 mL of Solution A, 68  $\mu$ L of Solution C, and 134  $\mu$ L of Solution B were mixed for each membrane. For Western blotting, the gel was removed from the glasses and the gel was placed into transfer buffer for 10 minutes. The PVDF membrane was cut as equal size with gel and immersed in 100% methanol for a few seconds to preset the membrane. Then the membrane was equilibrated in transfer buffer for 5 minutes. After that, the gel, PVDF membrane, Whatman papers and two fiber pads were placed in transfer sandwich as shown in Figure 2.1. The transfer sandwich was placed into Mini Trans-Blot module (Bio-Rad Laboratories, Richmond, CA, USA) and module was filled with transfer buffer. The transfer was carried out at 90 volt and 400 mA for 90 minutes.

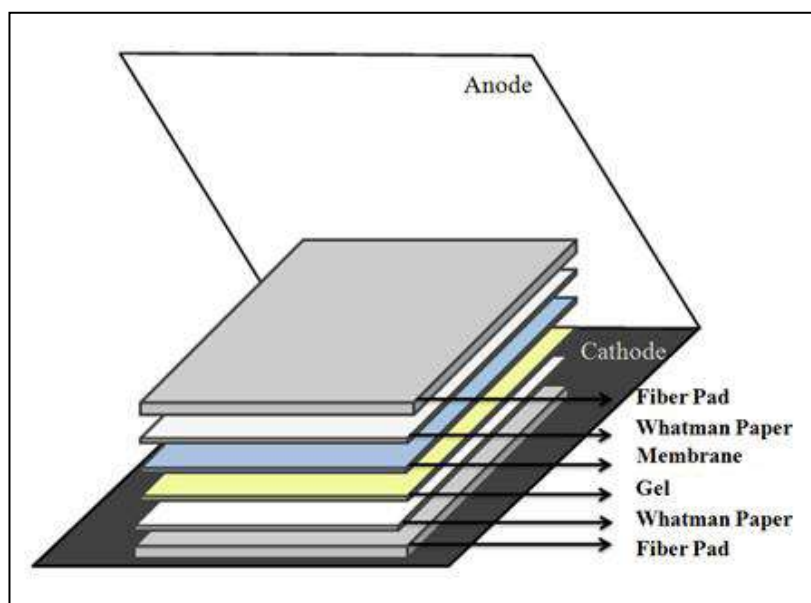


**Figure 2.1** Western blot sandwich.

After transfer was completed, the membrane was washed with TBST for 10 minutes. Then membrane was incubated with blocking solution in room temperature for an hour. After that, the membrane was incubated with 1/500 dilutions of ERK1/2, p-ERK1/2, IGF-I, COL1A1, IRS-1 and p-IRS-1 primary antibodies for 2 hours at room temperature by shaking. The membrane was washed with TBST for three times each of which is 10 minutes. After removal of unbound primary antibody, the membrane was incubated with 1/2000 dilutions of conjugated secondary antibodies for ERK1/2, p-ERK1/2, IGF-I, COL1A1, IRS-1 and p-IRS-1; and incubated with 1/2000 dilutions of alkaline phosphatase conjugated secondary antibodies for COL1A1 for an hour. Finally the membrane was incubated with appropriate substrate solution (ECL substrate solution or alkaline phosphatase substrate solution) for the conjugated enzyme on secondary antibody. For visualization of horseradish peroxidase conjugated secondary antibody, X-Ray Roentgen Method was used and the bands were visualized on the roentgen film. The band intensities were analyzed by Image J visualization software developed by NIH.

### 2.2.10 Fractionation of Crude Extract

Among the extracts, the extracts, which have the highest induction rate in Western blot and PCR analysis were focused and fractionation were started. The crude extract was fractionated into different fractions by partitioning into solvents of increasing polarity (Figure 2.2). It was thus fractionated into hexane, chloroform, ethyl acetate and the aqueous residue. After filtration of various solvents from the supernatant, crude extracts (CE) was obtained by evaporating in a vacuum rotary evaporator. Each fraction was obtained freeze-dried after eliminating the solvents.

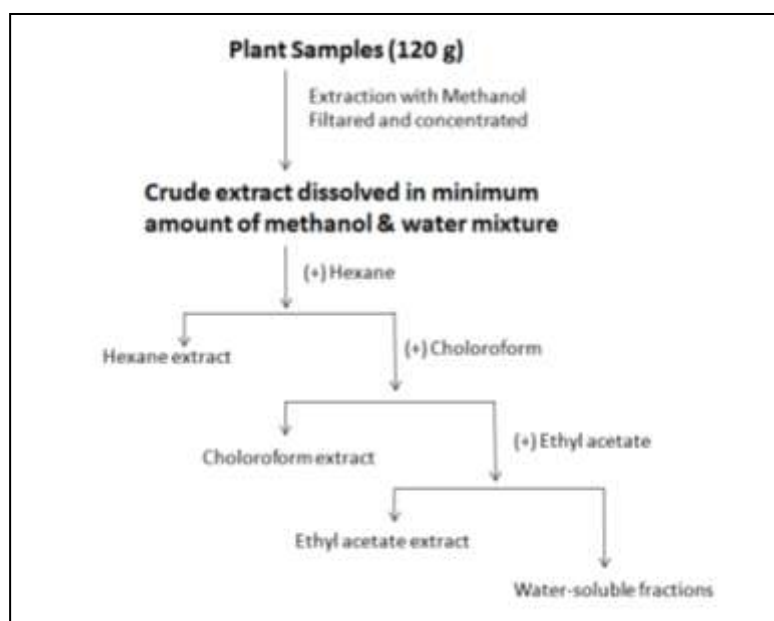


**Figure 2.2** Solvent – solvent fractionation scheme of *Achillea millefolium* aerial parts crude methanol extract using different solvents of increasing polarity sequentially.

## CHAPTER 3

### RESULTS

#### 3.1 EXTRACTION OF PLANT SAMPLES

120 g dry powder samples of each plant (*Achillea millefolium* aerial parts, *Hypericum perforatum* aerial parts, *Primula vulgaris* aerial parts and *Aesculus hippocastanum* seed cotyledon) were extracted with 1200 mL of methanol (1:10) (wt/v) in the rotating incubator (180 rpm) at 25°C for 24 hours. The extract was concentrated and dried through evaporation. Yield of the crude extracts are calculated in percentage and given in table 3.1.

**Table 3.1:** Yield of crude extracts

<b>Plant Sample</b>	<b>Yield of the Crude Extract (%)</b>
120 g of <i>Achillea millefolium</i> aerial parts	10.8
120 g of <i>Hypericum perforatum</i> aerial parts	12.1
120 g of <i>Primula vulgaris</i> aerial parts	11.2
120 g of <i>Aesculus hippocastanum</i> seed cotyledon	20.1

### **3.2 Antioxidant Activity Determination**

Before we performed molecular assays, initially we made free radical scavenging activity tests to make comparisons. Seed cotyledon of *Aesculus hippocastanum* and aerial parts of *Hypericum perforatum*, *Primula vulgaris*, *Achillea millefolium* were used for this purpose. Plant samples were prepared and extracted as described in sections 2.2.1 and 2.2.2. sections. These plant were evaluated for their antioxidant capacity.

#### **3.2.1 DPPH (2,2-diphenyl-1-picrylhydrazyl) Method**

Radical scavenging activities of *A. millefolium*, *H. perforatum*, *P. vulgaris* aerial parts and *A. hippocastanum* seed cotyledon extracts were investigated by DPPH method. The investigation method was described in section 2.2.3. Results of the experiments are given in Figure 3.1 and Table 3.1.

**3.2.1.1 Determination of Antioxidant Capacities of *A. millefolium*, *H. perforatum*, *P. vulgaris* Aerial Parts and *A. hippocastanum* Seed Cotyledon Extracts by DPPH Method.**

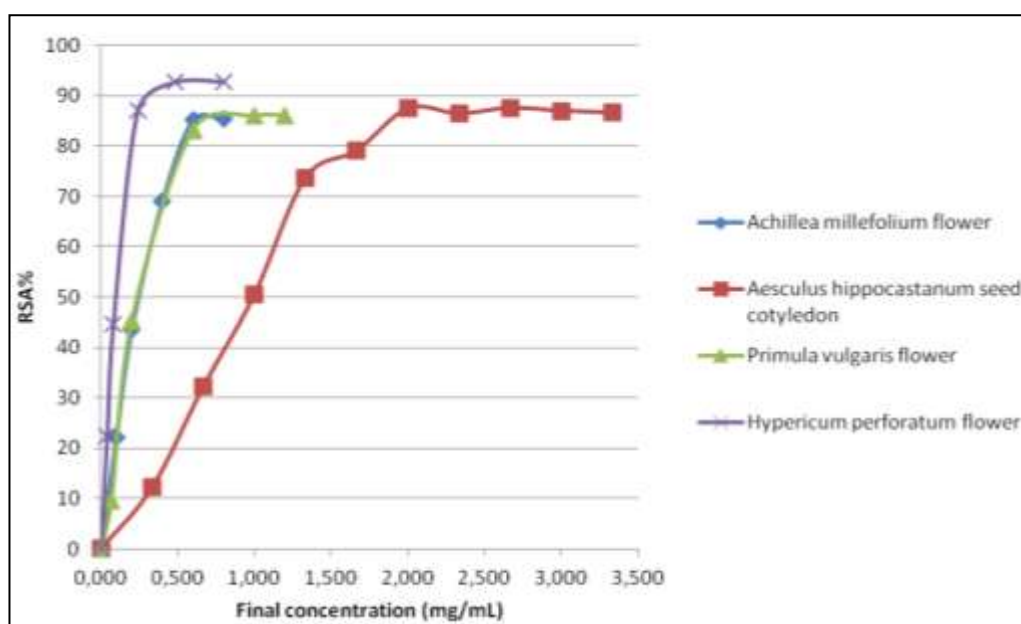


**Figure 3.1** DPPH radical scavenging activity of *A. millefolium*, *H. perforatum*, *P. vulgaris* aerial parts and *A. hippocastanum* seed cotyledon extracts. Radical scavenging activities were measured at 15th incubation period, at 517 nm, in percent versus extract concentrations (mg/mL)

Among selected extracts *Hypericum perforatum* aerial parts extract exhibited the most effective DPPH-scavenging activity with an EC<sub>50</sub> value of 0.189 mg/mL.

**Table 3.2** DPPH scavenging activity of *A. millefolium* aerial parts, *H. perforatum* aerial parts, *P. vulgaris* aerial parts and *A. hippocastanum* seed cotyledon extracts. Activities were measured at 15<sup>th</sup> incubation period, at 517 nm, in percent versus extract concentrations (mg/mL)

Samples	*DPPH RSA EC <sub>50</sub> (mg/mL)
<i>Achillea millefolium</i> aerial parts	0.313± 0,009
<i>Hypericum perforatum</i> aerial parts	0.189 ± 0,009
<i>Primula vulgaris</i> aerial parts	0.461 ± 0,008
<i>Aesculus hippocastanum</i> seed cotyledon	1,304 ± 0,029
DPPH RSA EC <sub>50</sub> : Effective concentration of plants extracts for 50% of DPPH radical scavenging activity. * Mean of three independent experiments in triplicates.	

### 3.2.2. ABTS [2,2'-azinobis-(3-ethylbenzothiazoline-6-sulfonic acid)] Method

ABTS radical scavenging activities was calculated according to RE et al., as described in section 2.2.3.2. Trolox standard curve was plotted as shown in Figure 3.2. and results were calculated according to this curve

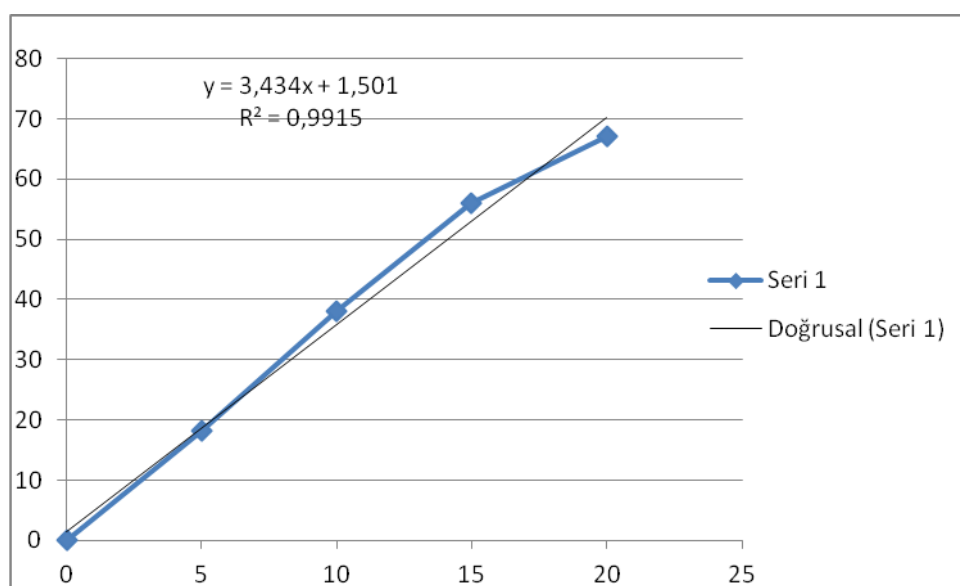


**Figure 3.2** Trolox standard curve to calculate Trolox equivalent antioxidant capacities of the extracts (at 734 nm). Each data were calculated by means of three independent experiments in triplicates.

### 3.2.2.1 Determination of Free Radical Scavenging Capacities of *A. millefolium*, *H. perforatum*, *P. vulgaris* Aerial Parts and *A. hippocastanum* Seed Cotyledon Extracts by ABTS Method.

Trolox equivalent antioxidant capacity (TEAC) values of *Achillea millefolium* aerial parts, *Hypericum perforatum* aerial parts, *Primula vulgaris* aerial parts and *Aesculus hippocastanum* seed cotyledon extracts are calculated (Table 3.3). The correlation was higher antioxidant capacity at higher TEAC value. *Hypericum perforatum* aerial parts extract was found as having the highest ABTS radical scavenging activity with the highest TEAC value of 3.867  $\mu\text{mol/g}$ . Extracts of *Aesculus hippocastanum* seed cotyledon, *Achillea millefolium* aerial parts, *Primula vulgaris* aerial parts and had TEAC values of 0.441, 2.001, 2.291  $\mu\text{mol/g}$ ; respectively with an increasing order.

**Table 3.3** Trolox equivalent antioxidant capacities (TEAC) of *A. millefolium*, *H. perforatum*, *P. vulgaris* aerial parts and *A. hippocastanum* seed cotyledon extracts.

Samples	*ABTS TEAC value ( $\mu\text{mol/g}$ ) $\pm$ SD
<i>Achillea millefolium</i> aerial parts	2,001 $\pm$ 0,022
<i>Hypericum perforatum</i> aerial parts	3,867 $\pm$ 0,005
<i>Primula vulgaris</i> aerial parts	2,291 $\pm$ 0,011
<i>Aesculus hippocastanum</i> seed cotyledon	0.441 $\pm$ 0,004
TEAC value: Radical scavenging activity $\mu\text{mol}$ equivalents of Trolox/g of extract. *Mean of three independent experiments in triplicates.	

### 3.2.3 CUPRAC ASSAY

Total antioxidant capacities of *A. millefolium*, *H. perforatum*, *P. vulgaris* aerial parts, *A. hippocastanum* seed cotyledon were assayed by Cuprac Assay as described in section 2.2.3.3. Trolox standard curve was plotted as shown in Figure 3.3. and results were calculated according to this curve.

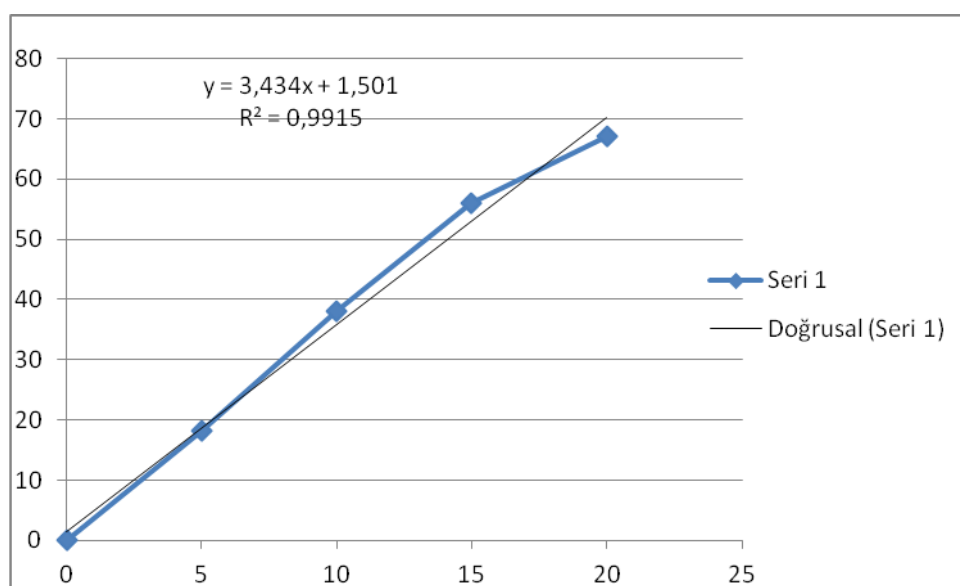


**Figure 3.3** Trolox standard curve to calculate Trolox equivalent antioxidant capacities of the extracts (at 734 nm). Each data were calculated by means of three independent experiments in triplicates.

### 3.2.3.1 Determination of Free Radical Scavenging Capacities of *A. millefolium*, *H. perforatum*, *P. vulgaris* Aerial Parts and *A. hippocastanum* Seed Cotyledon Extracts by CUPRAC Assay.

Trolox equivalent antioxidant capacity (TEAC) values of *A. millefolium* aerial parts, *H. perforatum* aerial parts, *P. vulgaris* aerial parts and *A. hippocastanum* seed cotyledon extracts were calculated (table 3.4). The correlation was higher antioxidant capacity at higher TEAC value. Therefore, *H. perforatum* aerial parts extract was found as having the highest radical scavenging activity with the highest TEAC value (1.919  $\mu\text{mol/g}$ ). Extracts of *A. hippocastanum* seed cotyledon, *A. millefolium* aerial parts, *P. vulgaris* aerial parts and had TEAC values of 0.121, 0.751, 0.757  $\mu\text{mol/g}$ ; respectively with an increasing order.

**Table 3.4** Trolox equivalent antioxidant capacities (TEAC) of *A. millefolium* aerial parts, *H. perforatum* aerial parts, *P. vulgaris* aerial parts and *A. hippocastanum* seed cotyledon extracts.

Samples	*CUPRAC TEAC value ( $\mu\text{mol/g}$ ) $\pm$ SD
<i>Achillea millefolium</i> aerial parts	0.751 $\pm$ 0.002
<i>Hypericum perforatum</i> aerial parts	1.919 $\pm$ 0.003
<i>Primula vulgaris</i> aerial parts	0.757 $\pm$ 0.003
<i>Aesculus hippocastanum</i> seed cotyledon	0.121 $\pm$ 0.002
TEAC value: Radical scavenging activity $\mu\text{mol}$ equivalents of Trolox/g of extract. *Mean of three independent experiments in triplicates.	

### 3.2.4 Total Phenolic Content Determination

Gallic acid (GA) standard curve was plotted (figure 3.4) and total phenolic content was determined as described in section 2.2.3.4

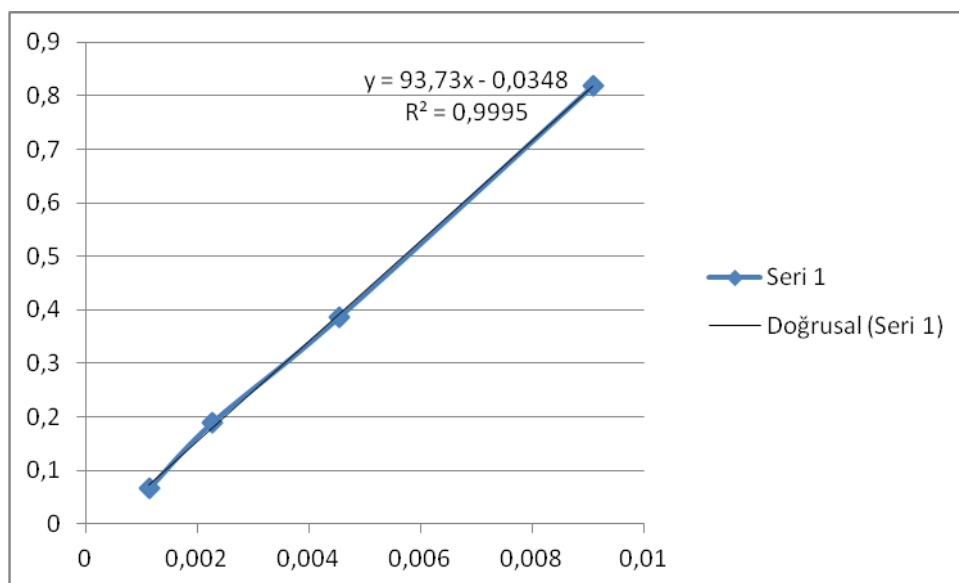


**Figure 3.4** Gallic acid standard curve. Each data was collected by means of three independent experiments in triplicates.

#### **3.2.4.1 Total phenolic Content of *A. millefolium*, *H. perforatum*, *P. vulgaris* Aerial Parts and *A. hippocastanum* Seed Cotyledon Extracts.**

Amount of phenolic compounds were searched, *H. perforatum* aerial parts extract has revealed the highest amount of (0.096 mg) gallic acid equivalence (GAE) in 1 mg of extract as can be seen in Table 3.5. *H. perforatum* aerial parts extract was also found as most effective radical scavenger in previous experiments.

**Table 3.5** Total phenolic content results of *A. millefolium*, *H. perforatum*, *P. vulgaris* aerial parts and *A. hippocastanum* seed cotyledon extracts.

Samples	*TP GAE (mg/mg)
<i>Achillea millefolium</i> aerial parts	0.050 ± 0.005
<i>Hypericum perforatum</i> aerial parts	0.096 ± 0.01
<i>Primula vulgaris</i> aerial parts	0.058 ± 0.009
<i>Aesculus hippocastanum</i> seed cotyledon	0.025 ± 0.009
TP GAE: Total phenolic content (mg equivalents of GA/mg of plant extract). *Mean of triplicate trials.	

### 3.2.5 Total Flavonoids Content

Calibration curves were plotted as absorbance at 734nm against concentration. Then total flavonoids content was calculated as catechin equivalent (Figure 3.5) as described in section 2.2.3.5.

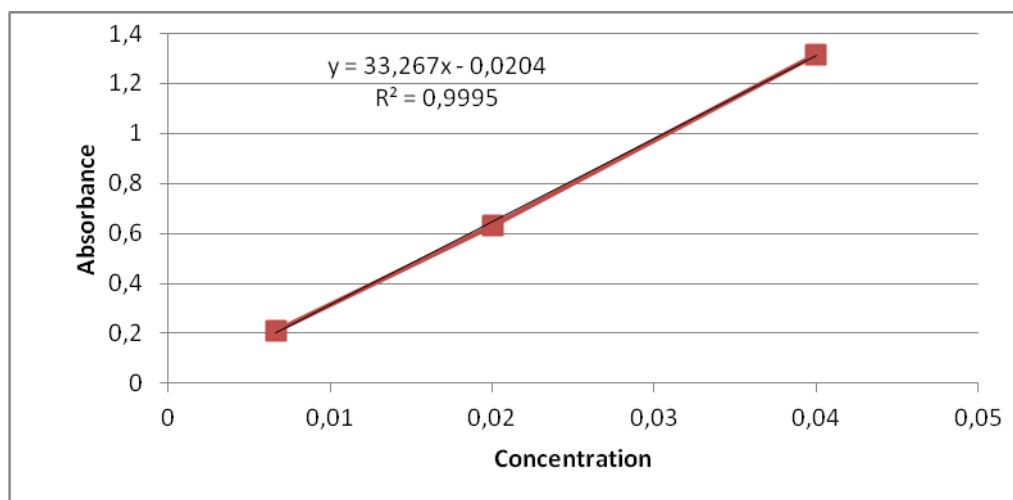


**Figure 3.5** Catechin standard curve

ABTS, DPPH, TP and TF test and their results for all selected parts of *Achillea millefolium*, *Hypericum perforatum*, *Primula vulgaris*, *Aesculus hippocastanum* are shown in Table 3.6.

**Table 3.6** Comparison of selected anti-oxidant methods for *A. millefolium* aerial parts, *H. perforatum* aerial parts, *P. vulgaris* aerial parts and *A. hippocastanum* seed cotyledon.

Samples	ABTS TEAC Value ( $\mu\text{mol/g}$ )	DPPH EC <sub>50</sub> (mg/mL)	Cuprac TEAC Value ( $\mu\text{mol/g}$ )	Total Phenol GAE (mg/mg)	Total Flavonoid (mg/mg)
<i>A. millefolium</i> aerial parts	2.001 $\pm$ 0.022	0.313 $\pm$ 0.009	0.751 $\pm$ 0.002	0.050 $\pm$ 0.005	0.029 $\pm$ 0.001
<i>H. perforatum</i> aerial parts	3.867 $\pm$ 0.005	0.189 $\pm$ 0.009	1.919 $\pm$ 0.003	0.096 $\pm$ 0.011	0.003 $\pm$ 0.001
<i>P. vulgaris</i> aerial parts	2.291 $\pm$ 0.011	0.461 $\pm$ 0.008	0.757 $\pm$ 0.003	0.058 $\pm$ 0.009	0.031 $\pm$ 0.002
<i>A. hippocastanum</i> seed cotyledon	0.441 $\pm$ 0.004	1.304 $\pm$ 0.029	0.121 $\pm$ 0.002	0.025 $\pm$ 0.009	0.065 $\pm$ 0.008

As the result of these assays *Hypericum perforatum* aerial parts extract was found as having the highest radical scavenging activity among other extracts with EC<sub>50</sub> value of 0.188627 mg/mL in DPPH method, TEAC value of 3,86721  $\mu\text{mol/g}$  in ABTS method and TEAC value of 1,9193  $\mu\text{mol/g}$  in CUPRAC Assay. Extracts of *Aesculus hippocastanum* seed cotyledon, *Achillea millefolium* aerial parts, *Primula vulgaris* aerial parts had radical scavenging activities respectively with an increasing order. Also amount of phenolic compounds and flavonoid compounds were searched in order to correlate anti-oxidant activities of the extracts. When phenolic compounds were searched, *Hypericum perforatum* aerial parts extract has revealed the highest amount of phenolic compounds as 0,096 mg gallic acid equivalence (GAE) in 1 mg of extract (Table 3.5). Total flavonoid content was calculated as catechin equivalent from catechin standard curve equation  $y=mx+n$  (Figure 3.5). *A. hippocastanum* seed cotyledon extract had the highest amount of flavonoid as 0,065 mg/mg.

After the antioxidant capacity determination of *Aesculus hippocastanum*, *Hypericum perforatum*, *Primula vulgaris* and *Achillea millefolium*, molecular mechanisms of these plant extracts at both transcriptional and translational levels are

studied to search for type I collagen biosynthesis-inducing plants and to select the most useful plant extract for herbal skin products. For that reason, the correlation between fibroblast number and alamarBlue<sup>®</sup> fluorescence intensity was determined with alamarBlue<sup>®</sup> assay. This experiment provides both the evaluation of the alamarBlue<sup>®</sup> assay as a first step and determination of fibroblast number for other experiments. Also, the fibroblast growth curve analysis was examined with the aid of alamarBlue assay as another preliminary step. The cellular growth curve of human dermal fibroblast line (ATCC: PCS-201-012) defines the growth characteristics for this cell line and the best time range for evaluating the effects of plant extracts on these cells. Then, in order to determine appropriate application concentrations of plant extracts, cell viability of fibroblasts treated with different concentrations of plant extracts was examined with alamarBlue<sup>®</sup> assay. Although, at the beginning the tested concentrations were in a wide range (from 0.1 mg/ml to 10 mg/ml); then this range was narrowed (from 0.1 mg/ml to 0.5 mg/ml).

### **3.3 Determination of Cell Viability (AlamarBlue<sup>®</sup> Assay)**

As a first step the fibroblast growth curve analysis were examined. Optimization of cell number and alamarBlue<sup>®</sup> intensity was done and cell volume was adjusted to  $4 \times 10^4$  cells/well.

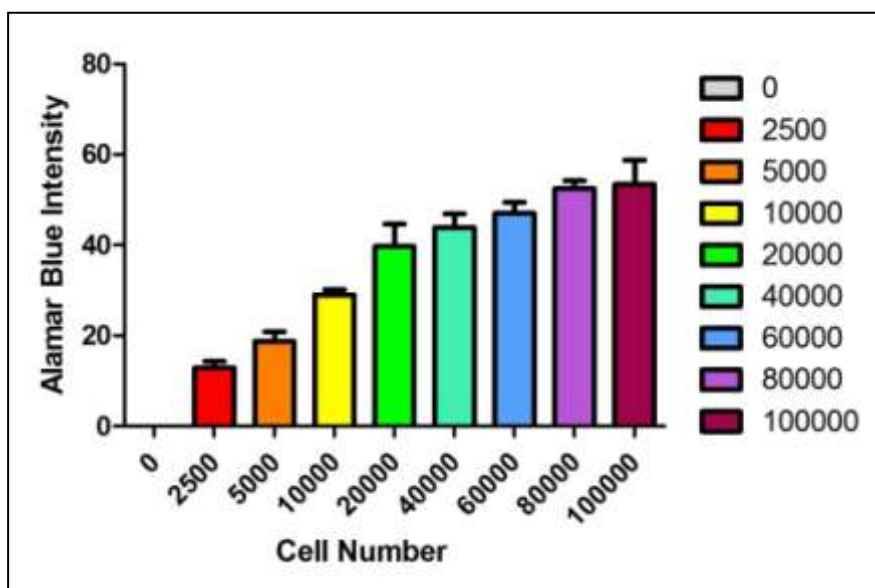


**Figure 3.6** Fibroblast number and alamarBlue® fluorescence correlation. (Cell volume was adjusted to  $4 \times 10^4$  cells/well).

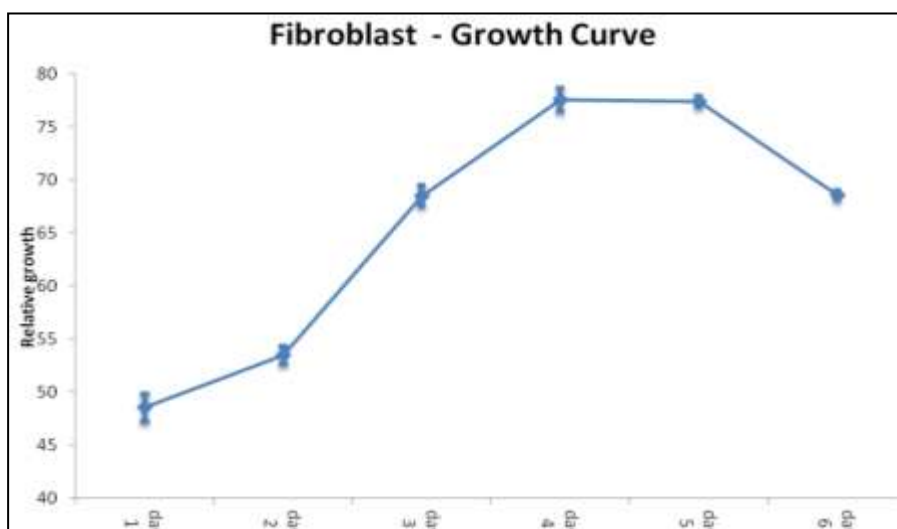


**Figure 3.7** Growth curve of primary human dermal fibroblasts (ATCC: catalog no. PCS-201-012).

Fibroblast growth curve analysis was done as described in section 2.2.5.1. Results were given in Figure 3.7 AlamarBlue assay was done as described in section 2.2.5 to investigate alamarBlue® based fluorescence and cell number correlation.

$4 \times 10^4$  fibroblasts/well were treated with increasing concentration (from 0.1 mg/ml to 10 mg/ml) of *Achillea millefolium* aerial parts, *Hypericum perforatum* aerial parts, *Primula vulgaris* aerial parts and *Aesculus hippocastanum* seed cotyledon extracts as described in section 2.2.5. Results are given in figures 3.8, 3.9, 3.10 and 3.11. Results are given in Figure 3.6.

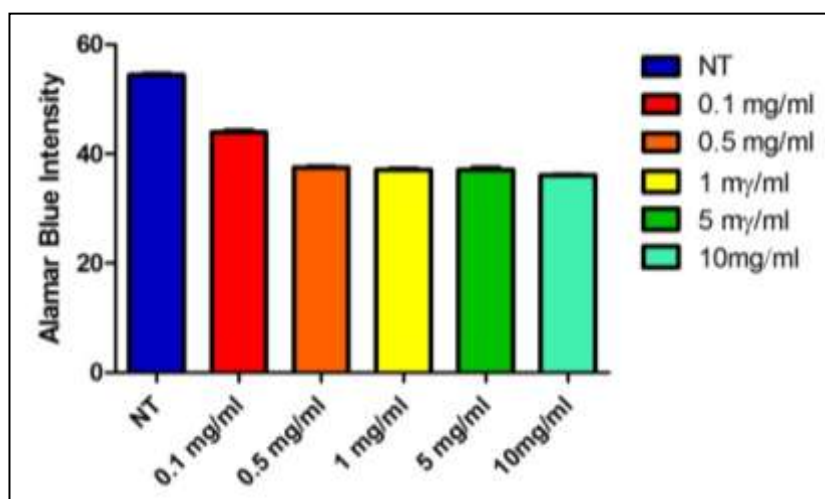


**Figure 3.8** Fibroblasts were treated with increasing concentration of *A. hippocastanum* seed cotyledon extract. Fibroblasts were dosed for 48 h with extract then 3 hours with alamarBlue.

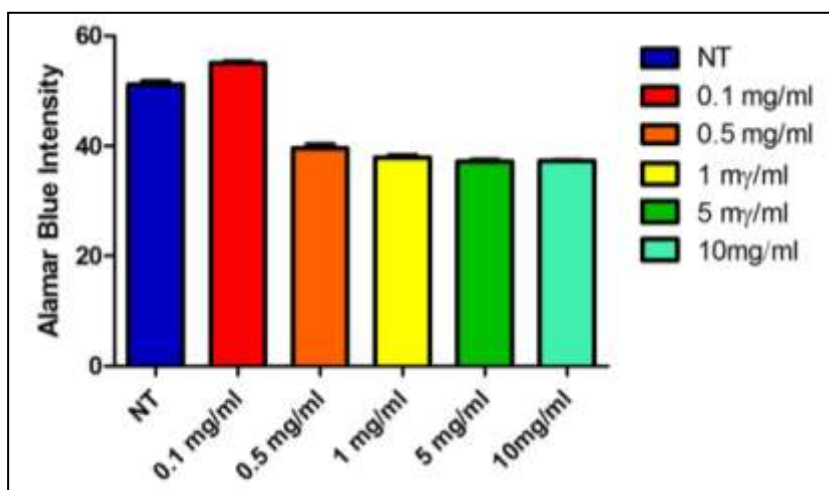


**Figure 3.9** Fibroblasts were treated with increasing concentration of *Achillea millefolium* aerial parts extract. Fibroblasts were dosed for 48 h with extract then 3 hours with alamarBlue.

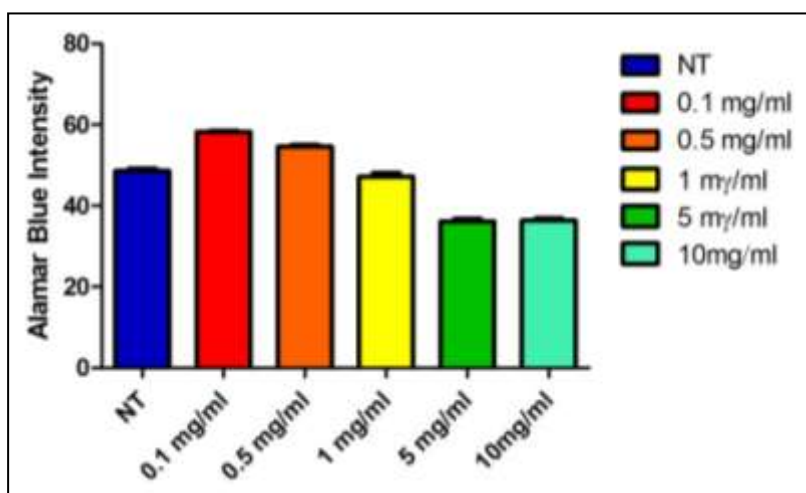


**Figure 3.10** Fibroblasts were treated with increasing concentration of *Primula vulgaris* aerial parts extract. Fibroblasts were dosed for 48 h with extract then 3 hours with alamarBlue.

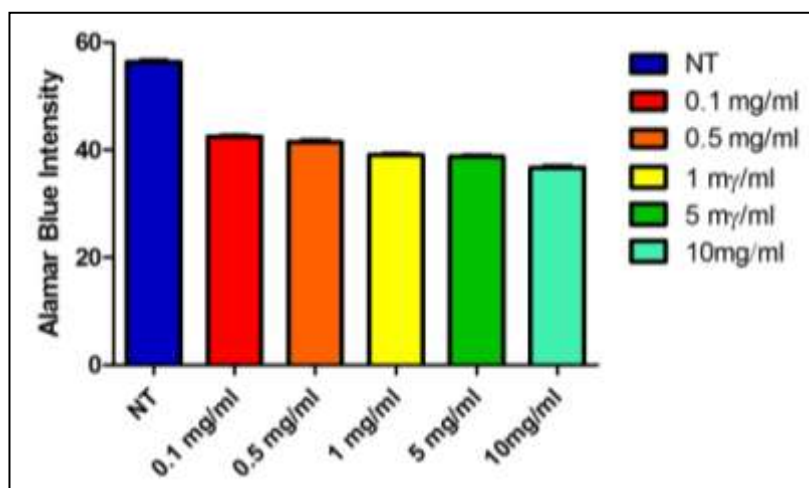


**Figure 3.11** Fibroblasts were treated with increasing concentration of *H. Perforatum* aerial parts extract. Fibroblasts were dosed for 48 h with extract then 3 hours with alamarBlue<sup>®</sup>.

There was an increase in fibroblasts which were treated with 0.1 mg/ml *A. millefolium* and *P. vulgaris*. Then to see exact optimum concentration of plant extracts,  $4 \times 10^4$  fibroblasts/well were treated with increasing concentration in narrower range (from 0.1 mg/ml to 0.5 mg/ml) of *Achillea millefolium* aerial parts, *Hypericum perforatum* aerial parts, *Primula vulgaris* aerial parts and *Aesculus hippocastanum* seed cotyledon extracts as described in section 2.2.5. Results are given in figures 3.11, 3.12, 3.13 and 3.14.

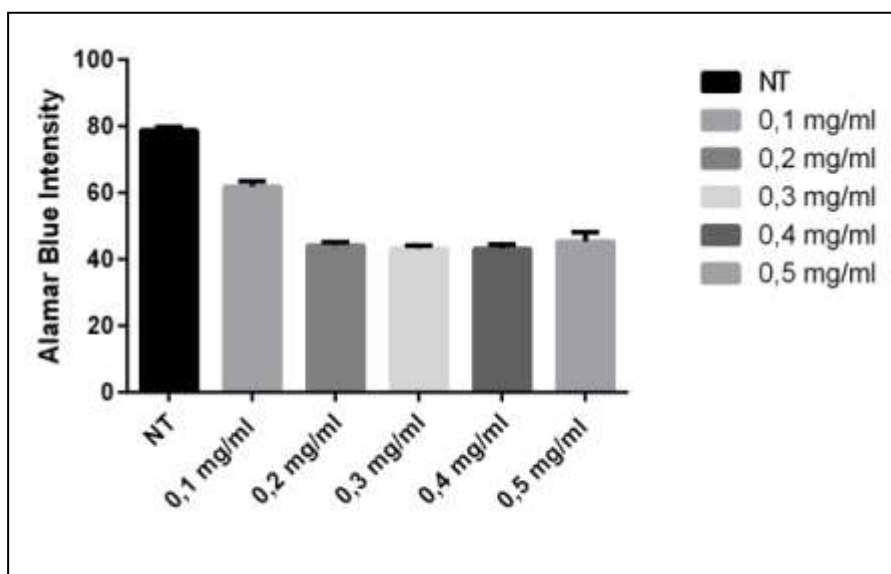


**Figure 3.12** Fibroblasts treated with increasing concentration of *Aesculus hippocastanum* seed cotyledon extract. Fibroblasts were dosed for 48 h with extract then 3 hours with alamarBlue<sup>®</sup>.

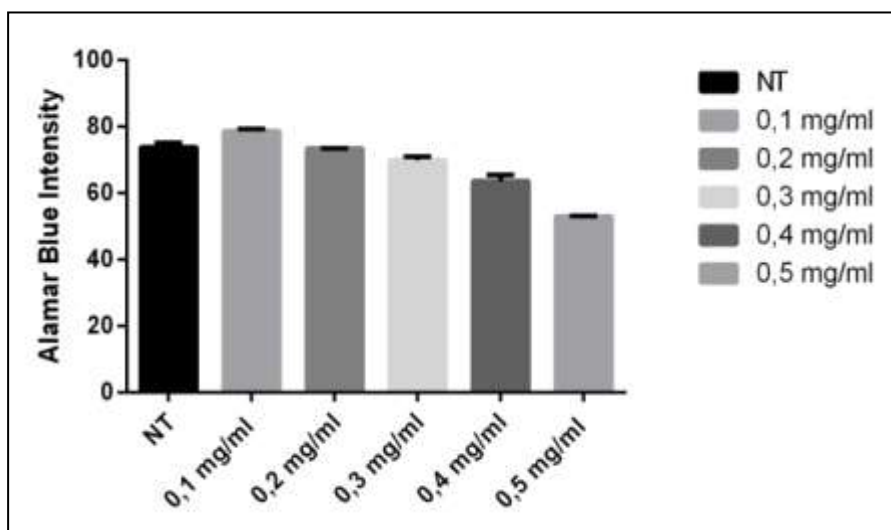


**Figure 3.13** Fibroblasts treated with increasing concentration of *Achillea millefolium* aerial parts extract. Fibroblasts were dosed for 48 h with extract then 3 hours with alamarBlue<sup>®</sup>.

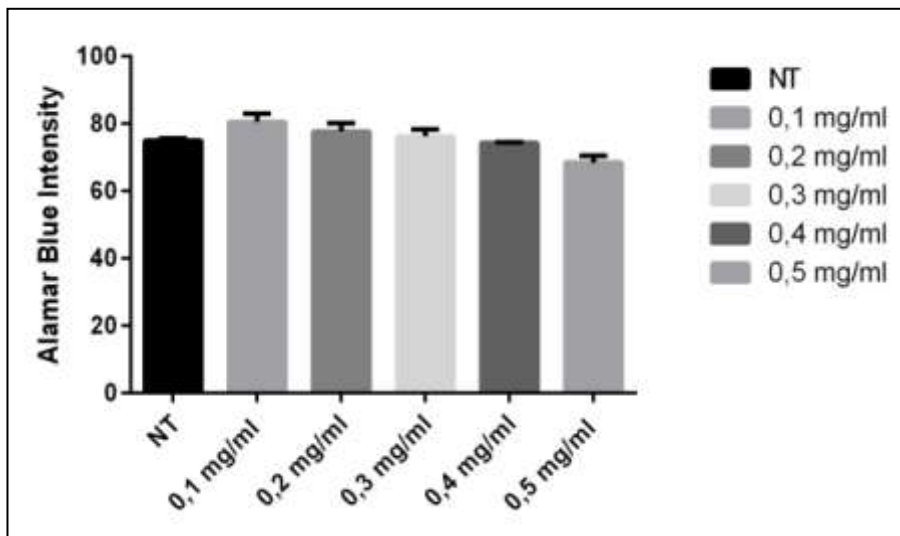


**Figure 3.14** Fibroblasts treated with increasing concentration of *P. Vulgaris* aerial parts extract. Fibroblasts were dosed for 48 h with extract then 3 hours with alamarBlue®.

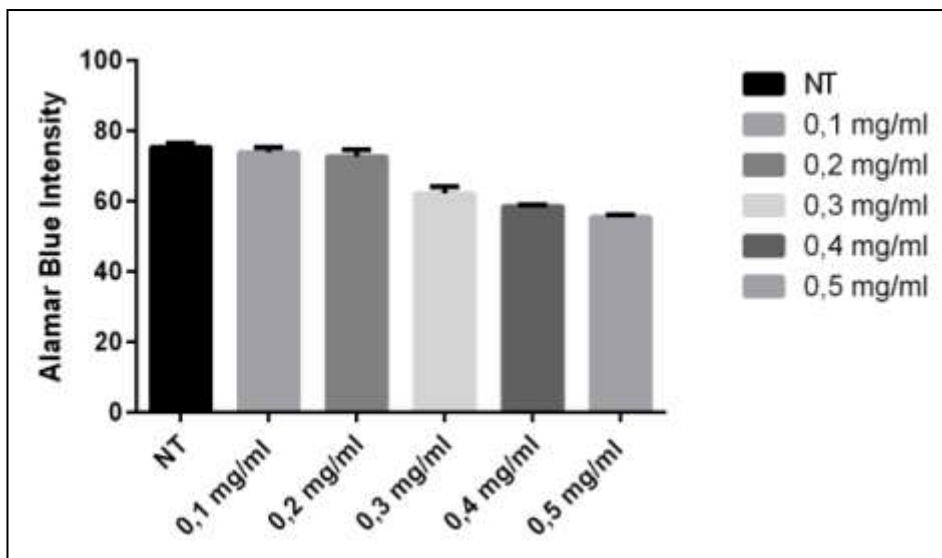


**Figure 3.15** Fibroblasts treated with increasing concentration of *H. perforatum* aerial parts extract. Fibroblasts were dosed for 48 h with extract then 3 hours with alamarBlue®.

According to cell viability results, there were an increase in fibroblast number treated with 0.1 mg/ml *Achillea millefolium* aerial parts extract and 0.1 mg/ml *Primula vulgaris* aerial parts extract. However, there was no increase in cell viability of fibroblasts treated with *Aesculus hippocastanum* seed cotyledon extract and *Hypericum Perforatum* aerial parts extract. For these extracts, least detrimental concentration dosage (0.1 mg/ml) was selected. It is obvious that although plant extracts can be useful in some concentration ranges, the same extracts can be very cytotoxic and harmful in higher concentration values. Therefore, adjustment of extract concentration and so doing cell viability assay is important for experiments. As a result of our experiments, 0.1 mg/ml plant extract amount for the continuous treatment experiments was determined.

Then next step, human fibroblasts were exposed extracts and then qPCR and Western blot techniques were performed respectively to determine the mRNA and protein expression levels of pro-type 1 collagen. The pro-type 1 collagen (Col1A1) mRNA and protein expressions in the plant extract treated and non-treated fibroblast line are shown in figure 3.20 and 3.21, respectively. Furthermore, the summary of results of the mRNA and protein expression analysis of Col1A1 from plant extract treated cells relative to non-treated cells is given in table 3.9.

### **3.4 COL1A1 mRNA Expression in the Fibroblast Line**

#### **3.4.1 COL1A1 mRNA Expression in Fibroblast Line**

The mRNA expression of COL1A1 determined by quantitative real time PCR (qRT-PCR) technique in the treated and non-treated cell lines. GAPDH was used as internal standard to calculate relative mRNA expression of COL1A1. Specific annealing temperatures of the primers (COL1A1 and GAPDH) were used.

Relative mRNA expression of COL1A1 was calculated in fibroblast line by producing standard curve from 1:10, 1:100, 1:500, 1:1000 and 1:5000 dilutions of cDNAs (Figure 3.16). The amplification plot shows changes in fluorescence of

SYBR green dye I versus cycle number of COL1A1 gene (Figure 3.17). Melt curve analysis was performed to check amplification of specific product (Figure 3.18).

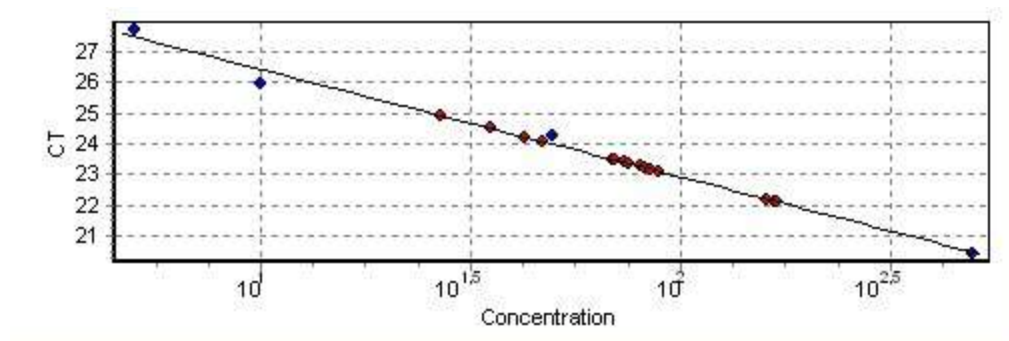


**Figure 3.16** standard curves generated from serial dilutions of control cDNA to calculate quantities of COL1A1 mRNAs in the treated and non treated fibroblast line.

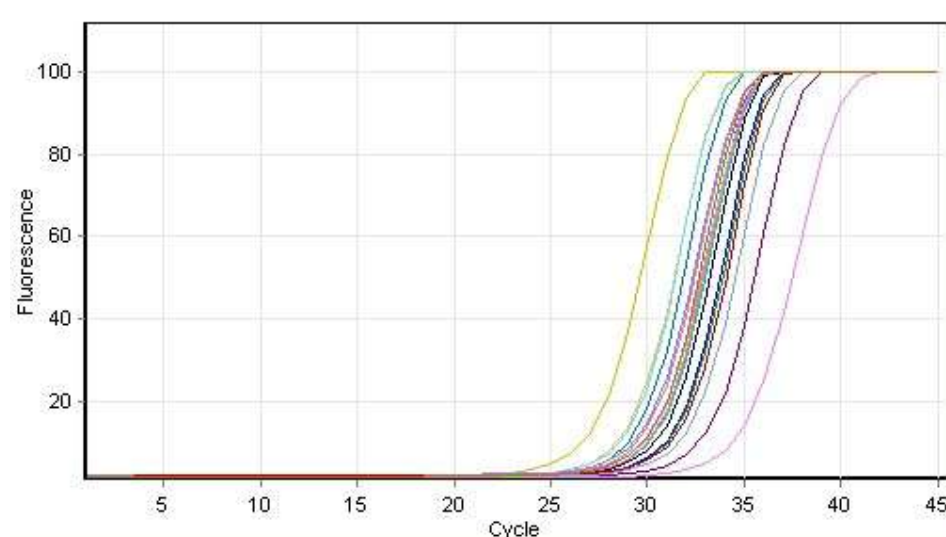


**Figure 3.17** Amplification curve showing the accumulation of fluorescence emission at each reaction cycle.

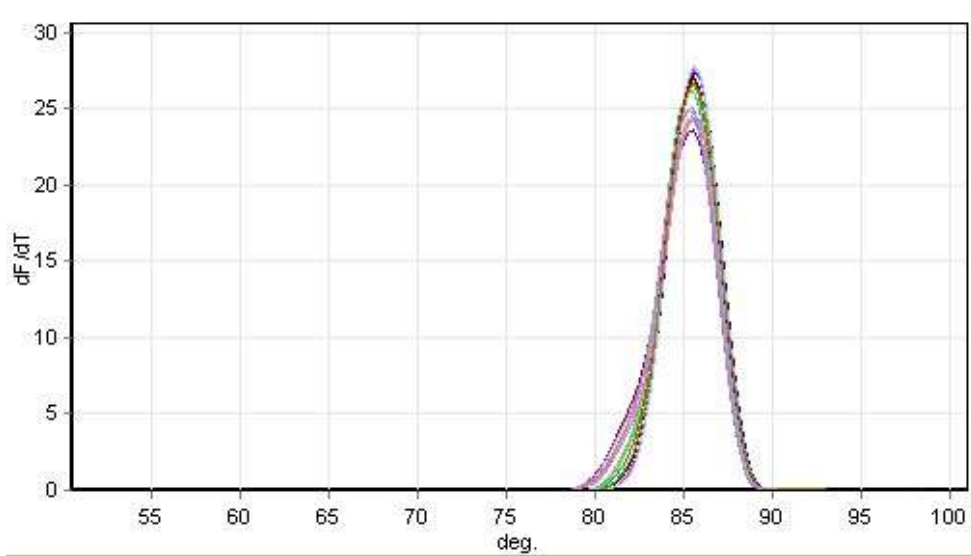


**Figure 3.18** Melting curve showing the fluorescence emission change versus temperature. Detection of single peak means single PCR product (Annealing Temp. is 60°C).

The results obtained, Livak method was used to determine mRNA expression of relative COL1A1 in cell lines by using Ct values. Formulation for Livak ( $2^{-\Delta\Delta Ct}$ ) method is given in Table 3.7. (Livak & Schmittgen 2001)

**Table 3.7** The Method of Livak (A method to calculate relative mRNA expression)

	Control	<i>A. hippocastanum</i>	<i>A. millefolium</i>	<i>P. vulgaris</i>	<i>H. perforatum</i>
Ct <sub>MAPK</sub>	27.72	26.77	22.27	21.72	21.33
Ct <sub>GAPDH</sub>	16.04	15.02	16.84	15.87	17.50
$\Delta Ct_{Cells} = Ct_{GAPDH} - Ct_{MAPK}$					
$\Delta Ct_{Reference} = Ct_{GAPDH} - Ct_{MAPK}$					
$\Delta Ct_{Cells}$	-11.68	-11.75	-12.06	-11.74	-12.12
$\Delta\Delta Ct_{Cells} = \Delta Ct_{reference} - \Delta Ct_{Cells}$					
$\Delta\Delta Ct$	0.00	0.07	0.38	0.06	0.44
$2^{-\Delta\Delta Ct}$	1.00	0.98	0.77	0.97	0.75

Figure 3.19 shows the relative COL1A1 mRNA expressions of treated and non-treated fibroblast line

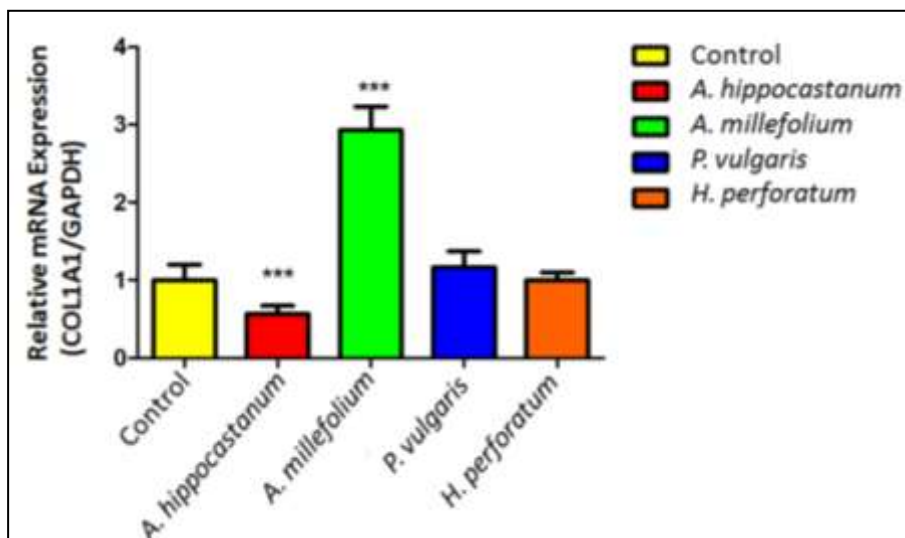


**Figure 3.19** Comparison of COL1A1 mRNA expression of treated and non-treated fibroblast line (Data was evaluated with student t-test \*\*\* $p < 0.0001$ )

### 3.5 Protein Concentrations of Lysates of the Treated and Non-Treated Cells

In this study protein expression of COL1A1 were carried out by using *A. Hippocastanum*, *A. millefolium*, *P. vulgaris*, *H. perforatum* treated and non treated (control) fibroblasts. For that purpose, protein extraction from four plates of each treated and non trated fibroblasts performed by using RIPA buffer procedure and the protein concentrations were determined by BCA method as described in material and methods part. Average protein concentrations of each ones are listed in Table 3.8

**Table 3.8** Average protein concentrations of whole cell lysates of the cells

Cells	Average Protein Concentrations (mg/ml)
Non treated fibroblast	2.00 ± 0.14
<i>A. hippocastanum</i> treated fibroblast	2.81 ± 0.15
<i>A. millefolium</i> treated fibroblast	2.11 ± 0.25
<i>P. vulgaris</i> treated fibroblast	2.19 ± 0.04
<i>H. perforatum</i> treated fibroblast	2.28 ± 0.08

### **3.6 Protein Expression Analyze of COL1A1 in the Treated and Non-Treated Fibroblasts**

Fibroblasts were treated with *A. millefolium*, *H. perforatum*, *P. vulgaris*, *A. hippocastanum*. Western blot experiments were performed on total cellular extracts of these treated and non-treated fibroblasts. COL1A1 protein expressions in treated and non-treated fibroblasts were determined by Western blot by using immunochemical detection specific antibodies.  $\alpha$ - tubulin (52 kDa) was used as internal standard.

COL1A1 primary rabbit polyclonal anti- Collagen I antibody (1/500 dilution) and alkaline phosphatase (AP) conjugated secondary goat anti-rabbit antibody were used for immunochemical detection of COL1A1 protein (Figure 3.20) Band intensities were quantified by using image J visualization software. Figure 3.21 shows the relative protein expressions.

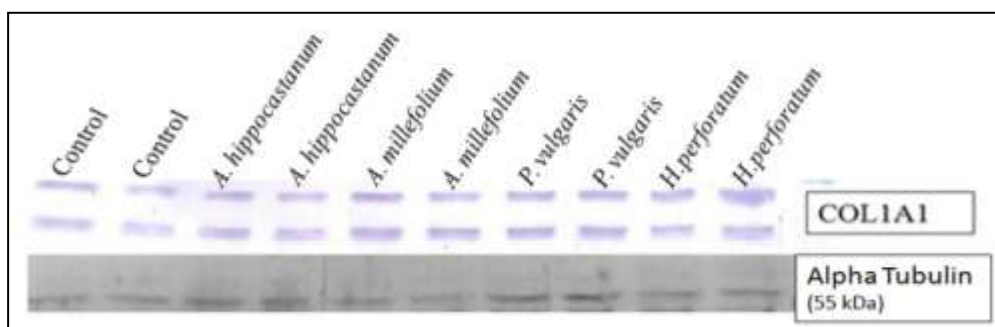


**Figure 3.20** Immunoreactive protein bands of cell lines representing COL1A1 and  $\alpha$ -tubulin used as internal standard.

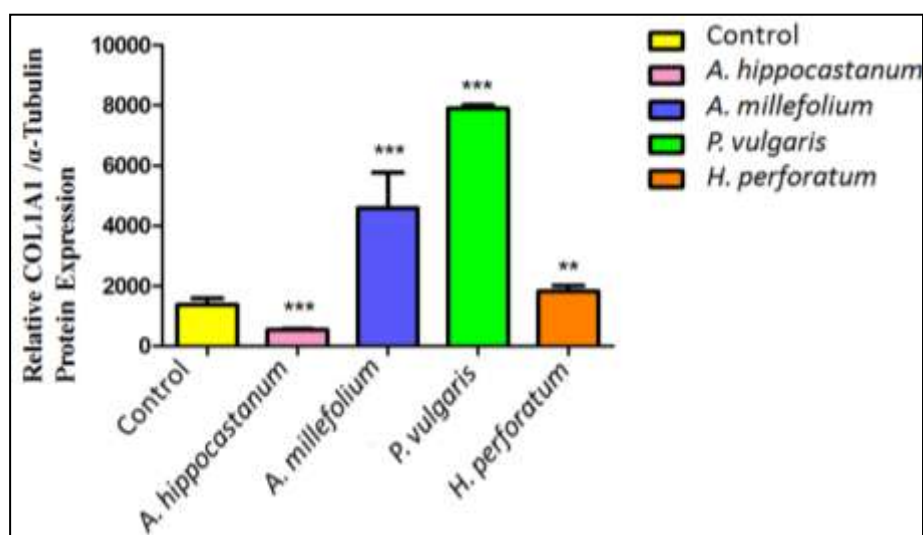


**Figure 3.21** Comparison of COL1A1 protein expressions of treated and non-treated fibroblast lines. The band quantifications are expressed as mean  $\pm$  SD of the relative intensity of three independent experiments (Data was evaluated with student t-test \*\*\* $p < 0.0001$ , \*\* $p = 0.0081$ )

**Table 3.9** Summary of the mRNA and protein expression analysis of Col1A1 from plant extract treated cells relative to non-treated cells.

	Col1A1	
	mRNA Expression (% of control)	Protein Expression (% of control)
<i>Aesculus hippocastanum</i> Treated	57	39,5
<i>Achillea millefolium</i> Treated	293	334,2
<i>Primula vulgaris</i> Treated	117	575,2
<i>Hypericum perforatum</i> Treated	100	132,9

In summary, *A. millefolium* aerial parts extract treated fibroblasts expressed Col1A1 mRNA significantly higher than others. In other words, *A. millefolium* aerial parts extract showed the highest induction rate in relative mRNA expression level. However, *Aesculus hippocastanum* seed cotyledon extract treated fibroblasts expressed Col1A1 mRNA significantly lower than others. Col1A1 relative mRNA expression was found at similar level for the other extract treatments. In addition, *A. millefolium* aerial parts extract treated and *Primula vulgaris* aerial parts extract treated fibroblasts expressed Col1A1 protein significantly higher than others. If we focus on the highest induction, *Primula vulgaris* aerial parts extract showed the highest induction rate in Western blot analysis. However, *Aesculus hippocastanum* seed cotyledon extract treated fibroblasts expressed significantly lower Col1A1.

According to our results and the purpose of this study about searching type I collagen biosynthesis inducing plants, *A. millefolium* (the highest Col1A1 mRNA expression) and *Primula vulgaris* (the highest Col1A1 protein expression) were focused and fractionated for continuous experiments.

### 3.7 Fractionation of Crude Extract

Among the extracts, *A. millefolium* aerial parts extract, which has the highest induction rate in qPCR analysis and *P. vulgaris* aerial parts extract, which has the highest induction rate in Western blot analysis were focused and fractionated.

A 120.0 g of dried crude extracts were dissolved in 3 liters of methanol-water mixture (70:30, v/v) to ensure the solubility of hydrophilic (phenolic) components.

Whole volume of the mixture was transferred into a separatory funnel. The organic phase was decanted of the funnel and evaporated each time. Same procedure was repeated by the next organic solvent specifically selected for their increasing polarity (hexane, chloroform, ethyl acetate). At the end of the final step of the fractionation, remaining aqueous phase was collected and was lyophilized as the aqueous fraction. All of these processes were repeated 3 times. In figure 3.22 and 3.23 the subsequent fractionations of *A. millefolium* and *P. vulgaris* are schemed respectively.

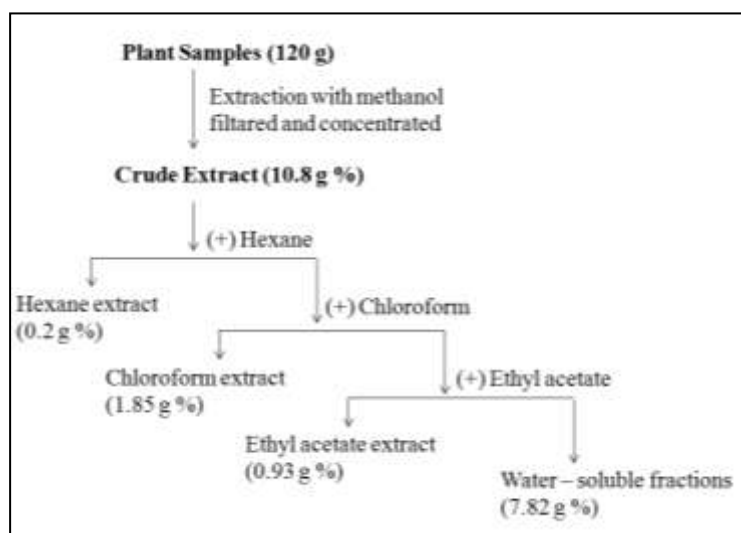


**Figure 3.22** Solvent – solvent fractionation scheme of *A. millefolium* aerial parts crude methanol extract using different solvents of increasing polarity sequentially.

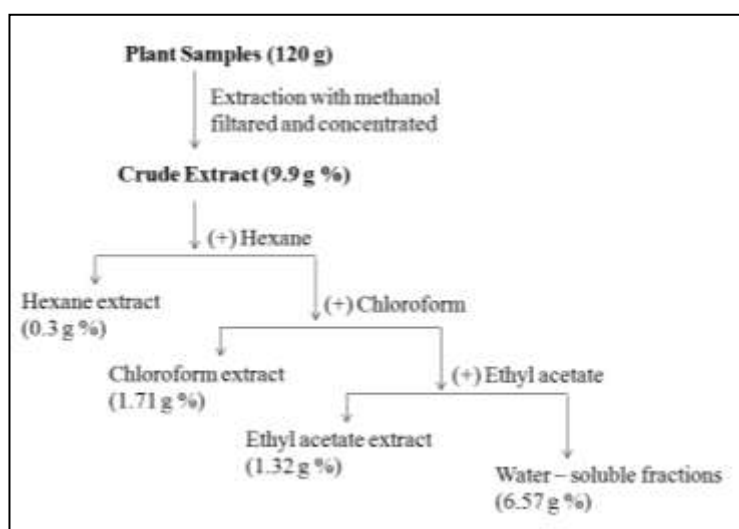


**Figure 3.23** Solvent – solvent fractionation scheme of *P. vulgaris* aerial parts crude methanol extract using different solvents of increasing polarity sequentially.

Crude extracts of many plants, contain carbohydrates and lipoidal materials, may comprise only low concentrations of the phenolic compounds. Therefore, the phenolic compounds of the plant extracts must be enriched before the analysis for the phenolic compositions. The liquid-liquid partitioning (fractioning) strategy based on the solvent polarity has been successfully used. Also, this approach by facilitating a bioactivity guided fractionation may be useful to understand concentrate the active components of the plant extracts. Separation of bioactive compounds present in crude extract can eliminate undesirable chemicals and help identifying the most important phenolic compounds (Faustino, 2010). Solvents such as hexane, dichloromethane and chloroform can be used to eliminate the lipoidal materials from crude extract (Ramirez-Coronel, 2004, Neergheen, 2006, Zhang, 2008).

After we fractionated *A. millefolium* and *P. vulgaris* we removed oils and fatty substances (hexane extract) and again started cell culture experiments with chloroform, ethyl acetate and water-soluble extracts. As a result 0,01 mg/ml plant extract amount for the continuous treatment experiments was selected. According to

cell viability assay, there was an increase in fibroblasts which were treated with ethyl acetate and water-soluble extracts. Therefore, we narrowed the search to *A. millefolium* ethyl acetate, water-soluble extracts and *P. vulgaris* ethyl acetate, water-soluble extracts. Human fibroblasts were exposed to those extracts and then the levels of pro-type 1 collagen were determined by qPCR and immunoblot analysis. The summary of results of the mRNA and protein expression analysis of Col1A1 from plant fractionated extract treated cells relative to non-treated cells is given in table 3.10.

**Table 3.10** Results of the mRNA and protein expression analysis of Col1A1 from plant fractionated extract treated cells relative to non-treated cells (summary)

	Col1A1	
	mRNA Expression (% of control)	Protein Expression (% of control)
<i>Primula vulgaris</i> Et. As. Ext. treated	47,2	145,3
<i>Primula vulgaris</i> Wat. Sol. Ext. treated	76,2	120,4
<i>Achillea millefolium</i> Et. As. Ext. treated	151,8	114,5
<i>Achillea millefolium</i> Wat. Sol. Ext. treated	164,8	117,4

According to qPCR analysis, there was an increase in Col1A1 mRNA expression treated with *A. millefolium* water-soluble extracts and *A. millefolium* ethyl acetate extracts. However, there was a decrease in col1A1 mRNA expression treated with *P.*

*vulgaris* water-soluble extracts and *P. vulgaris* ethyl acetate extracts. According to Western blot analysis, *P. vulgaris* ethyl acetate extract provided the most increase in collA1 protein expression, but this increase was not even two fold. The other fractionated extract treatments did not provide a significant increase in collA1 protein expression. Moreover, although there was a significant decrease in Col1A1 mRNA expression treated with *P. vulgaris* ethyl acetate extract, there was a significant increase in Col1A1 protein expression treated with *P. vulgaris* ethyl acetate extract.

### **3.8 Determination of Cell Viability (AlamarBlue® Assay of Chloroform, Ethyl Acetate and Water-Soluble Extracts)**

In previous sections, the correlation between fibroblast number and alamarBlue® fluorescence was examined. alamarBlue® assay was done as described in section 2.2.5. Optimization of cell number and alamarBlue® intensity was done and cell volume was adjusted to  $4 \times 10^4$  cells/well. Also growth curve was determined. Results were given in in section 3.3.

In this section, to determine optimum concentration of extracts,  $4 \times 10^4$  fibroblasts/well were treated with increasing concentration (from 0.1 mg/ml to 10 mg/ml) chloroform, ethyl acetate, water-soluble extracts of *Achillea millefolium* aerial parts and chloroform, ethyl acetate and water-soluble extracts of *Primula vulgaris* aerial parts as described in section 2.2.5. Results are given in figures 3.24, 3.25, 3.26, 3.27, 3.28 and 3.29.

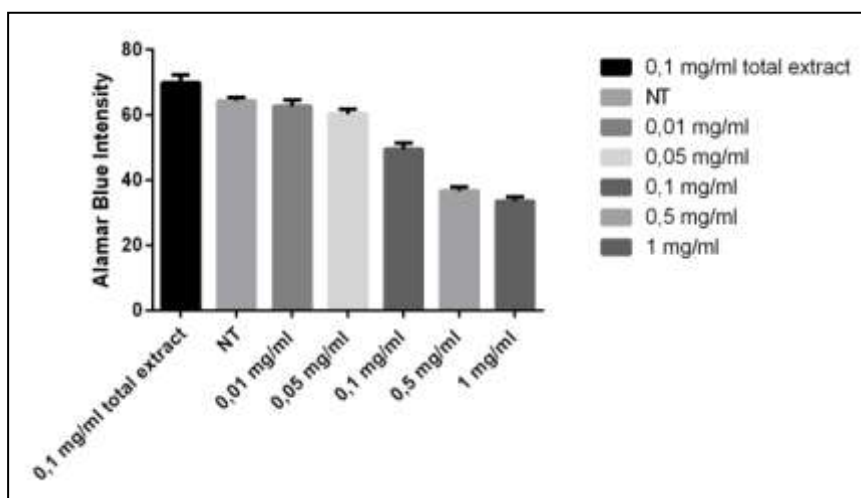


**Figure 3.24** Fibroblasts were treated with increasing concentration of *Primula vulgaris* aerial parts chloroform extract. Fibroblasts were dosed for 48 h with extract then 3 hours with alamarBlue®.

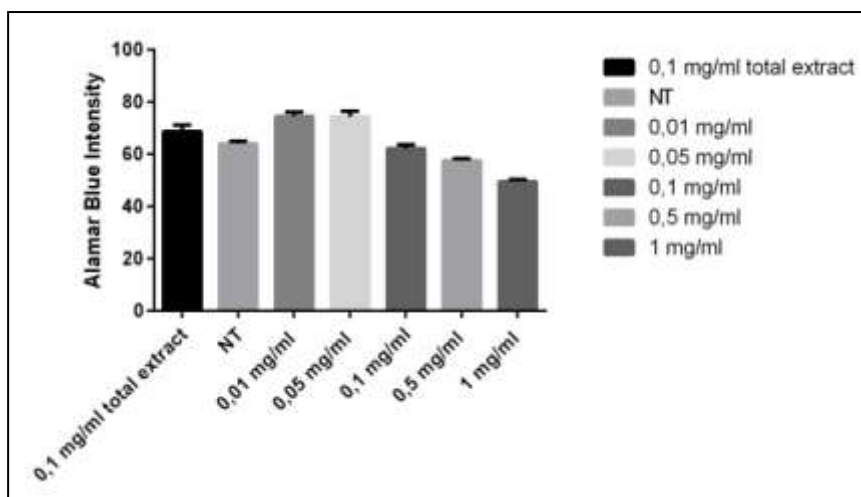


**Figure 3.25** Fibroblasts were treated with increasing concentration of *Primula vulgaris* aerial parts ethyl acetate extract. Fibroblasts were dosed for 48 h with extract then 3 hours with alamarBlue®.

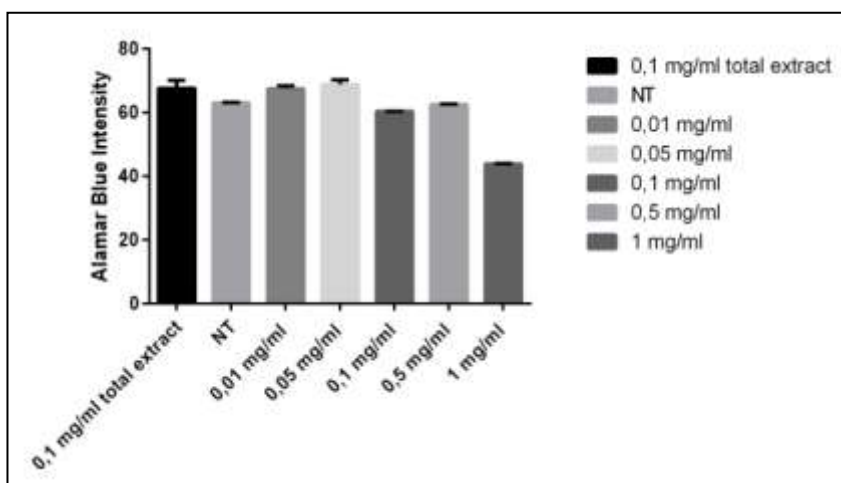


**Figure 3.26** Fibroblasts were treated with increasing concentration of *Primula vulgaris* aerial parts water-soluble extract. Fibroblasts were dosed for 48 h with extract then 3 hours with alamarBlue®.

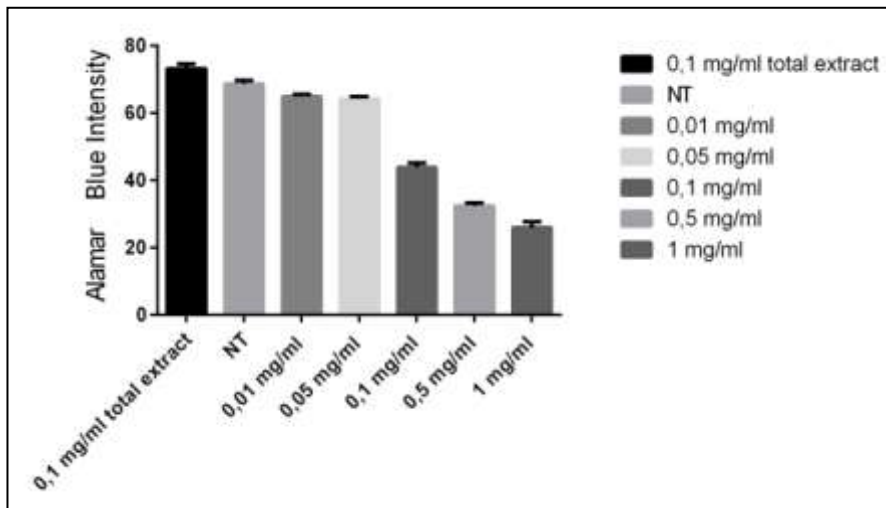


**Figure 3.27** Fibroblasts were treated with increasing concentration of *Achillea millefolium* aerial parts chloroform extract. Fibroblasts were dosed for 48 h with extract then 3 hours with alamarBlue®.

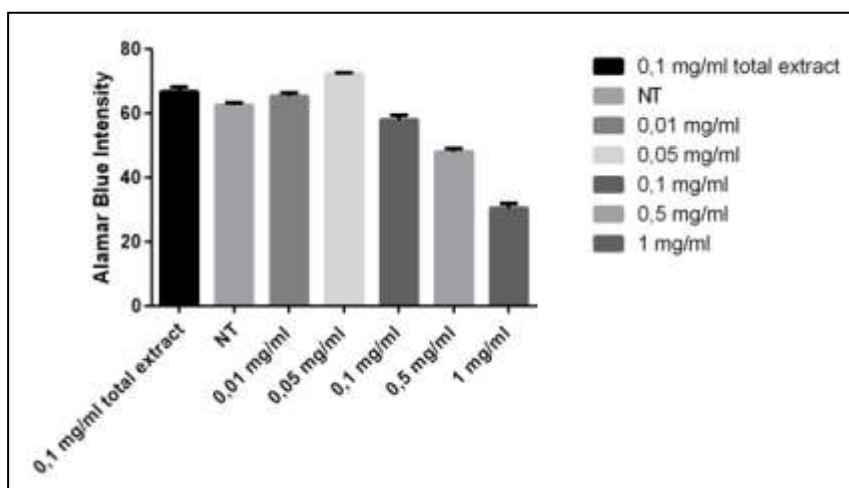


**Figure 3.28** Fibroblasts were treated with increasing concentration of *Achillea millefolium* aerial parts ethyl acetate extract. Fibroblasts were dosed for 48 h with extract then 3 hours with alamarBlue®.

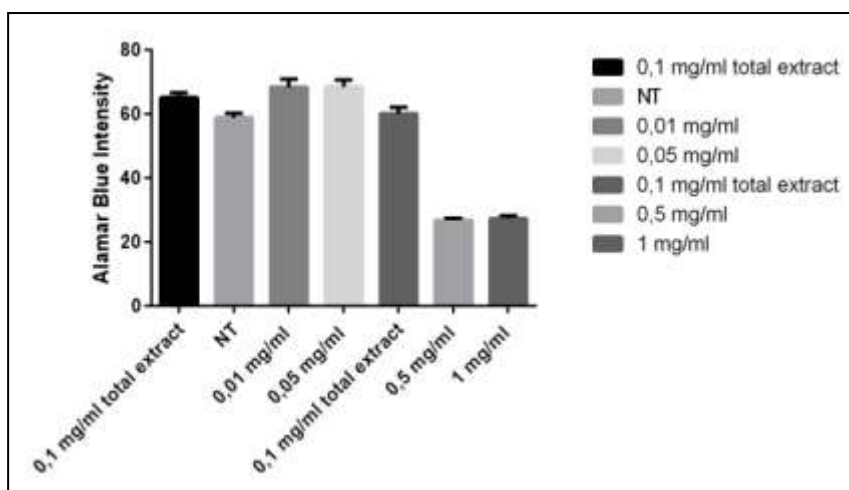


**Figure 3.29** Fibroblasts were treated with increasing concentration of *Achillea millefolium* aerial parts water-soluble extract. Fibroblasts were dosed for 48 h with extract then 3 hours with alamarBlue®.

### 3.9 COL1A1 mRNA Expression in the Fibroblast Line

The mRNA expression of COL1A1 was determined by quantitative real time PCR technique. To calculate relative mRNA expression of COL1A1 GAPDH was used as internal standard. Specific annealing temperatures of the primers of COL1A1 and GAPDH were used.

Relative mRNA expression of COL1A1 was calculated in fibroblast line by producing standard curve from 1:10, 1:100, 1:500, 1:1000 and 1:5000 dilutions of cDNAs (Figure 3.30). The amplification plot shows changes in fluorescence of SYBR green dye I versus cycle number of COL1A1 gene (Figure 3.31). Melt curve analysis was performed to check amplification of specific product (Figure 3.32).

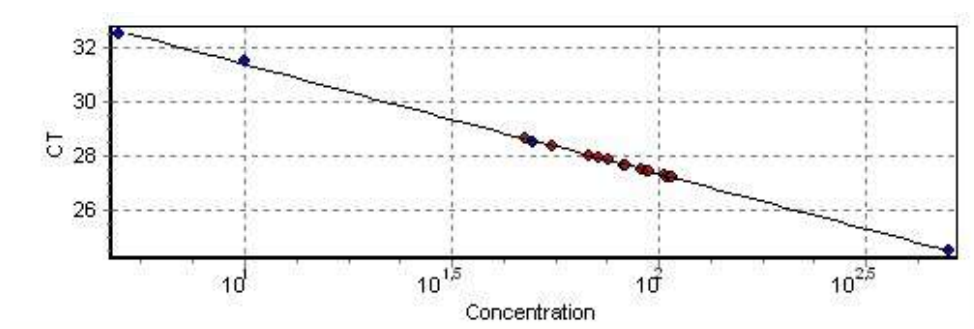


**Figure 3.30** Standard curve generated from serial dilutions of control cDNA to calculate quantities of COL1A1 mRNAs in the treated and non treated fibroblast line.

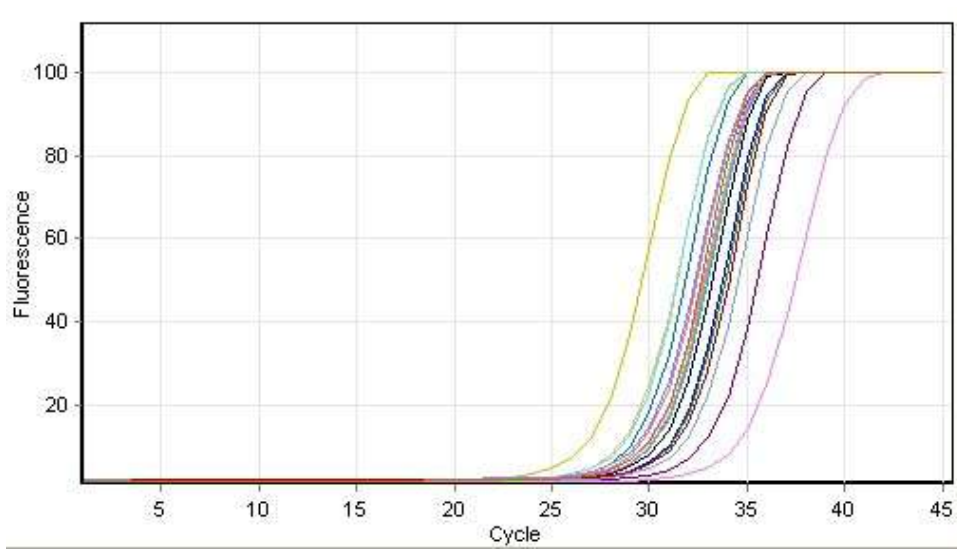


**Figure 3.31** Amplification curve showing the accumulation of fluorescence emission at each reaction cycle.

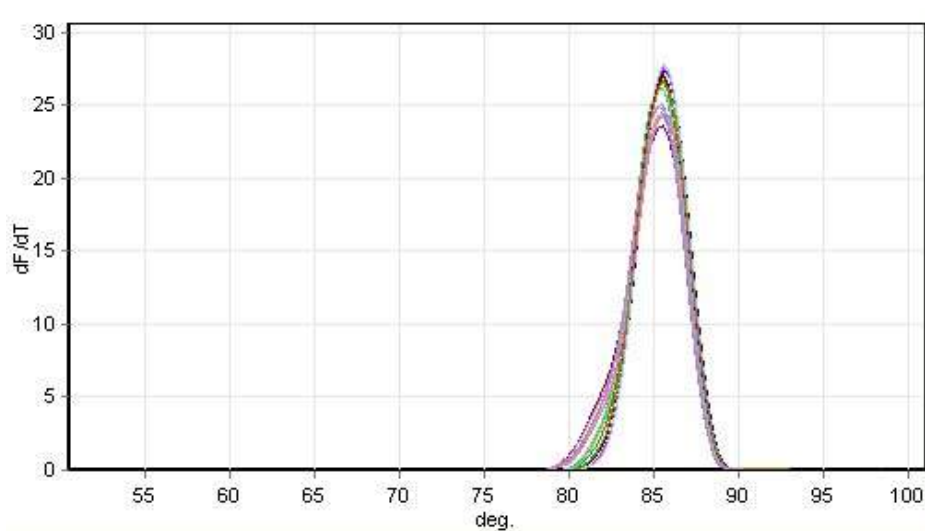


**Figure 3.32** Melting curve showing the fluorescence emission change versus temperature. Detection of single peak means single PCR product (Annealing Temp. is 60 °C).

Corbett Rotor-Gene 600 software was used to obtain the results. These results were normalized with internal standard GAPDH. Livak method was used to determine relative COL1A1 mRNA expression in cell lines by using Ct values (Livak & Schmittgen 2001). Formulation for Livak ( $2^{-\Delta\Delta Ct}$ ) method is given in Table 3.7

Figure 3.33 shows the relative COL1A1 mRNA expressions of treated and non-treated fibroblast line

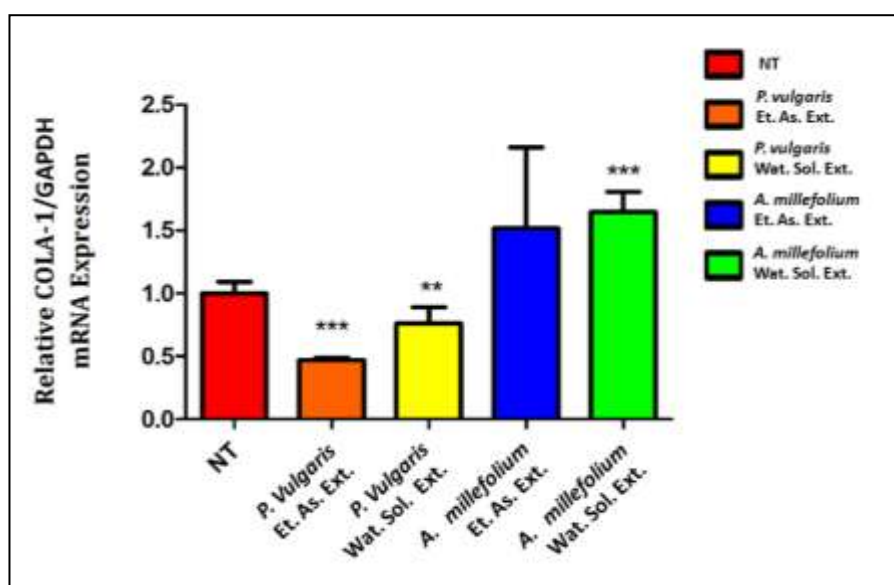


**Figure 3.33** Comparison of COL1A1 mRNA expression of treated and non-treated fibroblast line (Data was evaluated with student t-test \*\*\* $p < 0.0001$ , \*\* $p = 0.0044$ ).

Insulin-like growth factor-1 (IGF-1) stimulates collagen biosynthesis in fibroblasts. Crude extracts that increases pro-type 1 collagen expression level were examined on IGF-I signaling. mRNA expressions of MAPK, IGF-I, IGF-IR and protein

expressions of ERK 1/2, p-ERK1/2, IGF-I, IGF-IR, IRS-I, p-IRS-I were carried out. With this method, we get data for further researches.

### **3.10 Protein Expression Analysis of COL1A1 in the Treated and Non-Treated Fibroblasts**

Fibroblasts were treated with *A. millefolium* ethyl acetate extract, *A. millefolium* water soluble extract, *P. vulgaris* ethyl acetate extract, water soluble extract. Western blot experiments were performed on total cellular extracts of these treated and non-treated fibroblasts. COL1A1 protein expression in fibroblasts was determined by Western blot by using immunochemical detection specific antibodies.  $\alpha$ -tubulin (52 kDa) was used as internal standard.

#### **3.10.1 COL1A1 Protein Expression in Fibroblast Line.**

COL1A1 protein expression was determined by Western blotting. Primary rabbit polyclonal anti-collagen I antibody (1/500 dilution) and alkaline phosphatase (AP) conjugated secondary goat anti-rabbit antibody were used for immunochemical detection of COL1A1 protein (Figure 3.34) Band intensities were quantified by using Image J visualization software. Figure 3.35 shows the relative protein expressions.

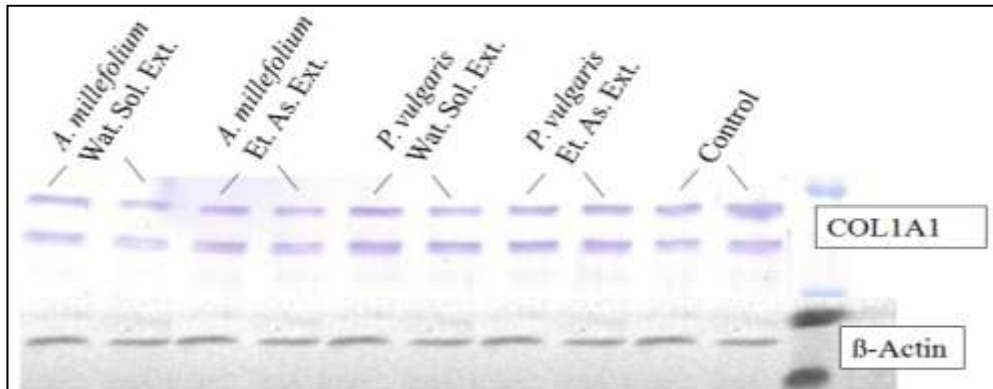


**Figure 3.34** Immunoreactive protein bands of cell lines representing COL1A1 and  $\beta$ -actin used as internal standard.

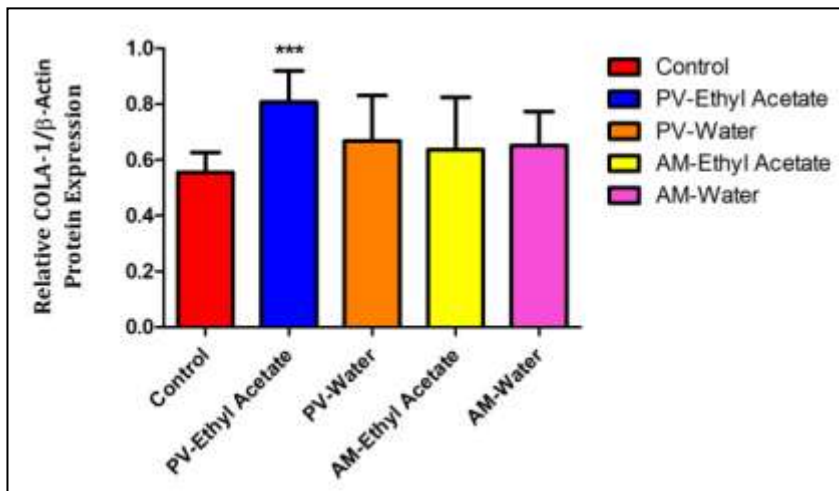


**Figure 3.35** Comparison of COL1A1 protein expressions of treated and non-treated fibroblast lines. The band quantifications are expressed as mean  $\pm$  SD of the relative intensity of three independent experiments (Data was evaluated with student t-test \*\*\* $p=0,0009$ ).

### 3.11 MAPK, IGF-I and IGF-IR mRNA Expressions in the Fibroblast Line

#### 3.11.1 MAPK mRNA Expression in the Fibroblast Line

Quantitative real time PCR technique was used to determine the mRNA expression of MAPK in the treated and non-treated fibroblast line. GAPDH was used as internal standard. Specific annealing temperatures of the primers (MAPK 60°C and GAPDH 58°C) were used.

Relative mRNA expression of MAPK was calculated in the treated and non-treated fibroblast line by producing standard curve from 1:10, 1:100, 1:500, 1:1000 and 1:5000 dilutions of cDNAs (Figure 36). The amplification plot shows changes in fluorescence of SYBR green dye I versus cycle number of MAPK gene (Figure 3.37). Melt curve analysis was performed to check amplification of specific product (Figure 3.38).

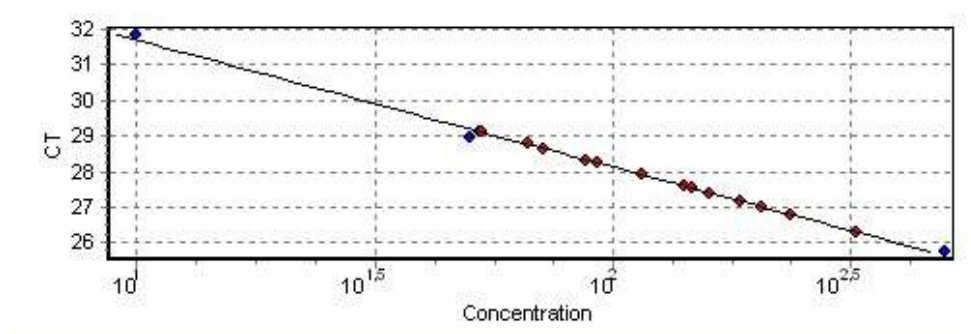


**Figure 3.36** Standard curves generated from serial dilutions of control cDNA to calculate quantities of MAPK 1 mRNAs in the treated and non treated fibroblast line.

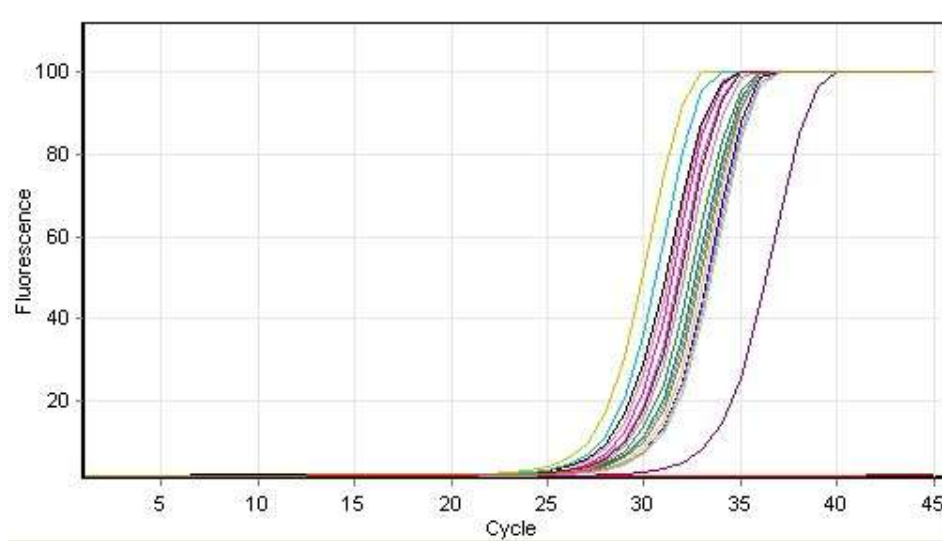


**Figure 3.37** Amplification curve showing the accumulation of fluorescence emission at each reaction cycle.

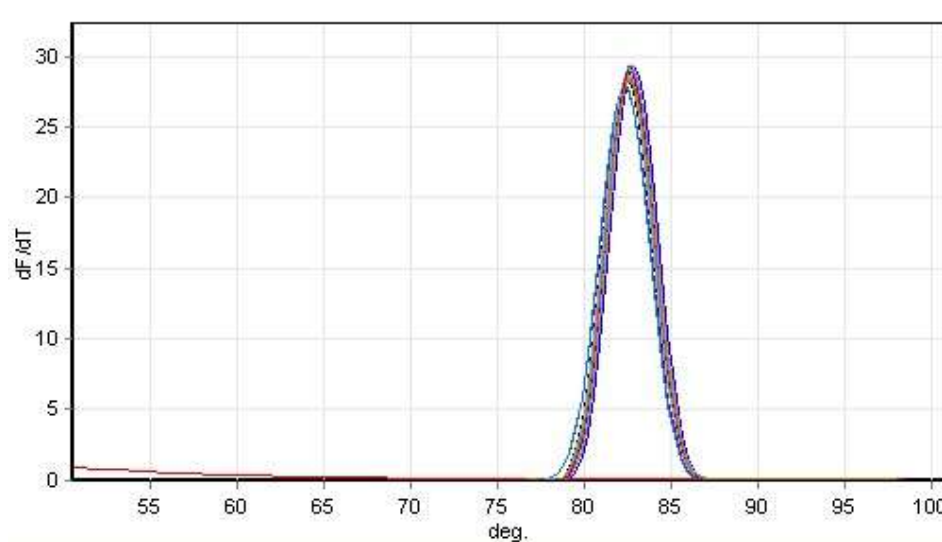


**Figure 3.38** Melting curve showing the fluorescence emission change versus temperature. Detection of single peak means single PCR product. (Annealing Temp. is 60 °C)

Corbett Rotor-Gene 600 software was used to obtain the results. These results were normalized with internal standard GAPDH. Livak method was used to determine relative COL1A1 mRNA expression in cell lines by using Ct values (Livak & Schmittgen 2001). Formulation for Livak ( $2^{-\Delta\Delta Ct}$ ) method is given in Table 3.7 For calculation of relative mRNA expression by using Livak method, Ct values of control fibroblast line were used as reference.

Figure 3.39 shows the relative MAPK mRNA expressions of treated and non-treated fibroblast line.

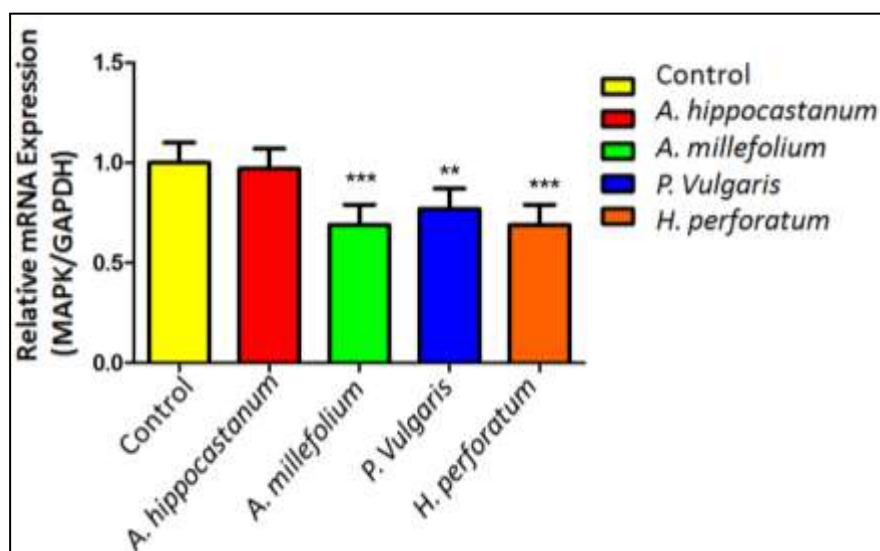


**Figure 3.39** Comparison of MAPK mRNA expression of treated and non-treated fibroblast line (Data was evaluated with student t-test \*\*\* $p < 0.0001$ , \*\* $p = 0.0026$ ).

### 3.11.2 IGF-I mRNA Expression in the Fibroblast Line

Quantitative real time PCR technique was used to determine the mRNA expression of IGF-I in the treated and non-treated fibroblast line. GAPDH was used as internal standard to calculate relative mRNA expression of IGF-I. Specific annealing temperatures of the primers of IGF-I and GAPDH were used.

Relative mRNA expression of IGF-I was calculated in the treated and non-treated cell line by producing standard curve from 1:10, 1:100, 1:500, 1:1000 and 1:5000 dilutions of cDNAs (Figure 3.40). The amplification plot shows changes in fluorescence of SYBR green dye I versus cycle number of IGF-I gene (Figure 3.41). Melt curve analysis was performed to check amplification of specific product (Figure 3.42).

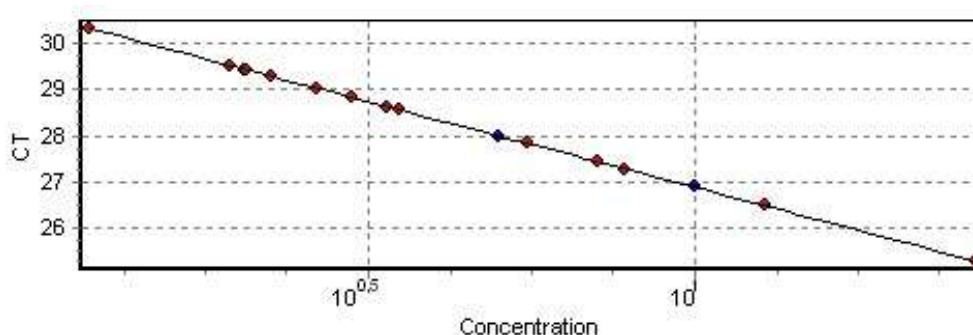


**Figure 3.40** Standard curve generated from serial dilutions of control cDNA to calculate quantities of IGF1 mRNAs in the treated and non treated fibroblast line.

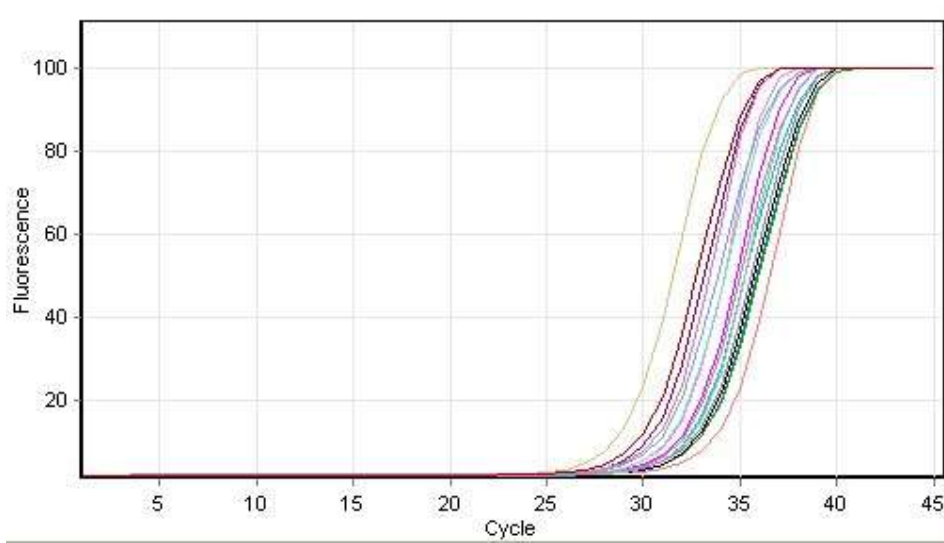


**Figure 3.41** Amplification curve showing the accumulation of fluorescence at each reaction cycle.

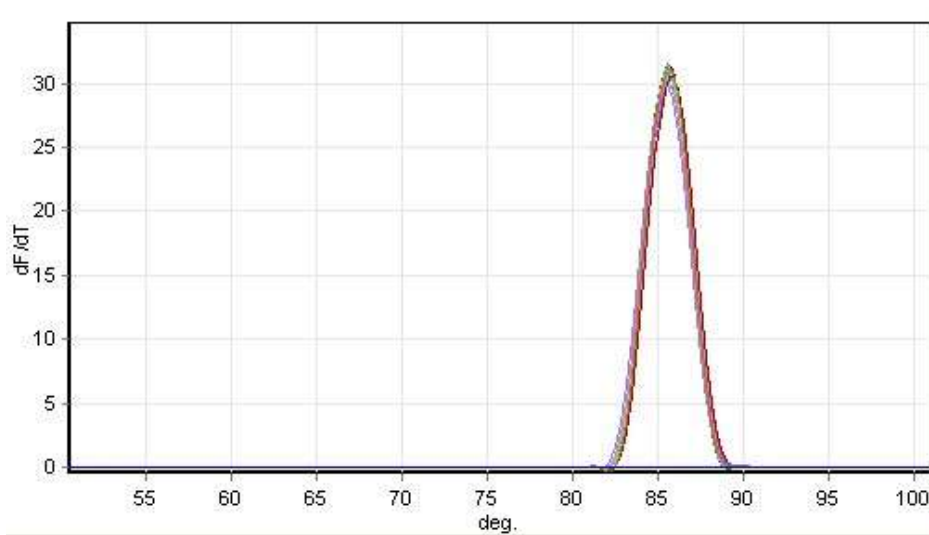


**Figure 3.42** Melting curve showing the fluorescence emission change versus temperature. Detection of single peak means single PCR product (Annealing Temp. is 62 °C).

Corbett Rotor-Gene 600 software was used to obtain the results. These results were normalized with internal standard GAPDH. Livak method was used to determine relative COL1A1 mRNA expression in cell lines by using Ct values (Livak & Schmittgen 2001). Formulation for Livak ( $2^{-\Delta\Delta Ct}$ ) method is given in Table 3.7 For calculation of relative mRNA expression by using Livak method, Ct values of control fibroblast line were used as reference.

Figure 3.43 shows the relative IGF-I mRNA expressions of treated and non-treated fibroblast line.

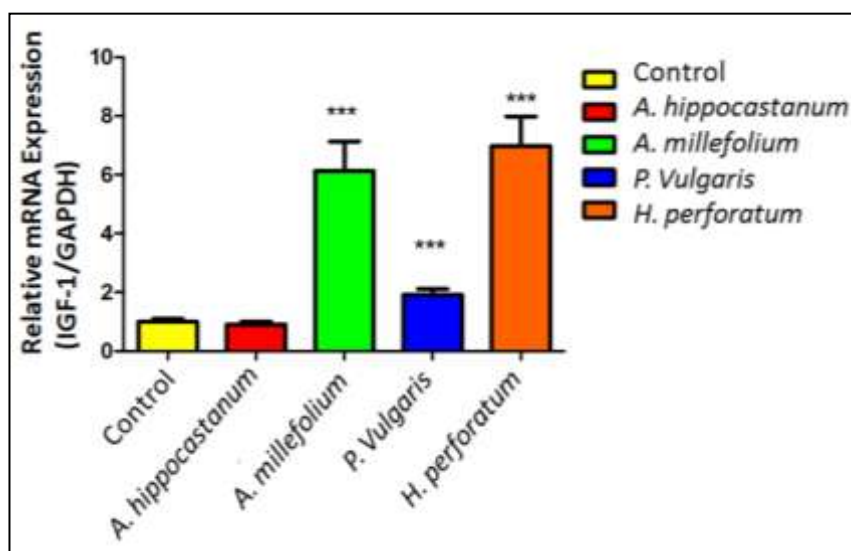


**Figure 3.43** Comparison of IGF-I mRNA expression of treated and non-treated fibroblast line (Data was evaluated with student t-test \*\*\* $p < 0.0001$ ).

### 3.11.3 IGF-IR mRNA Expression in the Fibroblast Line

Quantitative real time PCR technique was used to determine the mRNA expression of IGF-IR in the treated and non-treated cell lines. GAPDH was used as internal standard. Specific annealing temperatures of the primers (IGF1R and GAPDH) were used.

Relative mRNA expression of IGF-IR was calculated in fibroblast lines by producing standard curve from 1:10, 1:100, 1:500, 1:1000 and 1:5000 dilutions of cDNAs (Figure 44). The amplification plot shows changes in fluorescence of SYBR green dye I versus cycle number of IGF-IR gene (Figure 45). Melt curve analysis was performed to check amplification of specific product (Figure 46).

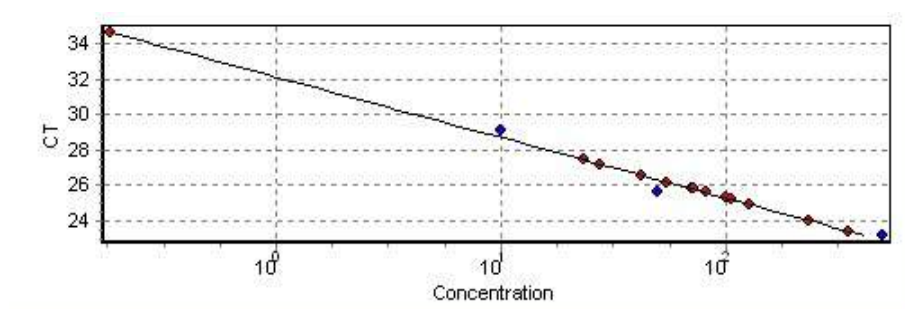


**Figure 3.44** Standard curve generated from serial dilutions of control cDNA to calculate quantities of IGF-IR mRNAs in the treated and non treated fibroblast line.

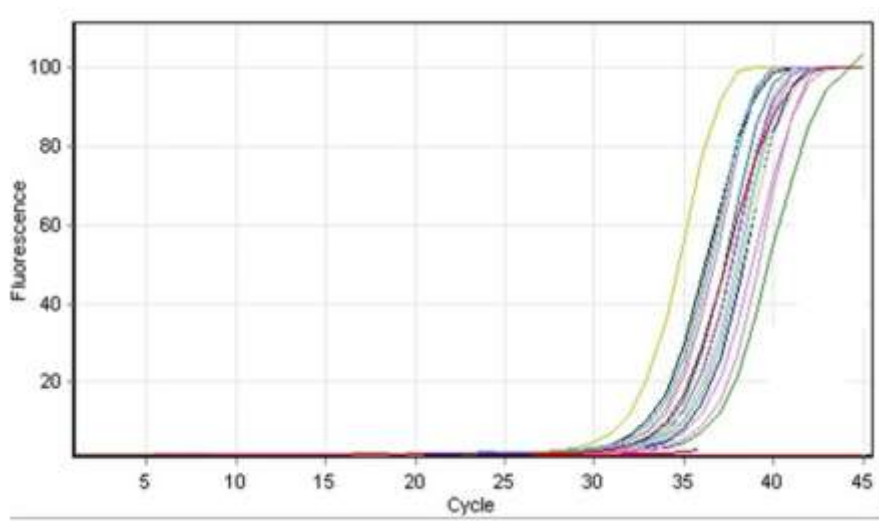


**Figure 3.45** Amplification curve showing the accumulation of fluorescence emission at each reaction cycle.

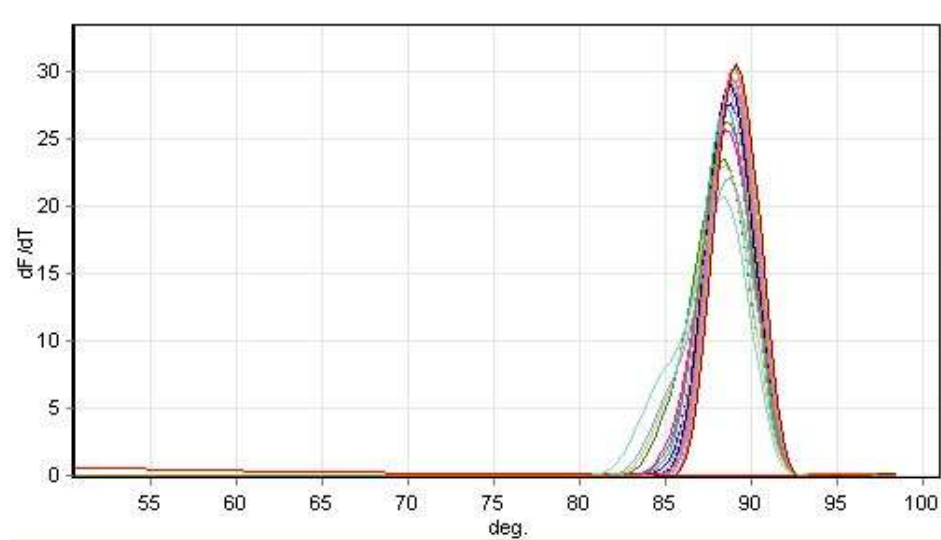


**Figure 3.46** Melting curve showing the fluorescence emission change versus temperature. Detection of single peak means single PCR product (Annealing Temp. is 62 °C).

Corbett Rotor-Gene 600 software was used to obtain the results. These results were normalized with internal standard GAPDH. Livak method was used to determine relative COL1A1 mRNA expression in cell lines by using Ct values (Livak & Schmittgen 2001). Formulation for Livak ( $2^{-\Delta\Delta Ct}$ ) method is given in Table 3.7 For calculation of relative mRNA expression by using Livak method, Ct values of control fibroblast line were used as reference.

Figure 3.47 shows the relative IGF-IR mRNA expressions of treated and non-treated fibroblast line.

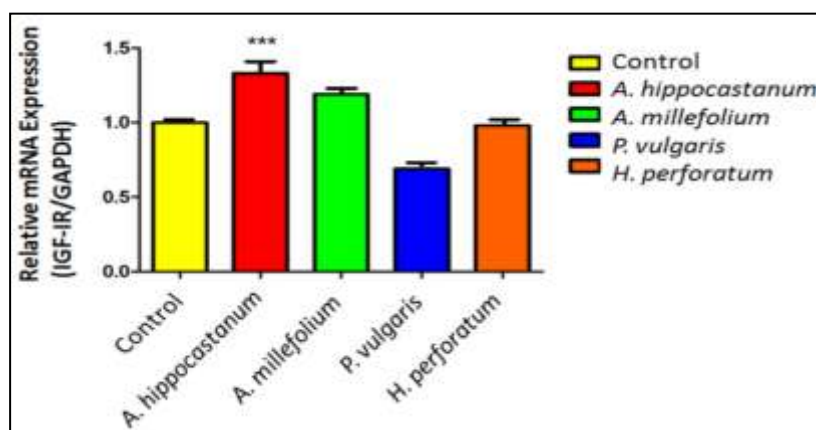


**Figure 3.47** Comparison of IGF-IR mRNA expression of treated and non-treated fibroblast line (Data was evaluated with student t-test \*\*\* $p < 0.0001$ ).

### 3.12 Protein Concentrations of Lysates of the Treated and Non-Treated Cells

In this study protein expressions of ERK 1/2, p-ERK1/2, IGF1, IGF1R, IRS1, p-IRS1 were carried out by using *A. hippocastanum*, *A. millefolium*, *P. vulgaris*, *H.*

*perforatum* treated and non treated (control) fibroblasts. For that purpose, protein extraction from four plates of each treated and non treated fibroblasts performed by using RIPA buffer procedure and the protein concentrations were determined by BCA method as described in material and methods part. Average protein concentrations of each ones were listed in Table 3.8 in section 3.5.

### **3.13 Protein Expression Analysis of ERK ½, p-ERK ½ IGF-I, IRS-1, p-IRS-1 in the Treated and Non-Treated Fibroblasts**

Fibroblasts were treated with *Achillea millefolium*, *Hypericum perforatum*, *Primula vulgaris*, *Aesculus hippocastanun*. Western blot experiments were performed on total cellular extracts of these treated and non-treated fibroblasts. ERK ½, p-ERK ½, IGF-I, IRS-1, p-IRS-1 protein expressions in treated and non-treated fibroblasts were determined by Western blot by using immunochemical detection specific antibodies.  $\alpha$ -Tubulin (52 kDa) was used as internal standard.

#### **3.13.1 ERK 1/2 Protein Expression in Fibroblast Line.**

ERK ½ protein expression was determined by Western blotting. Primary mouse polyclonal anti-IGF1 antibody (1/500 dilution) and a horseradish peroxidase (HRP) conjugated secondary rabbit anti-mouse antibody (1/2000 dilution) were used for immunochemical detection of ERK ½ protein (Figure 3.48). Band intensities were quantified by using Image J visualization software. Figure 3.49 shows the relative protein expressions.

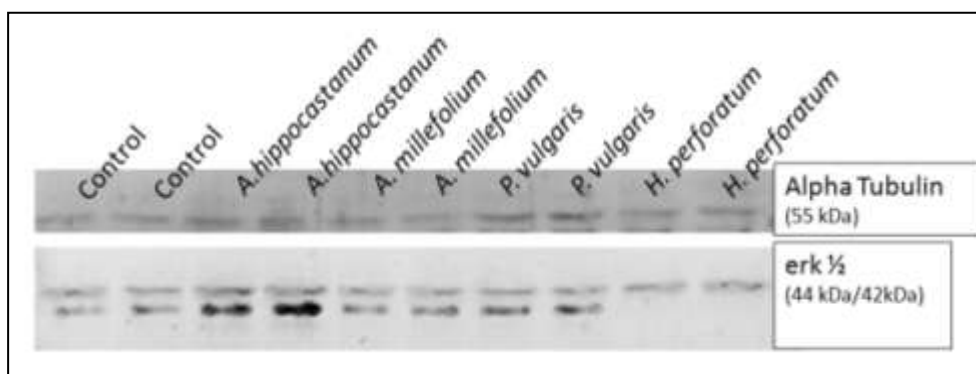


**Figure 3.48** Immunoreactive protein bands of cell lines representing ERK 1/2 and alpha tubulin used as internal standard.

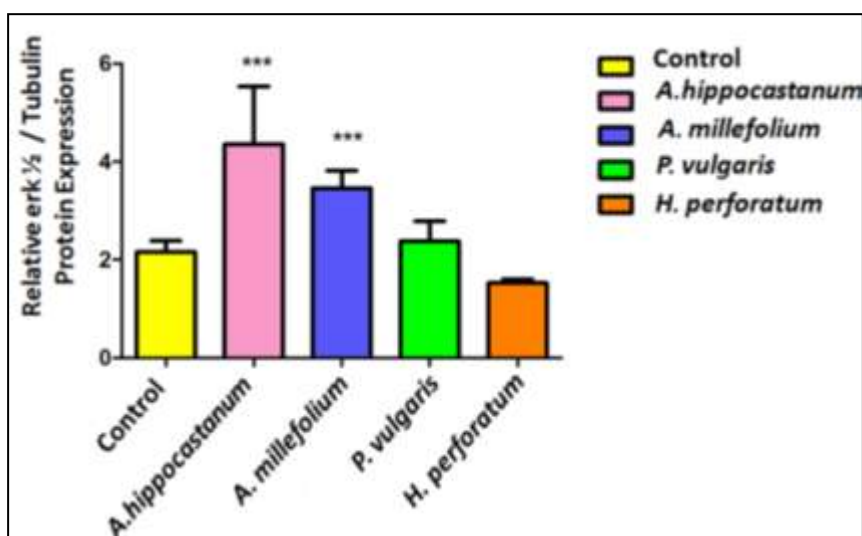


**Figure 3.49** Comparison of ERK 1/2 protein expressions of treated and non-treated fibroblast lines. The band quantifications are expressed as mean  $\pm$  SD of the relative intensity of three independent experiments (Data was evaluated with student t-test \*\*\* $p < 0.0001$ , \*\* $p = 0.0015$ , \* $p > 0.0189$ ).

### 3.13.2 p-ERK 1/2 Protein Expression in Fibroblast Line.

Expression of p-ERK 1/2 protein was determined by Western blotting. Primary mouse polyclonal anti-p-ERK 1/2 antibody (1/500 dilution) and a horseradish peroxidase (HRP) conjugated secondary rabbit anti-mouse antibody (1/2000 dilution) were used for immunochemical detection of p-ERK 1/2 protein (Figure 3.50). Band intensities were quantified by using Image J visualization software. Figure 3.51 shows the relative protein expressions.

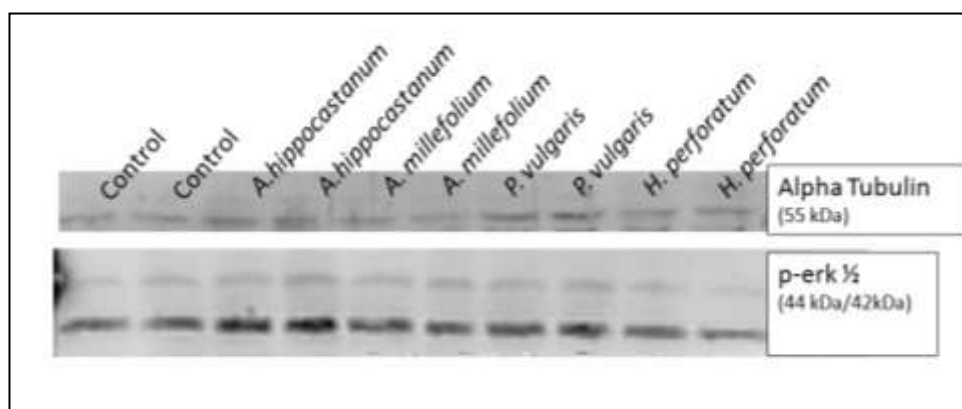


**Figure 3.50** Immunoreactive protein bands of cell lines representing p-ERK 1/2 and alpha tubulin used as internal standard.

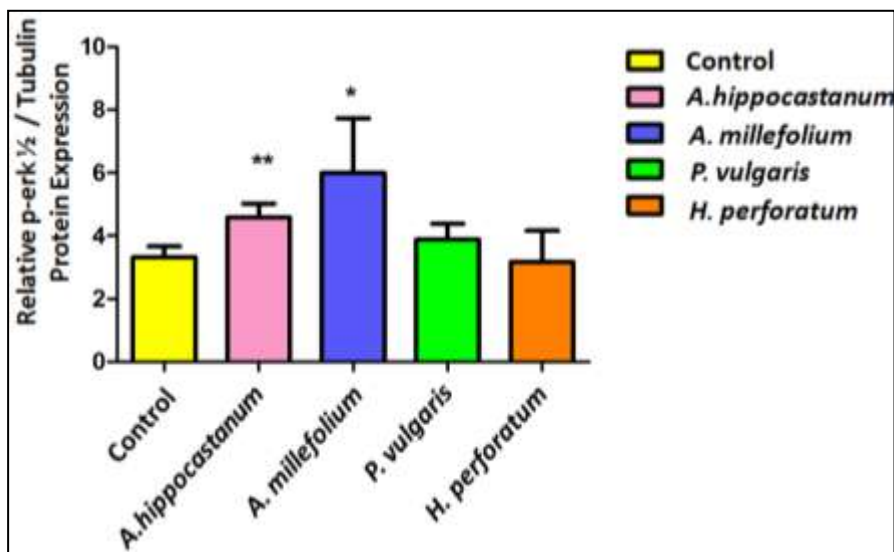


**Figure 3.51** Comparison of p-ERK 1/2 protein expressions of treated and non-treated fibroblast lines. The band quantifications are expressed as mean ± SD of the relative intensity of three independent experiments (Data was evaluated with student t-test \*\*p=0.0015, \*p=0.01).

### 3.13.3 IGF-I Protein Expression in Fibroblast Line.

IGF-I protein expression was determined by Western blotting. Primary goat polyclonal anti-IGF1 antibody (1/500 dilution) and a horseradish peroxidase (HRP) conjugated secondary mouse anti-goat antibody (1/2000 dilution) were used for immunochemical detection of IGF1 protein (Figure 3.52). Band intensities were quantified by using Image J visualization software. Figure 3.53 shows the relative protein expressions.

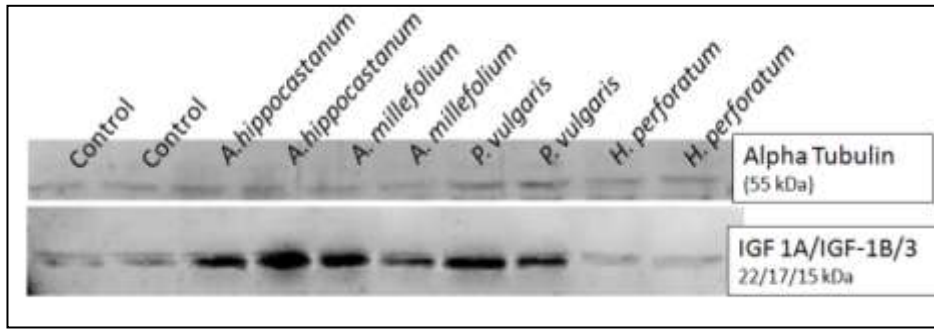


**Figure 3.52** Immunoreactive protein bands of cell lines representing IGF1 and Alpha tubulin used as internal standard.

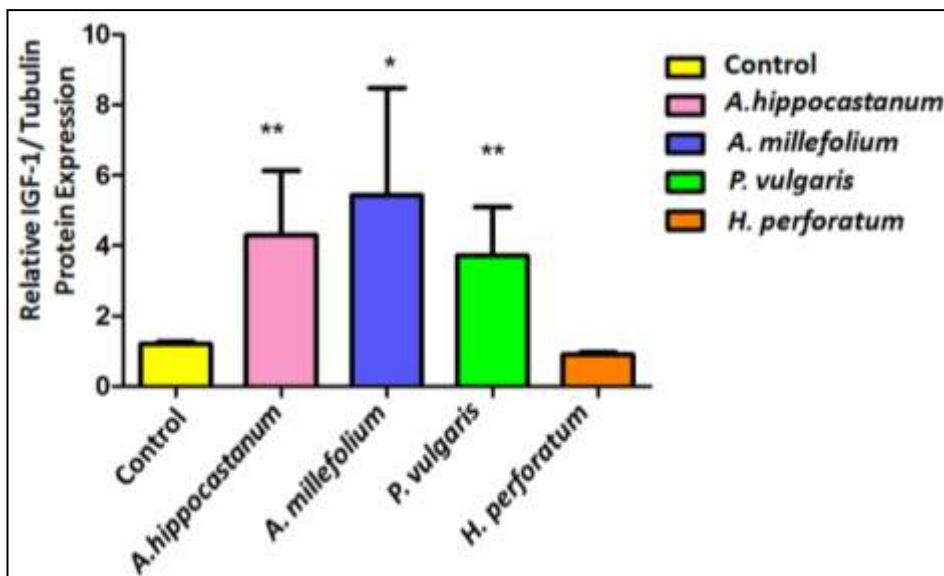


**Figure 3.53** Comparison of IGF-1 protein expressions of treated and non-treated fibroblast lines. The band quantifications are expressed as mean  $\pm$  SD of the relative intensity of three independent experiments (Data was evaluated with student t-test \*\* $p < 0.005$ , \* $p < 0.05$ ).

### 3.13.4 IRS-1 Protein Expression in Fibroblast Line

IRS-1 protein expression was determined by Western blotting. Primary rabbit polyclonal anti- IRS-1 antibody (1/500 dilution) and a horseradish peroxidase (HRP) conjugated secondary mouse anti-rabbit (1/2000 dilution) were used for immunochemical detection of IRS-1 protein (Figure 3.54 ) Band intensities were quantified by using Image J visualization software. Figure 3.55 shows the relative protein expressions.

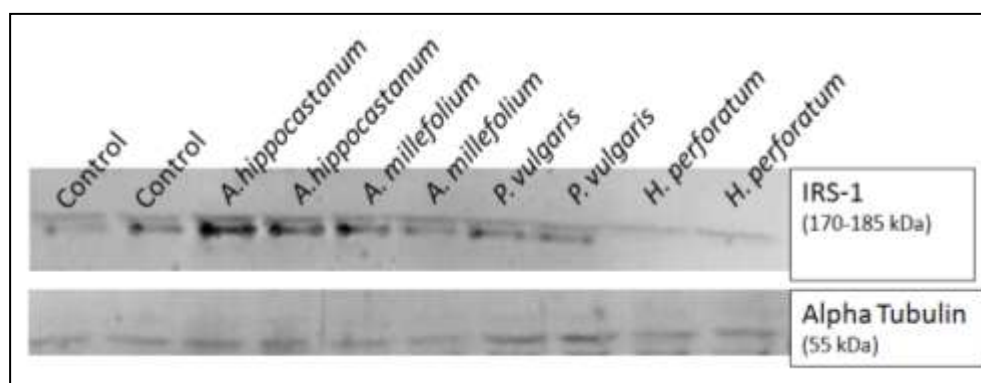


**Figure 3.54** Immunoreactive protein bands of cell lines representing IRS-1 and alpha tubulin used as internal standard.

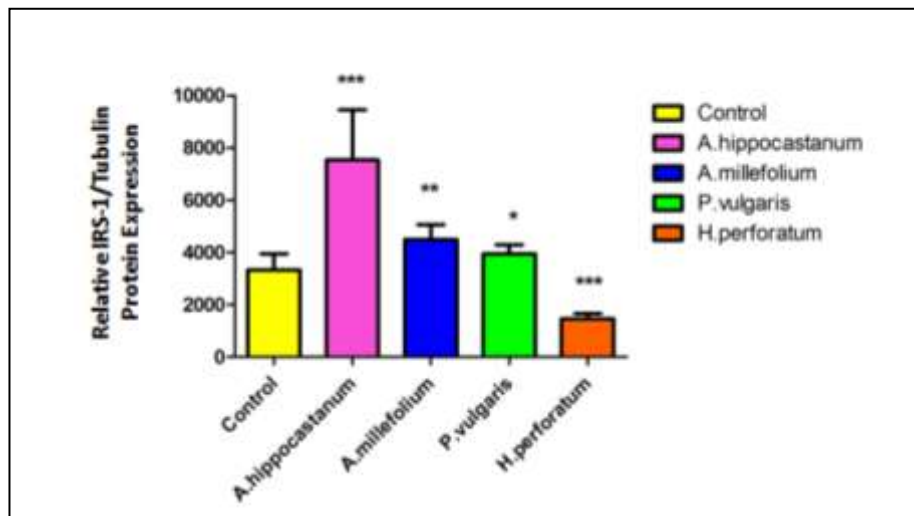


**Figure 3.55** Comparison of IRS-1 protein expressions of treated and non-treated fibroblast lines. The band quantifications are expressed as mean  $\pm$  SD of the relative intensity of three independent experiments (Data was evaluated with student t-test \*\*\* $p < 0.0001$ , \*\* $p = 0.0015$ , \* $p > 0.0189$ ).

### 3.13.5 p-IRS-1 Protein Expression in Fibroblast Line

p-IRS-1 protein expression was determined by Western blotting. Primary rabbit polyclonal anti-p-IRS-1 antibody (1/500 dilution) and a horseradish peroxidase (HRP) conjugated secondary mouse anti-rabbit antibody (1/2000 dilution) were used for immunochemical detection of p-IRS-1 protein (Figure 3.56) Band intensities were quantified by using Image J visualization software. Figure 3.57 shows the relative protein expressions.

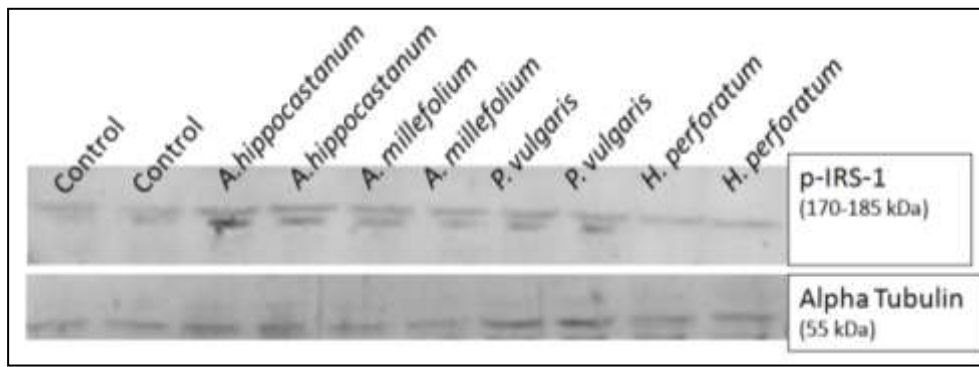


**Figure 3.56** Immunoreactive protein bands of cell lines representing p-IRS-1 and alpha tubulin used as internal standard.

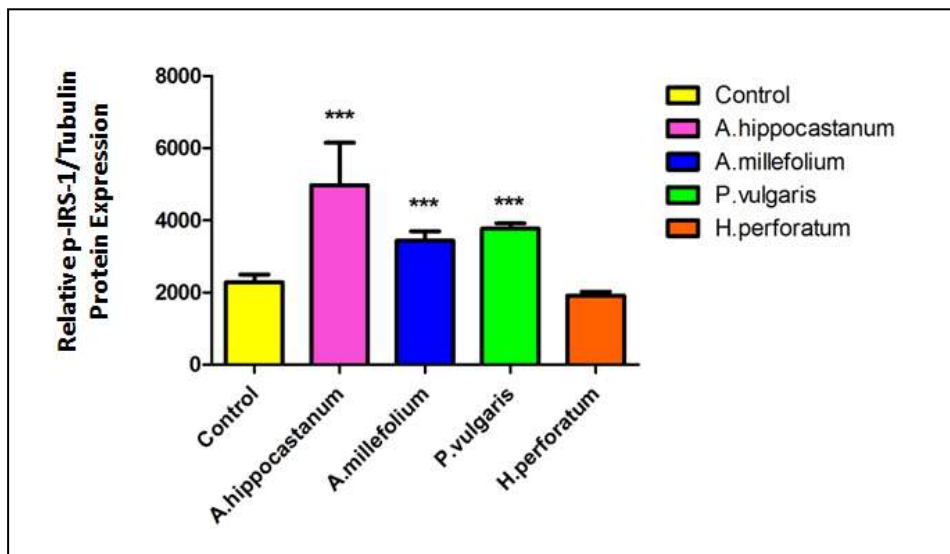


**Figure 3.57** Comparison of p-IRS-1 protein expressions of treated and non-treated fibroblast lines. The band quantifications are expressed as mean  $\pm$  SD of the relative intensity of three independent experiments (Data was evaluated with student t-test \*\*\* $p < 0,0001$ ).

## CHAPTER 4

### DISCUSSION

A skin dermis is primarily composed of collagenous extracellular matrix and dermal fibroblasts play an important role on its maintenance. Type I collagen, which is most abundant structural protein in skin and secreted by fibroblasts, plays the biggest role to maintain strength of the skin. Aged skin is characterized by decreased collagen levels in the dermis (Fisher et al. 2009). Getting old results in diminished synthesis of type I collagen, results in dermal elasticity loss (Fisher et al. 2002). Promoting type I collagen production is a good strategy against wrinkle formation. There have been many herbal products developed to repair the aging defects by triggering fibroblasts to produce collagen. These herbal products were built up based on the information from past to present and still continues to expand rapidly across the world. In addition to the benefits, some of those manufactured herbal products have the adverse effects as a result of unscientific production. Although there are many plants used in herbal products, *A. millefolium*, *A. hippocastanum*, *H. perforatum* and *P. vulgaris* are the most popular ones. In previous studies, extract of *A. millefolium* is described as a biological cosmetic additive; it has been shown to be effective on wrinkle formation by its anti-oxidant capacity (Masaki, 1995). *Hypericum perforatum* extract is also used in regenerative products; little research has been done about its cosmetic formulations but it has wide range applications, including wound healing and eczema (Butterweck, 2003; Maisenbacher and Kovar, 1992). *Primula vulgaris* has different areas to be applied especially within the food, cosmetic world and many researches were done about its activities (Demir, 2014). It has been known that reactive oxygen species play a main role in the biological events that lead to the clinical evidences of wrinkle formation therefore anti-oxidants are critical in skin aging (McCullough & Kelly 2006). There are many reports suggest an association between skin ageing and anti-oxidant activities of these plants (Wilkinson & Brown,

1999; Benedi et al., 2004). But little research was done about their molecular mechanism (Fujimura, et al. 2006). In this study, *in-vitro* experiment steps are planned to search for plants which induces type I collagen biosynthesis in human dermal fibroblasts. In vitro experiments are thought as preliminary, essential and fundamental steps for cosmetic research by providing directly usage of human cells without doing animal tests. These experiments provide to study cytotoxicity and molecular activity of various types of products influencing skin aging processes. Dermis fibroblast is considered as a good model for studying anti-wrinkle and aging-preventing components (Debowska, 2010). To determine useful plant extract for skin product, which has an ability to increase type I collagen synthesis, human dermal fibroblast line (ATCC: PCS-201-012) was used.

Initially we made free radical scavenging activity tests to make comparisons. Seed cotyledon of *A. hippocastanum* and aerial parts of *H. perforatum*, *P. vulgaris*, *A. millefolium* were used for this purpose. As the result of these assays *H. perforatum* aerial parts extract was found as having the highest radical scavenging activity among other extracts with EC<sub>50</sub> value of 0.188627 mg/mL in DPPH method, TEAC value of 3,86721 µmol/g in ABTS method and TEAC value of 1,9193 µmol/g in CUPRAC Assay. Extracts of *A. hippocastanum* seed cotyledon, *A. millefolium* aerial parts, *P. vulgaris* aerial parts had radical scavenging activities respectively with an increasing order. When phenolic compounds were searched, *H. perforatum* aerial parts extract has revealed the highest amount of phenolic compounds as 0,096 mg gallic acid equivalence in 1 mg of extract. Total flavonoid content was calculated and *A. hippocastanum* seed cotyledon extract had the highest amount of flavonoid as 0,065 mg/mg.

There isn't any study comparing antioxidant activities, total phenolic and flavonoids contents of methanol extracts of *A. hippocastanum* seed cotyledon, *A. millefolium* aerial parts, *P. vulgaris* aerial parts, *H. perforatum* aerial parts. But there are many studies done one by one about their anti-oxidant activities, total phenolic and flavonoids contents of different parts. The studied parts of the plants displayed different results from those observed from plants of other geographical origin. The scavenging ability of *H. perforatum* aerial parts methanol extract from v. Yagodina,

Rhodope Mountains (Zheleva-Dimitrova, 2010) was found has significant values and corresponds to the presence of high quantity of phenolic compounds ( $77.6\% \pm 0.5$  for DPPH and  $81.2\% \pm 0.4$  for ABTS). The scavenging ability of *A. Hippocastanum* seed cotyledon methanol extract from Turkey (Sagdicoglu Celep, 2012) was found has significant value with EC<sub>50</sub> value of 0.168 mg/mL in DPPH method.

After the antioxidant capacity determination molecular mechanisms of these plant extracts at both transcriptional and translational levels are studied to search for type I collagen biosynthesis-inducing plants and to select the most useful plant extract for herbal skin products. According to cell viability results, there were an increase in fibroblast number treated with 0.1 mg/ml *Achillea millefolium* aerial parts extract and 0.1 mg/ml *Primula vulgaris* aerial parts extract. However, there was no increase in cell viability of fibroblasts treated with *Aesculus hippocastanum* seed cotyledon extract and *Hypericum Perforatum* aerial parts extract. For these extracts, least detrimental concentration dosage was selected. As a result of our experiments, 0.1 mg/ml plant extract amount for the continuous treatment experiments was determined.

As a next step, mRNA and protein expression levels were determined by qPCR and Western blotting technique, respectively. The pro-type 1 collagen (Col1A1) mRNA and protein expressions in the plant extract treated and non-treated fibroblast line are shown in figure 3.20 and 3.21, respectively.

According to these experimental results, *A. millefolium* aerial parts extract treated fibroblasts expressed Col1A1 mRNA significantly higher than others. In addition, *A. millefolium* aerial parts extract treated and *Primula vulgaris* aerial parts extract treated fibroblasts expressed Col1A1 protein significantly higher than others. If we focus on the highest induction, *Primula vulgaris* aerial parts extract showed the highest induction rate in Western blot analysis. However, *Aesculus hippocastanum* seed cotyledon extract treated fibroblasts expressed significantly lower Col1A1.

If our experimental results are compared with researches in literature, although, there are many herbal products that contain *A. millefolium*, *A. hippocastanum*, *H. perforatum* and *P. vulgaris* extracts, molecular researches about them are not

enough. Indeed, there isn't any research in literature done about collagen synthesis action of *Achillea millefolium*, *Primula vulgaris* plant extracts. Also, there is little research about *Aesculus hippocastanum*, and *Hypericum perforatum* extracts about collagen proliferation in human dermal fibroblasts. We searched about the activity of seed cotyledon of *A. hippocastanum* and couldn't find any increase in collagen biosynthesis but Fujimura et al., demonstrated that *A. hippocastanum* leaf extract is able to induce collagen biosynthesis by contraction forces in fibroblasts. (Fujimura et al. 2006). Dikmen et al. and Öztürk showed that *H. perforatum* extract facilitates collagen biosynthesis (Dikmen, 2011 & Öztürk, 2007). Our result is consistent with Dikmen et al. and Öztürk's results.

Furthermore, our study can be the first research that provides to compare the effect of four plant extracts on collagen expression transcriptionally and translationally. Although there are few researches about collagen proliferation effects of our chosen plant extracts, it is known that there are many researches show that various species of plants have been increasing collagen proliferation. For example Takasao, et al. showed that cinnamon extract triggers collagen biosynthesis in dermal fibroblasts. (Takasao, 2012). Tanaka et al., also demonstrated (in a different study) that Aloe sterols stimulate collagen biosynthesis in human fibroblasts, and that Aloe vera gel powder containing Aloe sterols reduce facial wrinkles in women (Tanaka, 2015). These literature results show that plant extracts can provide an increase in collagen synthesis and also active components of these extracts can be found and can be compared.

According to our results and the purpose of this study about searching type I collagen biosynthesis inducing plants, *A. millefolium* (the highest Col1A1 mRNA expression) and *Primula vulgaris* (the highest Col1A1 protein expression) were focused and fractionated for continuous experiments. We removed oils and fatty substances (hexane extract) and again started cell culture experiments with chloroform, ethyl acetate and water-soluble extracts. According to cell viability assay, there was an increase in fibroblasts which were treated with ethyl acetate and water-soluble extracts. Therefore, we narrowed the search to *A. millefolium* ethyl acetate, water-soluble extracts and *P. vulgaris* ethyl acetate, water-soluble extracts. The summary

of results of the mRNA and protein expression analysis of Col1A1 from plant fractionated extract treated cells relative to non-treated cells is given in table 3.10.

According to qPCR analysis, there was an increase in Col1A1 mRNA expression treated with *A. millefolium* water-soluble extracts and *A. millefolium* ethyl acetate extracts. However, there was a decrease in col1A1 mRNA expression treated with *P. vulgaris* water-soluble extracts and *P. vulgaris* ethyl acetate extracts. According to Western blot analysis, *P. vulgaris* ethyl acetate extract provided the most increase in col1A1 protein expression, but this increase was not even two fold. The other fractionated extract treatments did not provide a significant increase in col1A1 protein expression. Moreover, although there was a significant decrease in Col1A1 mRNA expression treated with *P. vulgaris* ethyl acetate extract, there was a significant increase in Col1A1 protein expression treated with *P. vulgaris* ethyl acetate extract. This situation (no correlation between mRNA and protein) is seen in many experimental results. The reason can be post-transcriptional mechanisms involved in translating mRNA into protein like 5'capping, 3' polyadenylation and splicing. The other reason can be microRNAs (miRNAs), small noncoding RNAs. MicroRNAs (miRNAs) are 21–22-nucleotide RNAs that mediate generally post-transcriptional gene silencing by guiding Argonaute (AGO) proteins to RNA targets. Also, some studies propose that miRNAs also affect gene expression in different ways from post-transcriptional gene silencing by providing increase in target gene expression with threshold-linear response and miRNA sponging mechanism with pseudogenes, long non-coding RNA (lncRNA) and circular RNAs (circRNA) (Hausser & Zavolan, 2014).

If we compare both crude and fractionated extract treatments for protein expression (Table 4.3), it was seen that both extracts of *P. vulgaris* provided the induction in COL1A1 protein expression. If we compare fold change in protein expression, crude extract of *P. vulgaris* treatments resulted in much more fold increase than only *P. vulgaris* ethyl acetate or water soluble extracts treatments. However, this results were not surprising since crude *P. vulgaris* possesses both fractionated extracts (water-soluble and ethyl acetate extracts) and other components. Also, observing the increase in COL1A1 protein expression with *P. vulgaris* ethyl acetate extract helps

us to select the type I collagen biosynthesis inducing plant, which is *P. vulgaris*. At the end of these results, it can be said that *P. vulgaris* crude extract was more effective on pro-type 1 collagen synthesis.

Insulin-like growth factor-1 is one of the stimulator of collagen biosynthesis in fibroblasts (Svegliati-Baroni, 1999). After determination of the plant extract that has an increase pro-type I collagen expression, active components of these extracts, that mimics growth factor (IGF-1) is an area that can be used in further researches. For further researches, we started to study the IGF-I signaling pathway. In this study, crude extracts of four plant extracts (*A. millefolium*, *P. vulgaris*, *A. hippocastanum*, *H. perforatum*) were examined on IGF-I signaling, to get data for further researches. Active components that mimics growth factor (IGF-1) can be determined with this method. The exposure of the dermal fibroblasts to *A. millefolium* and *P. vulgaris* extracts can be contributed to activation of IGF-I receptor in the absence of IGF-I, in other words, a compound or some compounds in *A. millefolium* and *P. vulgaris* aerial parts extract could mimic the IGF-I.

If we focus on the MAPK expression results of our study, *A. millefolium*, *P. vulgaris*, *H. perforatum* treated fibroblasts showed decrease mRNA expression, but *A. hippocastanum* treated fibroblasts did not show any significant change according to non treated cells. However, *A. hippocastanum* and *A. millefolium* treated fibroblasts showed increase protein expression. This can be post transcriptional modifications.

Some plant constituents have been shown to mimic IGF-1 and trigger the IGF-I signaling pathway. (Cameron, 2007; Jarvill-Taylor, 2001; Chen, 2010). These findings show that, small molecules in the extracts of plants can regulate type I collagen expression by mimicking some proteins. Aging decreases the biological activities of dermal fibroblasts (also type I collagen secretion) due to the decrease in growth factor responsiveness (Edmondson, 2003). In addition, aging rates progress as growth hormone secretion diminishes, because of that acceleration of aging is related to the decrease of IGF-I blood levels (Bartke, 2005). In our study *A. millefolium*, *P. vulgaris* and *H. perforatum* treated groups showed significant increase in mRNA expression, *A. hippocastanum*, *A. millefolium* and *P. vulgaris* showed significant increase in protein expression. Our findings suggest that the

potentiating effects of *A. millefolium* and *P. vulgaris* aerial parts extract are beneficial in the prevention of the signs of aging. The activation of IGF-I signaling evoked by *A. millefolium* and *P. vulgaris* aerial parts extract may be indirectly attributed to the phosphorylation or dephosphorylation reaction of the IGF-I receptor. According to our IGF-1 receptor mRNA expression results, only *A. hippocastanum* treated group was found significantly high. In the insulin signaling pathway, first insulin binds to the insulin receptor, resulting in down-regulation of insulin signaling. Recent studies have demonstrated that PTP-1B inhibitors could lead to the activation of the insulin receptor in an insulin-independent manner by mimicking the insulin (Koren, 2007). So we can say that, PTP- 1B has recently emerged as a promising therapeutic molecular target in the effective management of type 2 diabetes. On the basis of these facts, we consider that some molecules can inhibit PTP-1B and thereby induce the activation of IGF-I receptor in the dermal fibroblasts. In our Western blot analysis *A. hippocastanum*, *A. millefolium* and *P. vulgaris* treated groups showed significantly high IRS-I and p-IRS-1 protein expressions.

In the present study, crude extracts of some plants varied in their effectiveness in type I collagen biosynthesis, suggesting that modest structural differences of some molecules may exert influence on the induction rate of collagen biosynthesis in the fibroblasts. Further studies are needed to understand the exact molecular mechanism underlying *Achillea millefolium* and *Primula vulgaris* aerial parts extract triggered activation of IGF-I signaling. In conclusion, we demonstrated for the first time that the *Primula vulgaris* aerial parts extract potentiates type I collagen biosynthesis in protein level within dermal fibroblasts.



## CHAPTER 5

### CONCLUSION

There have been many herbal products developed to repair the aging defects by stimulating collagen. In addition to the benefits, some of those manufactured herbal products have the adverse effects as a result of unscientific production. In this study, *in-vitro* experiment steps were planned to search for type I collagen biosynthesis-inducing plants using human dermal fibroblasts. Plants (seed cotyledon of *Aesculus hippocastanum* and aerial parts of *Hypericum perforatum*, *Primula vulgaris*, *Achillea millefolium*) were selected. Antioxidant capacities were evaluated. *Hypericum perforatum* aerial part extract was found as having the highest radical scavenging activity among other extracts. Then, cell culture experiments were started. The effects of crude extracts were investigated on the expression level of type 1 collagen. For this purpose, human fibroblasts were exposed to each extract and then the levels of *pro-type 1* collagen were determined by qPCR and immunoblot analysis. Among these extracts, *Achillea millefolium* aerial part extract, which has the highest induction rate in qPCR analysis and *Primula vulgaris* aerial part extract, which has the highest induction rate in Western blot analysis were focused and these extracts were fractionated with different solvents (hexane, chloroform, ethyl acetate, water). The effects of these fractions and crude extracts were again investigated on the expression level of type 1 collagen. The highest induction rates were again investigated in the groups which treated with crude extracts.

*Insulin-like growth factor-1* (IGF-1) is the most potent stimulator of collagen biosynthesis in fibroblasts. Crude extracts that increases *pro-type 1* expression level, were examined on IGF-I signaling. With this method, we get data for further researches. Active components that mimics growth factor (IGF-1) can be determined with this method.

In conclusion, the crude extract that has the highest induction rate in Western blot analysis (*Primula vulgaris* aerial parts extract) should be used to obtain cosmetic and dermatological skin care products due to its promotion of collagen biosynthesis. Active components of these extracts, that mimics growth factor (IGF-1) is an area used in further research.

*Insulin-like growth factor-1* is the most potent stimulator of collagen biosynthesis in fibroblasts. Crude extracts that increases *pro-type 1* expression level, were examined on *insulin-like growth factor-1* signaling. With this method, we get data for further researches. Active components that mimics growth factor (IGF-1) can be determined with this method.

## REFERENCES

- Alberts, B. et al., 2008. *Molecular Biology of the Cell*. Garland Science.
- Apak, R. et al., 2004. Novel Total Antioxidant Index for Dietary Polyphenols and Vitamins C and E, Using Their Cupric Ion Reducing Capability in the Presence of Neocuproine: CUPRAC Method. *Journal of Agricultural and Food Chemistry*, 52, pp.7970-7981.
- Bartke, A., 2005. Minireview: Role of the growth hormone/insulin-like growth factor system in mammalian aging. *Endocrinology*, 146(9), pp.3718-3723.
- Baserga, R. et al., 1997. The IGF-I receptor in cell growth, transformation and apoptosis, *Biochim. Biophys. Acta*, 1332(3), pp.105–126.
- Bella, J. et al., 1994. Crystal and molecular structure of a collagen-like peptide at 1.9Å resolution. *Science*, 266, pp.75–81.
- Benedi, J., et al., 2004. Antioxidant properties and protective effects of a standardized extract of *Hypericum perforatum* on hydrogen peroxide-induced oxidative damage in PC12 cell. *Life Science*, 75, pp.1263–1276.
- Blois, M.S., 1958. Antioxidant determinations by the use of a stable free radical. *Nature*, 26, pp.1199-1200.
- Berisio, R. et al., 2002. Crystal structure of the collagen triple helix model [(Pro-Pro-Gly)<sub>10</sub>]<sub>3</sub>. *Protein Sci.*, 11, pp.262–270.
- Bonni, A. et al., 1999. Cell survival promoted by the Ras-MAPK signaling pathway by transcription-dependent and -independent mechanisms. *Science*, 286(5443), pp.1358-1362.

- Bou-Gharios, G. et al., 1996. A potent far-upstream enhancer in the mouse pro- $\alpha$ 2 (I) collagen gene regulates expression of reporter genes in transgenic mice. *J Cell Biol.*, 134, pp.1333-1344.
- Butler, A.A. et al., 1998. Insulin-like growth factor-I receptor signal transduction: at the interface between physiology and cell biology. *Comp. Biochem. Physiol., Part B: Biochem. Mol. Biol.*, 121 (1), pp.19–26.
- Butterweck, V., 2003. Mechanism of action of St. John's Wort in depression. What is known? *CNS Drugs*, 17, pp.539–562.
- Cameron, C. et al., 2007. Effect of diet and ration on the relationship between plasma GH and IGF-1 concentrations in Arctic charr, *Salvelinus alpinus* (Linnaeus). *Aquaculture Research*, 38, pp.877-886.
- Canty, E.G. & Kadler K.E., 2005. Procollagen trafficking, processing and fibrillogenesis. *J Cell Sci*, 118, pp.1341–1353
- Chambard, J.C. et al., 2007. ERK implication in cell cycle regulation. *Biochim Biophys Acta*, 1773, pp.1299–1310
- Chambers, R.C. et al., 1998. Thrombin stimulates fibroblast procollagen production via proteolytic activation of protease-activated receptor 1. *Biochem J.*, 333, pp.121-127.
- Chen, L.H. et al., 2010. MicroRNA and aging: a novel modulator in regulating the aging network. *Ageing Res.*, 9, pp.559–566.
- Davis, P. H., 1965-1988. *Flora of Turkey and the East Aegean Islands*. Volume 1-10. Edinburgh Univ. Press.
- Debowska, R., 2010. In vitro and ex vivo tests in contemporary cosmetology. *Chemik*, 64(2), pp.74-79
- Demir, N. et al., 2014. The antioxidant and radical scavenging activities of Primrose (*Primula vulgaris*), *Euro. J. Exp. Bio.*, 4(2), pp.395-401.

- Dikmen, M. et al., 2011. Evaluation of the wound healing potentials of two subspecies of *Hypericum perforatum* on cultured NIH3T3 fibroblasts. *Phytotherapy Research*, 25, pp.208-211
- Dweck, A.C., 1996. Botanicals – research of actives. *Cosmet Toiletries*, 111, pp.45–57.
- Edmondson, S.R. et al., 2003. Epidermal homeostasis: the role of the growth hormone and insulinlike growth factor systems. *Endocr. Rev.*, 24 (6), pp.737–764.
- Fang, X. et al., 1999. Regulation of BAD phosphorylation at serine 112 by the Ras-mitogen-activated protein kinase pathway. *Oncogene*, 18, pp.6635-6640.
- Faustino, H. et al., 2010, Antioxidant Activity of Lignin Phenolic Compounds Extracted from Kraft and Sulphite Black Liquors. *Molecules*, 15, pp.9308-9322;
- Fisher, G. et al., 2002. Mechanisms of photoaging and chronological skin aging. *Arch Dermatol.*, 138, pp.1462–1470.
- Fisher, G.J. et al., 2009. Collagen fragmentation promotes oxidative stress and elevates matrix metalloproteinase-1 in fibroblasts in aged human skin. *Am. J. Pathol.*, 174, pp.101–114.
- Fujimura, T. et al., 2006. A horse chestnut extract, which induces contraction forces in fibroblasts, is a potent anti-aging ingredient. *J. Cosmet. Sci.*, 57, pp.369–376.
- Gillery, P. et al., 1992. Insulin-like growth factor-I (IGF-I) stimulates protein synthesis and collagen gene expression in monolayer and lattice cultures of fibroblasts. *J. Cell. Physiol.*, 152 (2), pp.389–396.
- Hausser, J. & Zavolan, M., 2014. Identification and consequences of miRNA-target interactions-beyond repression of gene expression. *Nat Rev Genet.*, 15, pp.599-612.

- Hazra, B., Biswas, S., & Mandal, N., 2008. Antioxidant and free radical scavenging activity of *Spondias pinnata*. *BMC Complementary and Alternative Medicine*, 8, p.63.
- Hematulin, A., 2010. Insulin-like Growth Factor 1 Signalling and Its Role in Cell Survival and Radiation Sensitivity. *Sriraj Med J*, 62(6), pp.263-267.
- Jarvill-Taylor, K.J., Anderson, R.A. & Graves, D.J., 2001. Ahydroxychalcone derived from cinnamon functions as a mimetic for insulin in 3T3-L1 adipocytes. *J. Am. Coll. Nutr.*, 20, pp.327–336.
- Klemow, K.M. et al. 2011. chapter 11: Medical Attributes of St. John's Wort (*Hypericum perforatum*). *Herbal Medicine Biomolecular and Clinical Aspects*. (2nd ed. ed.). CRC Press.
- Koren, S., 2007. Inhibition of the protein tyrosine phosphatase PTP1B: potential therapy for obesity, insulin resistance and type-2 diabetes mellitus. *Best Pract Res Clin Endocrinol Metab.*, 21, pp.621–640.
- Kuivaniemi, H., Tromp, G. & Prockop, D.J., 1991. Mutations in collagen genes: causes of rare and some common diseases in humans. *FASEB J.*, 5(7), pp.2052–2060.
- Laron, Z., 2001. Insulin-like growth factor 1 (IGF-1): a growth hormone. *Mol Pathol.*, 54(5), pp.311-316
- Lavan, B.E. et al., 1997. A novel 160-kDa phosphotyrosine protein in insulin-treated embryonic kidney cells is a new member of the insulin receptor substrate family. *J Biol Chem.*, 272(34), pp.21403-21407.
- Leung, A.Y. & Foster, S., 2014. *Encyclopaedia of Common Natural Ingredients used in Food, Drugs and Cosmetics*. pp.304–306.
- Li, J., Johnson, S.E., 2006. ERK2 is required for efficient terminal differentiation of skeletal myoblasts. *Biochem Biophys Res Commun.*, 345, pp.1425–1433.

- Livak, K.J. & Schmittgen, T.D., 2001. Analysis of relative gene expression data using real-time quantitative PCR and the  $2^{-\Delta\Delta C(T)}$  method. *Methods*, 25, pp.402–408.
- Mabey, R., 1996. *The Definitive New Guide to Britain's Wild Aerial parts, Plants and Trees*. Flora Britannica, pp. 480. Sinclair-Stevenson Ltd.
- Maisenbacher, P. & Kovar, K.A., 1992. Analysis and stability of Hyperici oleum. *Planta Med*, 58, pp.351–354
- Malone, J.P. & Veis, A., 2004. Heterotrimeric type I collagen C-telopeptide conformation as docked to its helix receptor. *Biochemistry*, 43(49), pp.15358-15366
- Marks, A., 1997. Herbal extracts in cosmetics. *Agro-Food- Industry Hi-Tech*, 8, pp.28-31.
- Masaki, H., Sakaki, S., Atsumi, T. and Sakurai, H., 1995. Active-oxygen scavenging activity of plant extracts. *Biol. Pharm. Bull.*, 18, pp.162–166.
- Mays, P.K., Bishop, J.E. & Laurent, G.J., 1988. Age-related changes in the proportion of types I and III collagen. *Mech. Ageing Dev.*, 45 (3), pp.203–212.
- McCullough, J., & Kelly, K., 2006. Prevention and Treatment of Skin Aging. *Understanding and Modulating Aging*, 1067, pp.323–331
- Mehta, R.C. & Fitzpatrick, R.E. 2007. Endogenous growth factors as cosmeceuticals. *Dermatol. Ther.*, 20(5), pp.350–359.
- Meloche, S. & Pouyssegur, J., 2007. The ERK1/2 mitogen-activated protein kinase pathway as a master regulator of the G1- to S-phase transition. *Oncogene*, 26, pp.3227–3239.
- Mescher, A.L., 2013. *Junqueira's basic histology*, 13th edition. Available at: [www.accessmedicine.com](http://www.accessmedicine.com)

- Neergheen, V.S., Soobrattee, M.A., Bahorun, T. & Aruoma, O.I., 2006. Characterization of the phenolic constituents of Mauritian endemic plants as determinants of their antioxidant activities in vitro. *J. Plant Physiol.*, 163, pp.787–799
- Nigel, P.B., 2005. Inherited diseases of collagen, elastin and keratin. *Medicine*, 33(1), pp.83–86.
- Orgel, J.P., San Antonio, J.D. & Antipova, O., 2011. Molecular and structural mapping of collagen fibril interactions. *Connect. Tissue Res.*, 52 (1), pp.2–17.
- Öztürk, N. et al., 2007. Wound-healing activity of St. John's Wort (*Hypericum perforatum* L.) on chicken embryonic fibroblasts. *J Ethnopharmacol.*, 111(1), pp.33-39
- Prockop, D.J., Kivirikko, K.I., Tuderman, L. & Guzman, N.A., 1979. The biosynthesis of collagen and its disorders (first two parts). *N Engl J Med*, 301, pp.13-23
- Prockop, D.J. & Kivirikko, K.I., 1984. Heritable diseases of collagen. *N Engl J Med*, 311, pp.376-386
- Proserpio, G., Gatti, S. & Genesi, P., 1980. Cosmetic uses of Horse-Chestnut (*Aesculum hippocastanum*) extract, of escin, and of the cholesterol/escin complex. *Fitoterapia*, 51, pp.113–28
- Ramirez-Coronel, S. et al., 2004. Characterization and estimation of proanthocyanidins and other phenolics in coffee pulp (*Coffee arabica*) by thiolysis-high performance liquid chromatography. *Journal of Agricultural and Food Chemistry*, 52(5), pp.1344-1349
- Rossert, J. & de Crombrughe B., 1996. Structure, synthesis, and regulation of type I collagen. *Principles of Bone Biology*, pp.127-142. Academic Press, Orlando
- Rossert, J., Eberspaecher, H. & de Crombrughe, B., 1995. Separate cis-acting DNA elements of the mouse pro- $\alpha$ 1(I) collagen promoter direct expression of

- reporter genes to different type I collagen producing cells in transgenic mice. *J Cell Biol*, 129, pp.1421-1432
- Sagdicoglu Celep, A. G.; Yilmaz, S. and Coruh, N., 2012. Antioxidant Capacity and Cytotoxicity of *Aesculus hippocastanum* on Breast Cancer MCF-7 Cells. *Journal of food and drug analysis*, 20, pp.692-698.
- Schmid, C., 1995. Insulin-like growth factors. *Cell. Biol. Int.*, 19(5), pp.445–457.
- Sengupta, P. et al., 2005. Collagen alpha1(I) gene (COL1A1) is repressed by RFX family. *J Biol Chem.*, 280(22), pp.21004-21014.
- Shimizu, A., et al., 1999. The dermatofibrosarcoma protuberans-associated collagen type I alpha1/platelet-derived growth factor (PDGF) B-chain fusion gene generates a transforming protein that is processed to functional PDGF-BB. *Cancer Res.*, 59(15), pp.3719-3723.
- Simonetti G. 1990. *Guide to Herbs and Spices*. Stanley Schuler. Simon & Schuster's Simon & Schuster ed., USA.
- Singleton, V. L. & Rossi, J. A., Jr., 1965. Colorimetry of total phenolics with phosphomolybdic- phosphotungstic acid reagents. *Am. J. Enol. Vitic.*, 16, pp.144-158
- Smith, P.K. et al., 1985. Measurement of protein using bicinchoninic acid. *Anal. Biochem.* 150(1), pp.76–85.
- Sun, X.J. et al., 1991. Structure of the insulin receptor substrate IRS-I defines a unique signal transduction protein. *Nature*, 352, pp.73–77.
- Sun, W., Hou, F., Panchenko, M.P. & Smith, B.D., 2001. A member of the Y-box protein family interacts with an upstream element in the alpha1(I) collagen gene. *Matrix Biol.*, 20(8), pp.527-541.
- Svegliati-Baroni, G., et al., 1999. Insulin and insulin-like growth factor- 1 stimulate proliferation and type I collagen accumulation by human hepatic stellate

- cells: differential effects on signal transduction pathways. *Hepatology*, 29(6), pp.1743–1751.
- Takasao, N. et al., 2012. Cinnamon extract promotes type i collagen biosynthesis via activation of IGF-I signaling in human dermal fibroblasts. *J Agric Food Chem.*, 60, pp.1193–1200.
- Tanaka, M. et al., 2015. Effects of plant sterols derived from Aloe vera gel on human dermal fibroblasts in vitro and on skin condition in Japanese women. *Clin Cosmet Investig Dermatol.* 8, pp.95-104.
- Teli, A., 1992. Regulation of cellular functions by extracellular matrix. *J. Am. Soc. Nephrol.* 2, pp.83–87.
- Werner, H. & Le Roith, D., 2000. New concepts in regulation and function of the insulin-like growth factors: implications for understanding normal growth and neoplasia. *Cell. Mol. Life Sci.* 57(6), pp.932–942.
- Wilkinson, J. & Brown, A., 1999. Horse chestnut: *Aesculus hippocastanum*: Potential applications in cosmetic skin-care products. *Int J Cosmet Sci* 21(6), pp.437-447
- Wölfle, U., Seelinger, G. & Schempp C.M. 2014. Topical application of St. John's wort (*Hypericum perforatum*). *Planta Med.* 80(2-3), pp.109–20.
- Zheleva-Dimitrova D., Nedialkov, P, Kitanov, G., 2010. Radical scavenging and antioxidant activities of methanolic extracts from *Hypericum* species growing in Bulgaria. *Phcog Mag.*, 6(22), pp.74-78.
- Zhang, Z. et al., 2008. Phenolic compounds and rare polyhydroxylated triterpenoid saponins from *Eryngium yuccifolium*. *Phytochemistry* 69, pp.2070–2080
- Zhishen, J., Mengcheng, T. & Jianming, W., 1999. The determination of flavonoid contents in mulberry and their scavenging effects on superoxide radicals. *Food Chem.*, 64(4), pp.555-559.

## CURRICULUM VITAE

### 1. PERSONAL INFORMATION

Surname, Name: KURT, Aslıgül

Nationality: Turkish (TC)

Date and Place of Birth: 26 October 1982, Ankara

Marital Status: Married

Phone: +90 533 636 70 06

email: asligulaksoy@gmail.com

### 2. EDUCATION

Degree	Institution	Year of Graduation
MS	Gazi University, School of Medicine, Department of Histology and Embryology	2008
BS	Ankara University, Faculty of Science, Biology	2005

### 3. WORK EXPERIENCE

Year	Place	Enrollment
2013- Present	Doku Biotechnology	General Manager
2012-2013	Ars Arthro Biotechnology	R&D Manager

#### 4. CONFERENCE PRESENTATIONS

1. A. Aksoy, M. T. Hatipoglu, D. Erdođan, S. Sahin, F. Helvaciođlu, G. T. Kaplanođlu. 2011. Age related distribution of estrogen, progesterone and follicule stimulating hormone receptors in rat ovaries. *FEBS J.* 278 (1), 424.
2. S. Sahin, G. T. Kaplanođlu, D. Erdogan, A. Aksoy and G. Goktas. 2011. Effects of age on estrogen receptor, progesterone receptor distribution in rat fallopian tubes. *FEBS J.* 278 (1), 427.
3. A. Aksoy, M. T. Hatibođlu, D. Erdogan, S. Sahin, F. Helvaciođlu, G. T. Kaplanoglu. 2012. Age-related changes in the ultrastructure of the rat ovaries. *FEBS J.* 279 (1), 187.
4. N. Ozdogan, S. Sahin, A. Aksoy, Y. Kumbet, N. oruh. 2012. An investigation on the antioxidant activities and total phenolics content of *Calendula officinalis*. *FEBS J.* 279 (1), 555.
5. N. Ozdogan, S. Sahin, Y. Kumbet, A. Aksoy, N. oruh. 2012. *Centaurea cyanus* Bitki zütünün Toplam Fenol ve Flavonoid ieriđinin ve Serbest Radikal Spürme Kapasitesinin Arařtırılması, XXIV Biyokimya Kongresi, Konya.
6. A. Aksoy, S. Sahin, Y. Kumbet, N. oruh. 2013. Anti-oxidant capacity of *Aesculus Hippocastanum* Fruit Parts as an Anti-aging Agent. *FEBS J.* 280 (1).